ATLAS

Version 1.0 (May 1989)
(reprinted April 1997)

ANALYSIS OF TIME-OF-FLIGHT DIFFRACTION DATA FROM LIQUID AND AMORPHOUS SAMPLES

A.K.Soper, W.S.Howells and A.C.Hannon

ISIS Facility
Rutherford Appleton Laboratory
Chilton, Didcot, Oxon OX11 0QX.

Tel: 01235-445543 (AKS)
01235-445680 (WSH)
01235-445358 (ACH)

TABLE OF CONTENTS

INTRODUCTION

The purpose of this manual is to describe a package of data analysis routines which have been developed at the Rutherford Appleton Laboratory for the analysis of time-of-flight diffraction data from liquids, gases, and amorphous materials. It seemed to us that a majority of users were put off analysing their data properly because of the apparent complexity of TOF data, although in actual fact the basic steps are the same as in a reactor experiment. Furthermore our experience to date has shown that there really is no fundamental barrier to diffraction data being accurately analysed to structure factor or even pair correlation function within a very short time of the completion of the experiment (always assuming the computer is "up" of course!). What has prevented this in the past has been a lack of understanding of what to do with the data and how to do it. For our part the relevant routines have been spread around different directories with different modes of input and operation, which has led to great inefficiencies for all concerned.

Therefore the package has now been set up with all the relevant routines in a single area of the computer in such a way that it requires a minimum of understanding of computing aspects on the part of the users, at the same time as allowing them to check that each stage of the analysis has been completed satisfactorily, and also enabling them to re-sequence the steps or add additional ones according to their own requirements. For example application of inelasticity corrections and calculation of the pair correlation function tend to be controversial stages with each user having his or her own preferences for how they should be achieved. While the package supplies suitable routines, the users can readily incorporate their own preferred routines as necessary. At several points the package requires an intelligent interaction with the user which means he or she is not entirely free from responsibilities. Hopefully after studying this manual he or she will be able to respond to the requests made of him confidently!

The other guiding principle we have adopted is that the users will not be willing to ship the very large raw data files generated in these experiments, but on the other hand will be willing to remain a short while at RAL after their experiments in order to complete the routine analysis. In this way they can return home with the much smaller files containing the structural information they are seeking for more detailed manipulations at their home institutions. This makes sense because most university users are not equipped to handle the size of typical ISIS data files, nor provide the necessary archive which is done at ISIS immediately after each run is completed. Having said that however we also request that users do NOT use the ISIS HUB computer for these subsequent manipulations because by doing so they simply slow down the HUB for other users, who also can only afford to spend a limited time at RAL analysing their data. Of course there are no restrictions on those users ambitious enough to take the raw data home and analyse it from scratch themselves: we will be happy to let such people have copies of any of our routines that they might need.

The package has been developed primarily for analysis of ISIS data, but is not limited to a specific instrument: the procedures will work equally well on any ISIS diffractometer, although LAD is used as the example throughout this manual. Because of its great versatility the GENIE command language, invented by Bill David, or variants of it, is used for the main stages. However the only stage which is strictly ISIS specific is the very first in which the raw data in ISIS format are converted into GENIE format. Therefore the package could in principle be used at other institutions which have the GENIE language, the only modification required being to the initial input of the raw TOF data.

Obviously while every effort has been made to ensure that the routines do what we say they do, we can accept no responsibility for errors which may occur: careful checking at each stage normally should show up any errors. We would welcome suggestions for ways in which the procedures can be corrected and improved.

This manual is in no way comprehensive. Further details are contained in the papers referred to. In particular the reader is encouraged to read Colin Windsor's book, "Pulsed Neutron Scattering" [1].

SECTION 1

TIME-OF-FLIGHT DIFFRACTION

1.1 THE TIME-OF-FLIGHT NEUTRON DIFFRACTION EXPERIMENT

There are seven principal components to a time-of-flight diffraction experiment: (1) production of neutrons in a target, (2) slowing down and thermalization in a moderator, (3) collimation of the neutrons into a beam, (4) a sample to scatter the neutrons, (5) a detector to analyse the "diffraction" pattern of the scattered neutrons, (6) a set of data acquisition electronics (DAE) with which the data are stored, initially in fast memory and eventually on computer memory, and finally (7) a data analysis package. Normally the user is involved in providing the sample and performing the data analysis, the rest being provided as part of the neutron facility.

Production of neutrons at a spallation neutron source is achieved by accelerating bunches of protons to sufficiently high energies (typically 500 - 800 MeV) that when they collide with a TARGET nucleus they produce highly excited nuclear states which decay either immediately or after a delay by throwing off nuclear particles such as neutrons, γ particles, neutrinos, etc. The maximum energy of neutrons produced in this way corresponds to the energy of the impinging proton beam, and if the target is uranium up to 30 neutrons per proton can be produced. Other, non-fissioning targets such as tantalum or tungsten produce about half this number of neutrons. The so-called "prompt" neutrons are the ones used for time-of-flight analysis while the "delayed" neutrons form a low level background in the diffractometer which is independent of time, but must in general be corrected for as it can be sample dependent. Normally the delayed fraction is on the order of a few tenths of 1 percent of the prompt neutrons, but in cases where an enriched booster target is installed, such as at the Argonne National Laboratory in the U.S., this fraction can be higher.

The proton beam is pulsed so that a pulse of neutrons less that 1μs wide is produced in the target. These neutrons are not useful however

because they typically have energies 10^9 times too high for diffraction effects to be seen. Therefore they are slowed down in a MODERATOR, which scatters the neutrons many times before they escape. Light atoms such as are in hydrogen-containing materials are used for the moderator since the energy transferred ina collision is greatest when the two particles have the same mass. Up to a point the thicker the moderator the slower the neutrons become, but the process is self limiting, because as well as slowing the neutrons down the moderator has the effect of broadening the initial very narrow pulse significantly. Therefore the moderator is designed to compromise between the production of slow neutons and the requirements for reasonably narrow neutron pulses: compared to a nuclear reactor the spallation target would be regarded as under-moderated. The target-moderator assembly is surrounded by neutron reflecting material, usually beryllium, to enhance the neutron production and pulse shape.

Figures 1.1 and 1.2 show a typical neutron spectrum from the methane moderator at ISIS, plotted as a function of energy and time-of-flight respectively. Two regions in the spectrum can be identified, the epithermal region where the intensity varies as 1/E or 1/t, respectively, and a Maxwellian "hump" which occurs when the neutrons in the moderator reach a temperature close to that of the moderator. The neutron spectrum is therefore described by two functions which are added together using a joining function [2]. The Maxwellian region is described by the function

$$\Phi_{max}(E) = J \frac{E}{T^2} \exp\{-E/T\} \qquad (1.1.1)$$

while the slowing down epithermal region is represented by

$$\Phi_{epi}(E) = \frac{\Phi_o}{E^A}. \qquad (1.1.2)$$

These two functions are combined by means of an empirical switch function, $\Delta(E)$:

$$\Phi(E) = \Phi_{max}(E) + \Delta(E)\Phi_{epi}(E) \qquad (1.1.3)$$

where

$$\Delta(E) = [1 + \exp\{ \frac{W_1}{\sqrt{E}} - W_2\}]^{-1}. \qquad (1.1.4)$$

In these equations J is the integrated Maxwellian intensity, T is the effective temperature of the Maxwellian in enegy units, Φ_o is the differential flux at 1 eV, A is a leakage parameter, and W_1, W_2 are two parameters which define the switch function. Table 1.1 lists the values of these constants for the methane and ambient moderators at ISIS.

TABLE 1.1 ISIS moderator constants

	CH_4	Ambient H_2O
Epithermal*		
Φ_0 (at 750MeV) $[10^{10}n(eVsr100cm^2\mu As)^{-1}]$	2.7	3.5
A	0.92	0.9
Maxwellian		
J $[10^{10}n(sr100cm^2\mu As)^{-1}]$	5.7	14.7
T (eV)	0.011	0.033
Joining function		
W_1 $(eV)^{1/2}$	1.7	4.0
W_2	7.0	10.6

*N.B. The above numbers for Φ_0 refer to 750MeV proton energy. The $100cm^2$ refers to the area of the moderator normally viewed.

The neutrons emerge from the moderator in all directions and so to be useful for diffraction they must be COLLIMATED. An essential difference between TOF and reactor diffraction is that there is no monochromator for the TOF experiment which means the full spectrum of

neutron energies, from 800 MeV downwards, is incident on the sample. Therefore materials like cadmium and gadolinium which might be used in a reactor situation are useless in the TOF case, and may even be detrimental because of the high energy γ's produced by neutron capture in those materials. Instead boron, which has a 1/v capture cross section over a wide energy range, is the primary component, with large amounts of iron and hydrogen (the latter usually in the form of wax or resin) to provide the basic scattering cross section. Because the final scattered intensities are small compared to the incident beam intensity, and because it is essential to provide a radiation free environment for people working near the diffractometer the TOF collimator is a massive construction: at ISIS the collimator plus shielding measures typically ~1.5m square. Figure 1.3 shows a diagram of the prototype SANDALS collimator. This collimator is surrounded on all four sides by about 0.4m of iron, and a further 0.3m borated wax outside the iron.

The collimator defines a NEUTRON BEAM at the sample position. This must be sufficiently well collimated to give adequate angular resolution for the type of experiment being undertaken, but large enough to give an acceptable count rate. Crystalline powder experiments generally need high resolution in order to discriminate effectively between adjacent Bragg reflections and also to determine the sample constribution to the shape of individual reflections. However because Bragg reflections are so sharp the count rate is rarely a severe constraint, unless special effects are being determined, such as the change in structure as a function of time. For liquids and amorphous materials however the structure factor consists of a few broad peaks which merge together, continuously. Detailed analysis of these requires absolute measurements which can only be achieved through careful and accurate measurements. In many examples, particularly those which involve measuring changes in structure as a function of pressure, temperature or isotope, count rate can be of paramount importance because of the intrinsic weakness of the signal. Increases in resolution can only be used if a count rate appropriate to the resolution is available.

The SAMPLE is normally held in a CONTAINER: in addition if the temperature is to be different from ambient then a FURNACE is required to go above room temperature, and a CCR (CLOSED CYCLE REFRIGERATOR), for temperatures down to ~20K, or HELIUM CRYOSTAT, for temperatures down to 4.2K, is required. Somewhat lower temperatures can be achieved by pumping on the helium in the crystat.

For accurate structure factor measurements the mounting and containment of the sample can be crucial since the diffractometer is sensitive to small positioning offsets on the order of 1mm. This sensitivity arises from the small variations in final flight path and scattering angle which can occur from one sample to another if each sample is not placed in exactly the same position as its predecessor. One solution to this difficulty which is applicable if the sample will not be under pressure is to use a flat plate sample can with an area larger than the beam area. This largely avoids the positioning problems. In general however cylindrical cans must be used for pressure or furnace experiments and so it is essential to ensure that if cylindrical cans are used the sample positioning is accurate to 0.1mm.

Ideally the container should be made of a purely incoherent scattering material (vanadium or zirconium-titanium are the closest to this ideal), otherwise the Bragg reflections from the container can be hard to subtract completely: the problem arises because the front and back of the sample container correspond to slightly different scattering angles at the detector so that Bragg peaks from front and back arrive at slightly different times-of-flight. Thus when the container is measured empty and then filled with sample the neutron attenuation by the sample causes the Bragg peaks from the front of the container to be attenuated preferentially compared to those from the rear, causing an apparent shift in the position of the peaks in time. Once again the ideal of an incoherent container may be hard to meet if a particularly corrosive sample requires a special material for containment. Fortunately zirconium-titanium alloy is suitable for many pressure vessels.

The next diffractometer component, the DETECTOR, adopts one of two forms. It is usually a gas proportional counter, with ^{3}He gas the primary neutron absorber, but at ISIS there has been considerable development work on neutron scintillator detectors. If all goes well the user should not have to be particularly concerned about which kind of detector he is using, although he should be aware of its efficiency and deadtime. The reasons for choosing scintillator detectors for liquids and amorphous materials centre on their much lower cost, compared to He tubes, and on the fact that they can be made at least twice as efficient as the He tube. In this way the epithermal part of the neutron spectrum can be used more effectively.

The primary object of the DATA ACQUISITION ELECTRONICS, DAE, is to record each neutron event and give it a label corresponding to the number of the detector in which it occurred and to the time of arrival at the detector. The clock which measures this time of arrival is started by an electronic pulse which is generated when a burst of protons hits the target. At ISIS this occurs 50 times a second. Once the label is generated, a word of memory corresponding to the label is incremented. In this way a histogram of events is built up. The experiment is controlled by a FRONT END MINIcomputer (FEM) which is a computer to store, manipulate and display the data.

After transmission through the sample the neutrons and other particles are absorbed in a BEAM STOP, which again at ISIS is of a massive construction, as it must absorb all potentially dangerous particles which come down the beam line. In fact different pulsed neutron sources have adopted different modes of operation: at the HARWELL linac and at the LANSCE facility at Los Alamos, parts of the facility are inaccessible while the beam is on, in order to protect experimenters from radiation exposure. At ISIS on the other hand the shielding is sufficiently comprehensive that even when running at full power the background radiation levels are certainly low enough for people to remain near the diffractometers for extended periods.

The time of arrival, t_0, of a neutron at the detector is given by its "TIME-OF-FLIGHT", TOF, which is the time (in μs) taken by the neutron to travel 1m, multiplied by the total total flight path in m. Several useful relationships can be written down between the neutron's time of flight TOF (μs/m), velocity v (in m/s), wavelength λ (in Å), wavevector (in $Å^{-1}$) and energy E (in meV). Thus

$$\begin{aligned} v\ (m/s) &= 10^6/TOF\ (\mu s/m) \\ \lambda\ (Å) &= 0.0039562TOF = 0.0039562t_0(\mu s)/L(m) \\ t_0\ (\mu s) &= 252.77\lambda L \\ k\ (Å^{-1}) &= 2\pi/\lambda = 1588.2/TOF \\ E\ (meV) &= 81.807/\lambda^2 \end{aligned} \qquad (1.1.5)$$

Using these relationships we can write down the incident flux distribution as a function of wave vector or wavelength in terms of the energy distribution:

$$\begin{aligned} \Phi(\lambda) &= \Phi(E)\left(\frac{\partial E}{\partial \lambda}\right) = 2\Phi(E)\left(\frac{E}{\lambda}\right) \\ \Phi(k) &= \Phi(E)\left(\frac{\partial E}{\partial k}\right) = 2\Phi(E)\left(\frac{E}{k}\right), \text{ etc.} \end{aligned} \qquad (1.1.6)$$

Note that since in the epithermal region $\Phi(E) \simeq \Phi_0/E$, then

$$\Phi(\lambda) = 2\Phi_0/\lambda,\ \Phi(k) = 2\Phi_0/k, \text{ etc.}$$

An important characteristic of any diffractometer is its resolving power: it is the Q-RESOLUTION which makes the primary distinction between a powder diffractometer, where there are many sharp peaks close together and so requires high resolution, and the liquids and amorphous diffractometer where the peaks are broader, merge together continuously, and hence requires relatively low resolution. For liquids and amorphous materials diffraction, irrespective of whether it is constant wavelength or time-of-flight diffraction, the scattered intensity, which is proportional to the structure factor S(Q) (see section 1.2), is measured versus the momentum transfer, ħQ, where for elastic scattering

$$Q = 4\pi \sin\theta / \lambda \qquad (1.1.7)$$

2θ is the scattering angle and λ the neutron wavelength. In the case of TOF, λ is measured by time-of-flight with θ held constant. In that case we see that the resolution, ΔQ, has two components:

$$\Delta Q = \left(\frac{\partial Q}{\partial \theta}\right)\Delta\theta + \left(\frac{\partial Q}{\partial \lambda}\right)\Delta\lambda$$

$$= Q\,[\cot\theta\Delta\theta + \Delta\lambda/\lambda]. \qquad (1.1.8)$$

The wavelength uncertainty, $\Delta\lambda/\lambda$, arises from the intrinsic pulse width of the incident neutron beam and from the flight path uncertainty to the detector, $\Delta L/L$, where L is the total flight path from moderator to detector. A more detailed account of contributions to the resolution function is given in Appendix A. We note that for a given TOF channel the width of the pulse, Δv, as a function of neutron velocity, v, is proportional to v, i.e. $\Delta v/v = \Delta\lambda/\lambda \simeq$ constant. Similarly since for a given time channel

$$\lambda \sim 1/L(m)$$

it will be seen that the flight path uncertainty also gives rise to a wavelength uncertainty such that $\Delta\lambda/\lambda = \Delta L/L$ = constant as a function t_0. Hence we see from (1.1.3) that the resolution $\Delta Q/Q$ is roughly a constant as a function of TOF for a given scattering angle.

Further details about the effects of resolution are given in Appendix A. The count rate on a diffractometer is denoted by its "count rate number" or "C-number" (see Appendix B for details). Table 1.2 lists the resolutions and C-numbers for LAD and Table 1.3 lists the projected numbers for SANDALS.

TABLE 1.2 Some Specifications for LAD

Moderator:	Methane, 100K
Incident Flight Path:	10m
Beam Cross Section:	Rectangular
Maximum Beam Aperture:	20 (wide) x 50 (high)mm
Final Flight Path:	~1m
Detectors:	10 atm ^{3}He detectors at 5°, 10° and 150°, Li-glass scintillators at other angles.

Range In 2θ (deg.)	Detector Solid Angle (sr)	Resolution $\Delta Q/Q(\%)$	C-number (at $Q=10\text{Å}^{-1}$)
5	0.0002	11	0.04
10	0.0002	6	0.04
20	0.016	2.8	3.1
35	0.027	1.7	5.2
58	0.027	1.2	5.2
90	0.027	0.8	5.2
150	0.048	0.5	9.3

TABLE 1.3 Some Specifications for SANDALS

Moderator:	Methane, 100K
Incident Flight Path:	11m
Beam Cross Section:	Circular
Maximum Beam Aperture:	32mm (diameter)
Final Flight Path:	0.75m - 4.0m
Detectors:	Zinc sulphide sandwich detectors 200 (high) x 10 (wide) x 20 (deep) mm 30% efficient at 10eV

Range In 2θ	Detector Solid Angle	High Resolution Res.	High Resolution C-number	Low Resolution Res.	Low Resolution C-number
(deg.)	(sr)	$\Delta Q/Q(\%)$	($Q=10\text{Å}^{-1}$)	$\Delta Q/Q(\%)$	($Q=10\text{Å}^{-1}$)
3 - 11	0.039	11 - 2	0.3	16 - 4	6
11 - 21	0.110	2	1.4	4 - 3	32
19 - 31	0.202	1.5	3.5	3	76
29 - 41	0.275	1.3	5.5	2.5	120

1.2 OVERVIEW OF DIFFRACTION THEORY

The quantity being sought in a diffraction experiment on any crystalline or disordered material is the STRUCTURE FACTOR, $S(\underline{Q})$, where

$$S(\underline{Q}) = 1 + \rho \int d\underline{r}\ (g(\underline{r}) - 1)\ \exp(i\underline{Q}.\underline{r}) \qquad (1.2.1)$$

and ρ is the number density of atoms in the material, $g(\underline{r})$ is the pair correlation function at position $\underline{r}$ given an atom at the origin, and $\underline{Q}$ is the reciprocal lattice vector or wave vector transfer in the diffraction experiment. The integral is taken over the entire volume of the sample. $S(\underline{Q})/\rho$ is to be regarded as the density of points in reciprocal space, just as $\rho g(\underline{r})$ is the density of points in real space.

The definition of the structure factor (1.2.1) although different from the normal definition for structure factor used in crystallography is nonetheless valid irrespective of whether the sample is a single crystal, polycrystalline, amorphous or fluid. However for powders, glasses and fluids an immediate simplification is possible because $S(\underline{Q})$ and $g(\underline{r})$ then depend only on the magnitude of $\underline{Q}$ and $\underline{r}$ respectively and not on their directions. (This statement is equivalent to saying the points in reciprocal space and space real are distributed uniformly into shells of radius Q and r respectively). Hence the integral over spherical polar angular coordinates in (1.2.1) can be performed directly:

$$S(Q) = 1 + 4\pi\rho/Q \int_0^\infty rdr\ (g(r) - 1)\ \sin(Qr) \qquad (1.2.2)$$

Although this is now a one-dimensional integral, it is important to bear in mind that the diffraction experiment probes S(Q) in three dimensions.

For a multicomponent system there is a term like (1.2.1) or (1.2.2) for each distinct pair of atomic types, α,β; all the partial structure factors, $S_{\alpha\beta}(Q)$, are summed together in the TOTAL STRUCTURE FACTOR with weights proportional to the product of the scattering lengths for each atomic type:

$$F(Q) = \sum_{\alpha} c_\alpha \overline{b_\alpha^2} + \sum_{\alpha,\beta} c_\alpha \overline{b_\alpha} c_\beta \overline{b_\beta} \, (S_{\alpha\beta}(Q)-1) \qquad (1.2.3)$$

where c_α is the atomic fraction, b_α is the scattering length, of element α, and the bars indicate averages over the spin and isotope states of each element, assuming of course these are not correlated with position. The first term in (1.2.3) is called the "SELF" or "SINGLE ATOM" scattering, while the second is called the "INTERFERENCE" or "DISTINCT" scattering, because it contains the basic structural information on atomic positions.

The quantity measured in a neutron diffraction experiment is strictly NOT the structure factor, but the DIFFERENTIAL CROSS-SECTION, which is defined as

$$\frac{d\sigma}{d\Omega}(\lambda,2\theta) = \frac{\left(\begin{array}{l}\text{Number of neutrons scattered per unit time}\\ \text{into the small solid angle } d\Omega \text{ at angle } 2\theta\end{array}\right)}{N\,\Phi(\lambda)\,d\Omega} \qquad (1.2.4)$$

where N is the number of atoms (or scattering units if such a definition is more convenient) in the sample, and $\Phi(\lambda)$ is the incident neutron flux at wavelength λ. As for the structure factor the differential cross-section can be split into "self" and "distinct" terms:

$$\frac{d\sigma}{d\Omega} = \frac{d\sigma}{d\Omega_S} + \frac{d\sigma}{d\Omega_D} \qquad (1.2.5)$$

In the absence of any corrections for attenuation, multiple scattering

and inelasticity effects the differential cross section is equal to the total structure factor, F(Q). This known as the STATIC APPROXIMATION. In particular the self and distinct parts are defined as

$$\frac{d\sigma}{d\Omega_S} = \sum_\alpha c_\alpha \overline{b_\alpha^2}$$

and

$$\frac{d\sigma}{d\Omega_D} = \sum_{\alpha,\beta} c_\alpha \overline{b_\alpha} c_\beta \overline{b_\beta} \, (S_{\alpha\beta}(Q)-1) \qquad (1.2.6)$$

In neutron scattering the nucleus recoils under neutron impact and so the neutron can exchange energy with the scattering system (an "INELASTIC" collision. Hence even with diffraction experiments dynamic effects almost invariably have to be considered. These are described by the van Hove dynamic structure factor, $S(Q,\omega)$, [3], with separate terms for self and interference scattering as before. The single atom term for atom α will be represented here by $S_\alpha(Q,\omega)$, and the interference term between α and β by $S_{\alpha\beta}(Q,\omega)$. In terms of these quantities the so-called "STATIC STRUCTURE FACTORS" are defined by

$$S_\alpha(Q) = \int_{-\infty \text{ const.}Q}^{\infty} S_\alpha(Q,\omega)\, d\omega = 1.$$

$$S_{\alpha\beta}(Q)-1 = \int_{-\infty \text{ const.}Q}^{\infty} S_{\alpha\beta}(Q,\omega)\, d\omega \qquad (1.2.7)$$

where the integrals are taken along a path of constant Q. It will be readily apparent that the diffraction experiment ideally should integrate $S(Q,\omega)$ over all energy transfers and so obtain an ensemble averaged "snap shot" view (t=0) of the material. It is quite different from the ELASTIC diffraction experiment which probes only S(Q,0) and so determines the residual structure after waiting a long time ($t=\infty$).

In terms of these partial dynamic structure factors the total dynamic structure factor for a material is defined in the same way as (1.2.3):

$$F(Q,\omega) = \sum_{\alpha} c_\alpha \overline{b_\alpha^2}\, S_\alpha(Q,\omega) + \sum_{\alpha,\beta} c_\alpha \overline{b}_\alpha c_\beta \overline{b}_\beta\, S_{\alpha\beta}(Q,\omega) \qquad (1.2.8)$$

The inelasticity associated with the scattering causes a particular effect in that neutrons can arrive either earlier or later than they would have done if the scattering were elastic (no exchange of energy). If k and k′ are the neutron wavevectors before and after the scattering then the TIME-OF-FLIGHT EQUATION states that

$$\frac{L}{k} + \frac{L'}{k'} = \frac{L + L'}{k_e} \qquad (1.2.9)$$

where L is the incident flight path, moderator to sample, L′ is the flight path sample to detector, and k_e is the elastic wavevector for a particular time channel. The TOF equation combines with the usual kinematic equations for the neutron:

$$Q^2 = k^2 + k'^2 - 2kk' \cos 2\theta \qquad (1.2.10)$$

and

$$2m\hbar\omega = \hbar^2 k^2 - \hbar^2 k'^2, \qquad (1.2.11)$$

to define the path through (Q,ω) space over which $F(Q,\omega)$ is integrated. Hence instead of measuring (1.2.3) for the sample directly, as we would ideally like to do, the TIME-OF-FLIGHT DIFFERENTIAL CROSS SECTION, TDCS, is obtained in practice:

$$\Sigma(Q_e,\theta) = \int \frac{k'}{k} F(Q,\omega) \frac{\Phi(k)}{\Phi(k_e)} \left(\frac{\partial k}{\partial k_e}\right)_\omega \frac{E(k')}{E(k_e)}\, d\omega \qquad (1.2.12)$$

where $\Phi(k)$ is the incident spectrum expressed as a function of k, as described in section 1.1, $E(k')$ is the detector efficiency at the final

final wave vector, k_e is the wavevector for elastic scattering, and $Q_e = 2k_e\sin\theta$. The dependence of Σ on θ as well as Q is shown to emphasize that for a given Q value the TDCS is still a function of scattering angle. The partial derivative can be evaluated using 1.2.11 in 1.2.9:

$$\left(\frac{\partial k}{\partial k_e}\right)_\omega = \frac{(1 + R)k^2/k_e^2}{1 + Rk^3/k'^3} \qquad (1.2.13)$$

where $R = L'/L$. Egelstaff [4] calls this a "sampling factor" because it controls the way $F(Q,\omega)$ is sampled.

Note that the TDCS is to be distinguished from the differential cross section (1.2.4) by virtue of the finite final flight path: if R were to go to zero then the TDCS is identical to the differential cross sention. The denominators in equation (1.2.12) imply that the measured data have been normalized to the incident beam and detector efficiencies at the elastic energy. This is achieved in practice by dividing the TOF data by the scattering from a standard sample, usually vanadium, which scatters almost entirely incoherently. Even so some spectrum dependence is found in the TDCS because of the inelastic scattering of some detected neutrons.

Strictly speaking the integral in (1.2.12) implies we cannot do the experiment because we don't know $F(Q,\omega)$, and even if we measured it we could never obtain it over wide enough ω range to perform the integrals in (1.2.4) accurately. However, as has been shown by Placzek [5] and many others since then [e.g.4,6-13], the difference between F(Q) and $\Sigma(Q,\theta)$ is small enough in many cases that we can estimate the difference

$$P(Q,\theta) = F(Q) - \Sigma(Q,\theta) \qquad (1.2.14)$$

by using an approximate model for $F(Q,\omega)$. For example such a model might satisfy the first two moments of the true $F(Q,\omega)$, which are often known. $P(Q,\theta)$ is called the PLACZEK or INELASTICITY CORRECTION, and note that it too is a function of both Q and θ.

There is a different Placzek correction for each term in (1.2.3), so we label the single atom Placzek correction as $P_\alpha(Q,\theta)$ and the interference correction as $P_{\alpha\beta}(Q,\theta)$. Each Placzek correction has to be evaluated by an integral like (1.2.12), but with $F(Q,\omega)$ replaced by the appropriate partial dynamic structure factor. There are several approximate ways of doing this, either by putting in a model for $S(Q,\omega)$, or else by a Taylor expansion about the static values. With the exception of simple molecules it is normally not possible to evaluate the interference Placzek correction, which however is expected to be small (see section 2.10 for further details).

With these definitions we can rewrite (1.2.12) in a form similar to (1.2.3):

$$\Sigma(Q,\theta) = \sum_\alpha c_\alpha \overline{b_\alpha^2}[1+P_\alpha(Q,\theta)] + \sum_{\alpha,\beta} c_\alpha \overline{b_\alpha} c_\beta \overline{b_\beta} [S_{\alpha\beta}(Q)-1+P_{\alpha\beta}(Q,\omega)] \qquad (1.2.15)$$

The basic steps in data analysis should now be apparent:

(1) derive $\Sigma(Q,\theta)$ from a set of diffraction data;

(2) estimate and subtract the single atom scattering, i.e. the first term in (1.2.15);

(3) derive g(r) after removing any interference Placzek corrections.

The bulk of this manual is concerned with the first of these steps, although we will also suggest ways of tackling the other two stages.

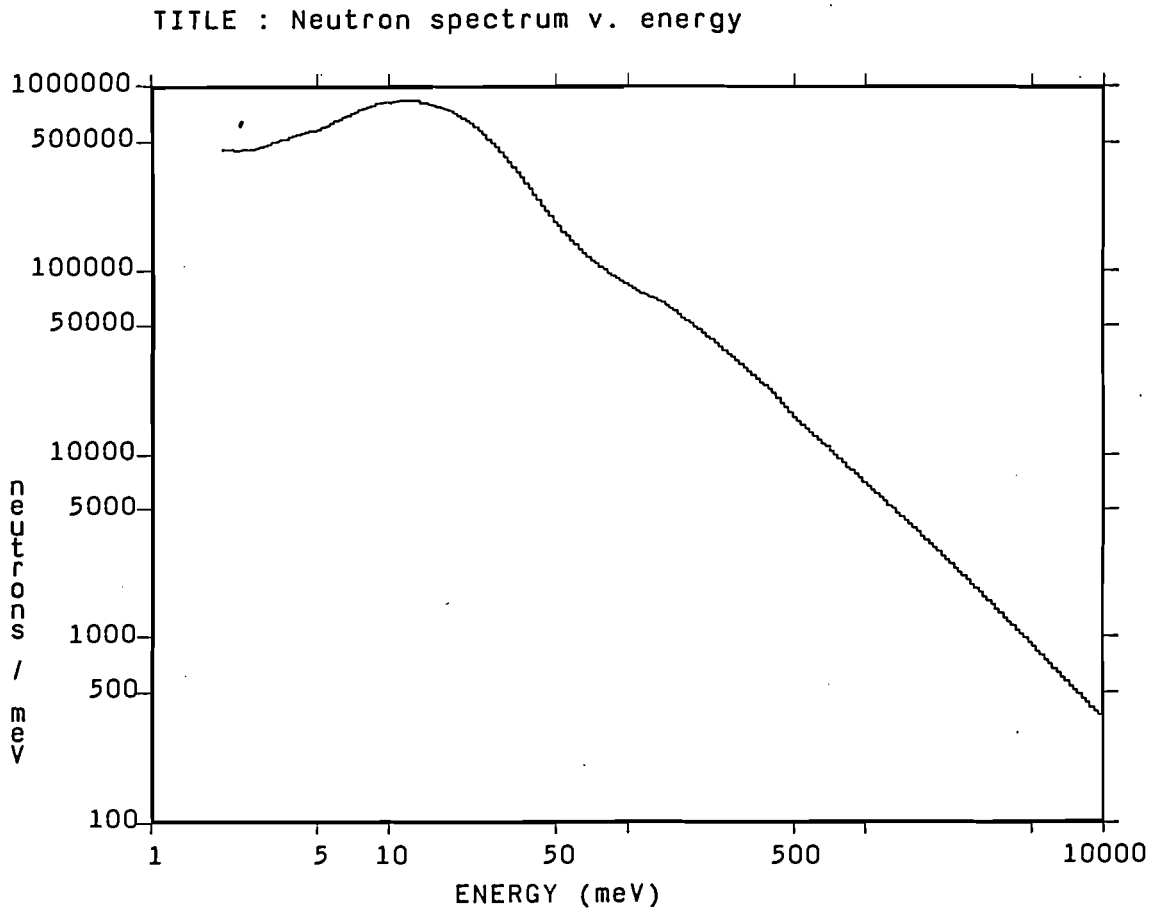

Figure 1.1 Time-of-Flight neutron spectrum as a function of energy. Note the log scales used in the graph

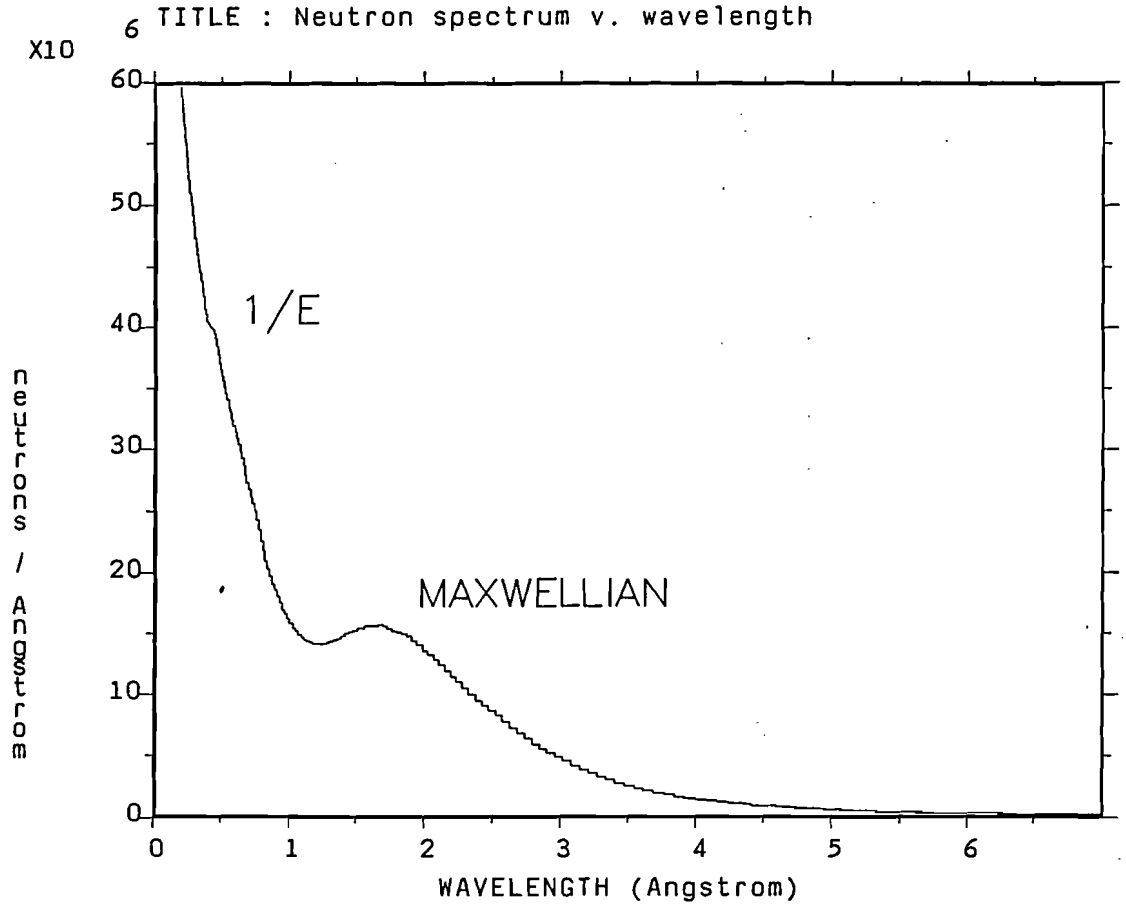

Figure 1.2 Time-of-Flight spectrum as a function of neutron wavelength

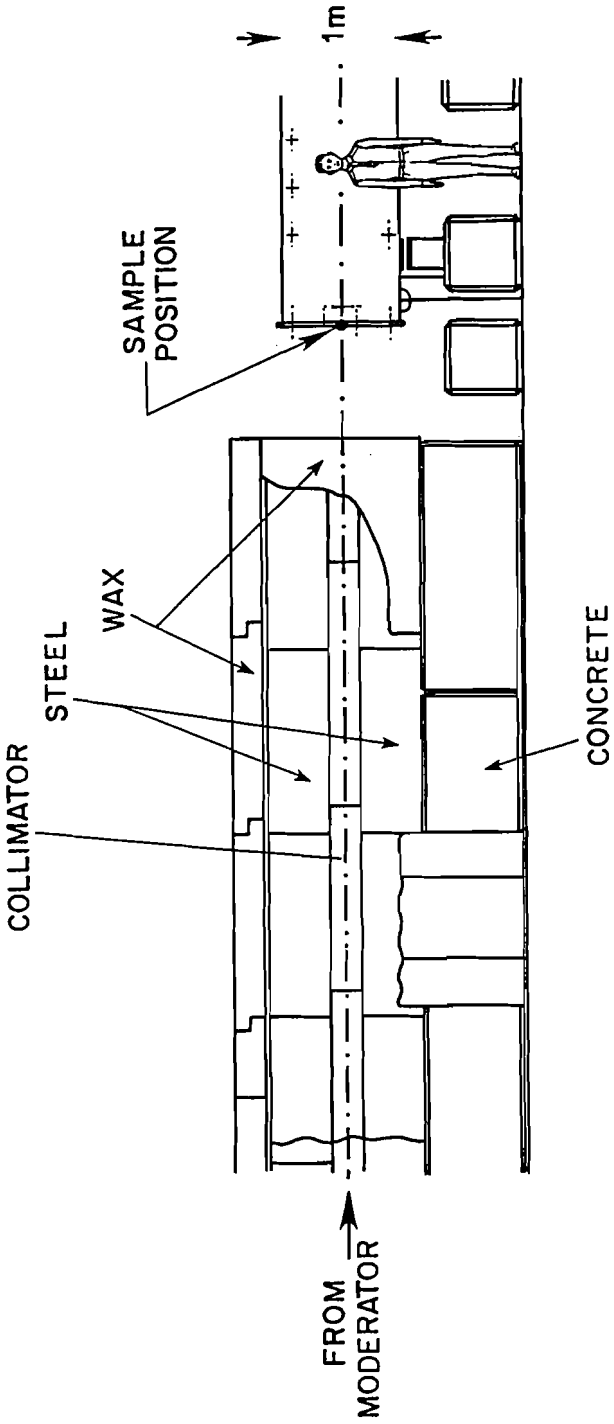

Figure 1.3 Diagram of the prototype SANDALS collimator illustrating the bulkiness of neutron shielding at ISIS.

SECTION 2

STEPS IN DATA ANALYSIS OF TOF DIFFRACTION DATA

2.1 INTRODUCTION

The initial goal of the experimenter is to obtain the TDCS of his or her sample. The success of subsequent analysis to g(r) or partial structure factors depends critically on obtaining the TDCS accurately. A number of corrections are required to the measured data: these are straightforward to apply but nonetheless easy to get wrong. Four main sources of error can be identified:

(i) the experimenter doesn't have complete information about his or her sample, e.g. dimensions, densities, cross sections, etc.;

(ii) incorrect data analysis procedures are used;

(iii) the detectors are not sufficiently stable;

(iv) sample environment equipment introduces unexpected backgrounds and sample positioning errors.

The last two causes require action by the instrument scientists, but there is little or nothing that can correct for poorly characterised samples or incorrect data analysis procedures.

Occasionally on LAD we have achieved absolute accuracies of 1%, accuracy being measured by the difference between the measured high Q limit of the TDCS and the expected high Q limit. With care this accuracy could be achieved routinely. However at present we typically obtain accuracies on the order of 5%, and in the majority of cases the reason for this is either because the sample is poorly characterised or because the data analysis is inadequate.

With the exceptions of sections 2.9 and 2.11, which concern the estimation of inelasticity corrections and transforming the final result to g(r), we believe the methods of analysis of diffraction data from liquids and amorphous samples are well understood and routine. In the sections which follow we have attempted to describe the correct sequence of steps.

As seen in section 1.1, the scattered intensity is measured as a function of time-of-flight which in turn is proportional to wavelength. The data can also be presented as a function of wave vector, k, wave vector transfer, Q, or energy, E, by using the relationships (1.1.5) to apply the appropriate rescaling. The choice is subject to the preference of the experimenter, although the Q representation is the most common as it relates to the reciprocal space in which the structure factor is defined, equation (1.2.1). Therefore we shall use the Q representation here. Thus if the sample is very small so that the effects of attenuation and multiple scattering are negligible, the detected count rate would be proportional to the incident flux, $\Phi(k_e)$ the TDCS of the sample, $\Sigma(Q_e)$, the detector solid angle, $\Delta\Omega$, and the detector efficiency, $E_d(k_e)$:

$$I(k_e) = \Phi(k_e)\, N\, \Sigma(Q_e)\, E_d(k_e)\, \Delta\Omega \qquad (2.1.1)$$

where N is the number of scattering units in the neutron beam, and $Q_e = 2k_e\sin\theta$. The incident flux and detector efficiency are represented here as a function of k_e to emphasize that they are not a function of the scattering angle of the detector.

Equation (2.1.1) is an idealized count rate: the first correction that must be applied is for detector deadtime.

2.2 DEADTIME CORRECTIONS

No matter how well made a detector is always "dead" for a short while after a neutron event has occurred. For a ^{3}He tube this DEADTIME might be 3μs, whilst for a glass scintillator it is perhaps 250ns, before another event can be recorded. The zinc sulphide detectors will have a deadtime of betweeen 2 and 10 μs, depending on how they are set up. Normally the correction for deadtime is a few percent and so can be made by a simple formula. Suppose τ is the deadtime in μs for a detector. First consider the case where the time channel is broad compared to the deadtime. If R_m is the measured count rate in the time

channel (in cts/μS), then the detector is dead for a time

$$D = \Delta R_m \tau \qquad (2.2.1)$$

where Δ is the width of the time channel in μS. Hence the count rate, R, which would have been measured if the detector had zero deadtime, is greater than R_m in proportion to the time that the detector is dead:

$$R = \frac{\Delta}{(\Delta - D)} R_m = \frac{R_m}{(1 - R_m \tau)} \qquad (2.2.2)$$

At the other extreme if the time channels are narrower than the deadtime, then some of the previous time channels may contribute to the deadtime in a particular channel. For example if channels n to m contribute to the deadtime in channel m, then the length of time channel m is dead is given by

$$D_m = \tau \sum_{j=n,m} \Delta_j R_j \qquad (2.2.3)$$

where Δ_j and R_j are the channel width and count rate in channel j respectively. The limits of j are determined by inspection. This correction is used in the same way as before, with D_m in place of D in (2.2.2).

A subtlety occurs in practice that renders the correction more complicated. When many detectors exist it is not practical to have a separate input for each detector into the DAE. Instead an ENCODER is used to create a binary address which describes which detector fired. If the deadtime of the encoder is longer than that of the detector, then it is the encoder's deadtime which determines the detector deadtime. Moreover since the encoder can process only one event at a time, <u>all</u> the detectors that feed into that encoder are effectively dead when any one detector fires. Therefore in this situation the sum in (2.2.3) should include a sum over all channels which feed into a decoder. In that case if $R_{j,k}$ is the count rate in time channel j and encoder channel k, then the detector deadtime is given by

$$D_m = \tau \sum_{j=n,m} \sum_{k} \Delta_j R_{j,k} \qquad (2.2.4)$$

and the sum over k is over all detector channels that feed into the encoder. In the situation when (2.2.4) applies Δ_j is the encoder's deadtime, NOT the detector's. Hence even though the deadtime for an individual detector may be small, the grouping of say 50 detectors into an encoder results in a 50-fold enhancement in the count rate as far as deadtime is concerned. So the deadtime correction could be much larger than might be apparent from the count rate in an individual detector.

2.3 NORMALIZING TO THE INCIDENT BEAM MONITOR

Having corrected $I(Q_e)$ for deadtime, the next stage is to divide out the incident spectrum, which is measured by means of a MONITOR detector placed in the incident beam before the sample. The spectrum is divided out at this stage because small variations in moderator temperature and proton beam steering can modify the energy dependence of the spectrum from time to time at the 1-2% level. Since the calibration run must be performed before or after the sample run, it will only give a reliable result if the dependence on the incident spectrum is removed at the end of each run. The count rate in the monitor detector, which of course must also be corrected for deadtime, is proportional only to the incident spectrum and the monitor efficiency:

$$I_m(k_e) = \Phi(k_e)\, E_m(k_e) \qquad (2.3.1).$$

Thus when used to normalize the scattered neutron count rate, a NORMALIZED count rate is obtained:

$$NRM(Q_e) = I(k_e)/I_m(k_e) = N\, \Sigma(Q_e)\, \frac{E_d(k_e)}{E_m(k_e)}\, \Delta\Omega \qquad (2.3.2).$$

A second measurement which is made at the same time as the scattered count rate from the sample is the fraction of neutrons transmitted by the sample. This number is monitored by a TRANSMISSION MONITOR, with efficiency $E_t(k_e)$, placed after the sample. Again this fraction cannot be measured directly, but must be determined by ratioing different runs, e.g. with and without sample. If $I_t(k_e)$ is the count rate in the transmission monitor, then this count rate is proportional to the incident flux, the transmission monitor efficiency and the TRANSMISSION of the sample, $T(k_e)$, which will be defined in the next section and is dependent on the total neutron cross section of the sample. Hence when normalized to the incident monitor, the transmitted intensity is given by

$$MON(k_e) = I_t(k_e)/I_m(k_e) = T(k_e) \frac{E_t(k_e)}{E_m(k_e)} \qquad (2.3.3).$$

The transmission monitor is used to provide information on the neutron cross section and density of the sample: it can often confirm that the sample is what it is supposed to be.

There will then be a set of NRM files for every detector or detector group, and a MON file, for every run, whether it be sample, container, vanadium (calibration) or background. The stages covered by sections 2.2 and 2.3 are obtained by running the NORM program of section 3.6

2.4 MEASURING THE NEUTRON CROSS SECTION

a) The Total Neutron Cross Section

Neutron cross sections arise from two primary processes: scattering and capture. Provided there are no nuclear resonances in the energy region of interest, the probability for capture is inversely proportional to neutron velocity, i.e. proportional to neutron wavelength, and the constant of proportionality, usually defined for 2200m/s neutrons (λ = 1.8Å), is called the CAPTURE CROSS SECTION, σ_a.

There is a value of σ_a for every nucleus, although in many cases it is quite small or zero.

The SCATTERING CROSS SECTION, $\sigma_s(\lambda)$, on the other hand has no such simple dependence on energy or wavelength, because it represents the integral of the DIFFERENTIAL SCATTERING CROSS SECTION, $d\sigma/d\Omega$ at a particular wavelength over all scattering angles:

$$\sigma_s(\lambda) = \int \frac{d\sigma}{d\Omega}(\lambda)\, d\Omega = 4\pi \int \frac{d\sigma}{d\Omega}(\lambda) \sin 2\theta\, d\theta \qquad (2.4.1)$$

As an example of the application of this result we will assume the static approximation applies and that the liquid under inverstigation is a hard sphere fluid of reduced density $\rho\sigma^3 = 0.5$, where σ, the hard core diameter, is 3.142Å. In that case S(Q) is known exactly in the Percus-Yevick approximation, and so (2.4.1) can be integrated numerically for all wavelengths, using

$$\frac{d\sigma}{d\Omega}(\lambda) = b^2\, S(Q) = b^2\, S(\frac{4\pi\sin\theta}{\lambda}) \qquad (2.4.2)$$

where b is the bound scattering length of the fictitious nucleus. The result is shown in figure 2.1: it will be seen that the scattering cross section for a material with structure will certainly deviate from the bound value. In particular the scattering cross section will display a similar structure to that seen in the differential scattering cross section.

For light atoms such as hydrogen and deuterium the consequences are quite drastic: the differential cross section falls dramatically with scattering angle at all but the longest neutron wavelengths, and the shape of the fall, which depends on the details of $S(Q,\omega)$, also varies with energy. Thus at low energies the neutron can excite only diffusional type motions, while at high energies the neutron can excite all possible modes, including dissociation of molecules if present. Thus the scattering cross section must vary between its so-called "BOUND" and "FREE" values as we go from low energy to high. The "bound"

values are those quoted in tables of neutron scattering lengths such as the compilation by Koester et. al. [14] or Sears [15] and correspond to the case of an immovable nucleus: they are essentially nuclear parameters. The corresponding "free" values at high energies can be computed by multiplying the "bound" cross sections by the ratio

$$\left(\frac{A}{A+1}\right)^2$$

where A is the mass of the nucleus in question. This has the value 0.25 for hydrogen and 0.44 for deuterium, which tells us to expect a large fall in the scattering cross section of these materials with increasing energy. Such a fall is readily visible in the transmission data from hydrogen containing samples. For heavy atoms on the other hand this factor is close to unity and so within the likely accuracy of the transmission measurement is not significant.

In practice it is not possible to ever obtain the true bound cross section for a liquid containing light atoms since the low energy cross section is intimately related to the details of $S(Q,\omega)$ at small Q and ω. However the free cross section should appear as the asymptotic limit as $\lambda \Rightarrow 0$, since then all neutron capture processes have gone to zero.

Figure 2.1 also shows a second quantity, the TOTAL NEUTRON CROSS SECTION, $\sigma_t(\lambda)$, where

$$\sigma_t(\lambda) = \sigma_s(\lambda) + \sigma_a(\lambda) \qquad (2.4.3)$$

In this case it has been assumed that the fictitious material has a capture cross section $\sigma_a = 0.4$ at λ=1.8Å. It can be seen that the approximation of treating the total cross section as a sum of a constant plus linear term in λ will be inadequate for accurate work at long wavelengths.

If nuclear resonances are present in the total cross section then the above treatment must be modified. A nuclear resonance occurs when the neutron excites the nucleus to an excited state, and so is

(slightly) analogous to an absorption edge in X-ray scattering. However the possible nuclear states are quite complicated in general and can be accompanied by several processes, including the emission of a γ photon. Usually both scattering and capture are not simple at a resonance, and full treatment of the effects of this on the data analysis are beyond the present purpose, and certainly are not included in any of the correction routines. At present the only recourse is to ignore the energy regions where resonances occur and hope that there is sufficient angular coverage that all Q values can be obtained away from a resonance. Figure 2.2 shows the measured total cross section for a solution of ^{148}Sm-perchlorate in D_2O. Note the strong resonance at $\lambda \simeq$ 1Å, corresponding to a nuclear resonance in a ^{149}Sm impurity. This resonance was so broad that analysis of these data to TDCS was impossible. Appendix E lists the more commonly occurring resonances.

b) Measuring the Neutron Cross Section

We have seen above that the total cross section depends on the STRUCTURE and DYNAMICS of the sample, which in turn relates to the thermodynamic state of the sample. Therefore it strictly has to be measured for each and every sample, and this is why a transmission monitor is placed after the sample. In practice it is difficult to measure the total cross section on an ABSOLUTE scale with the necessary precision, so the transmission monitor is used to obtain the ENERGY DEPENDENCE of the total cross section, with absolute values obtained by reference to the known free and bound values at short and long wavelengths. Note that using a separate experiment to measure transmissions is very time consuming and not necessarily useful since it is not always possible to reproduce the exact conditions of the experiment at a later time.

If the sample is a flat plate which uniformly covers the beam then the TRANSMISSION of the sample is given simply by

$$T(k_e) = \exp\{-\rho\sigma_t(\lambda)L\} \qquad (2.4.4)$$

where ρ is the number density and L is the neutron flight path within the sample. Hence if $T(k_e)$ can be obtained from monitor ratios as described in section 2.3 then it is a trivial inversion to obtain σ_t.

For any other shape of sample however the flight path through the sample is a function of position within the beam. Figure 2.3 shows the geometry of the problem in this case. If x measures the perpendicular distance from one edge of the beam then L becomes a function of x and the transmission in this case can be written as

$$T(k_e) = \int_0^W \exp\{-\rho\sigma_t(\lambda)L(x)\}\, dx \,/\, W \qquad (2.4.5)$$

where W is the width of the beam. In this case there is no simple inversion to σ_t, which has to be obtained by trial and error. However if a Newton-Raphson technique is used to do this convergence to a solution is quite rapid. Further efficiency can be gained by noting that only a finite number of terms in the exponential are needed. Writing $\mu = \rho\sigma_t$, we see that

$$T(k_e) = 1 - \mu M_1 + (\mu M_2)^2 - (\mu M_3)^3 + \ldots \qquad (2.4.6)$$

where

$$M_n = \frac{1}{n!}\int_0^W L^n(x)\, dx \,/\, W \qquad (2.4.7)$$

The latter integrals are dependent only on the shape of the sample and not on neutron energy and so need only be evaluated once.

If the sample is contained in a holder then the monitor ratio that is used is the ratio of sample plus can to can alone. In that case the measured transmission is given by

$$T(k_e) = \frac{\int_0^W \exp\{-[\mu_S L_S(x)+\mu_C L_C(x)]\}\, dx}{\int_0^W \exp\{-\mu_C L_C(x)\}\, dx} \qquad (2.4.8)$$

where the capital suffix S applies to the sample and C applies to the container. Similar expansions of the top exponential term can be used as before. However the values of μ_C must be supplied separately or obtained in a separate transmission experiment on the container alone. Finally note that if the beam profile is not uniform a simple modification of the above formulae is needed: because the profile function can be included in the moments (2.4.7) it does not lead to any increase in computing time.

2.5 ATTENUATION AND MULTIPLE SCATTERING CORRECTIONS

Much of the underlying methodology for calculating ATTENUATION and MULTIPLE SCATTERING corrections has been covered in numerous previous publications and so will not be repeated here. Although there are a number of approaches to the calculation, the formalism of Soper and Egelstaff [16], which uses numerical integrations to estimate corrections for the cylindrical geometry, is used here, because it is written in a sufficiently general form to allow corrections for furnaces and radiation shields if they are sufficiently absorbing or scattering to require a separate correction. These latter corrections will be the subject of the next section.

The most common case is that of a sample contained in a holder. In that case two measurements are needed: one for the sample plus can, $I_{SC}(k_e)$, and one for the can alone, $I_C(k_e)$. These two quantities are each affected by attenuation and multiple scattering so our simple definition (2.1.1) has to be modified for the general case:

$$I_{SC}(k_e) = \Phi(k_e)[N_S\Sigma_S(Q_e)A_{S,SC} + N_C\Sigma_C(Q_e)A_{C,SC} + M_{SC}(k_e)] \times E_d(k_e)\,\Delta\Omega \qquad (2.5.1)$$

$$I_C(k_e) = \Phi(k_e)[N_C\Sigma_C(Q_e)A_{C,C} + M_C(k_e)]\ E_d(k_e)\ \Delta\Omega \qquad (2.5.2)$$

Here N_S and N_C are the number of atoms in the sample and container respectively, while $A_{S,SC}$, $A_{C,SC}$ and $A_{C,C}$ are the usual Paalman and Pings [17] attenuation factors. For example $A_{S,SC}$ is the attenuation factor for scattering in the sample and attenuation in the sample plus container. The quantities M_{SC} and M_C are the total multiple scattering differential scattering cross sections for sample plus can and can alone respectively. Note that the multiple scattering terms cannot in general be included in first scattering terms because they are not linear in N_S and N_C. Both attenuation and multiple scattering terms are functions of neutron energy by virtue of the energy dependence of the scattering and capture cross sections.

The attenuation factors depend only on the sample geometry and the total neutron cross section and so can be evaluated exactly in the static approximation, within the limits of numerical precision.

On the other hand the multiple scattering terms can never be evaluated very accurately since in principle they require detailed knowledge of the sample's structure (and dynamics if the inelastic scattering is significant). The method of calculation normally employed makes use of the measured total transmission cross section to give the scattering cross section at each neutron energy, but then assumes the scattering at this energy to be isotropic with scattering angle. This is called the ISOTROPIC approximation. (This is NOT the same as assuming that the multiple scattering is isotropic, an approximation introduced by Blech and Averbach [18] which is not needed in practice.) Sears [19] has described how the isotropic approximation can be improved although direct calculation with a Monte Carlo algorithm which includes the measured TDCS is probably the best way to cope with multiple scattering from thick samples. Given the speed of modern computers this is not an unreasonable approach. Howells has a program, ELMS, (Elastic Multiple Scattering) which does this and it can be made available if there is sufficient demand.

There is a general consensus that the isotropic approximation is expected to be acceptable if the sample scatters less than ~20% of the incident beam, although there has never been a quantitative study of the size of sample at which this approximation starts to introduce a serious systematic error in the measured structure factor. Clearly it greatly assists the multiple scattering problem if the container can be made of an incoherent scatterer, such as vanadium or zirconium-titanium, or of an amorphous material, such as silica, since Bragg peaks introduce a severe difficulty to any quantitiative multiple scattering calculation.

In summary, to be confident that multiple scattering will not introduce too large a systematic error it is a useful rule of thumb to ensure that the sample scatters between 10% and 20% of the incident neutron beam.

2.6 FURNACE CORRECTIONS

If the sample and container are in a furnace and the furnace element contributes significantly to the attenuation and scattering processes then three measurements are needed: sample plus can plus furnace, $I_{SCF}(k_e)$, empty can plus furnace, $I_{CF}k_e)$, and furnace alone, $I_C(ke)$. These three quantities are related to the corresponding differential cross sections by:

$$I_{SCF}(k_e) = \Phi(k_e)[N_S\Sigma_S(Q_e)A_{S,SCF} + N_C\Sigma_C(Q_e)A_{C,SCF} + N_F\Sigma_F(Q_e)A_{F,SCF} + M_{SCF}(k_e)]\ E_d(k_e)\ \Delta\Omega \qquad (2.6.1)$$

$$I_{CF}(k_e) = \Phi(k_e)[N_C\Sigma_C(Q_e)A_{C,CF} + N_F\Sigma_F(Q_e)A_{F,CF} + M_{CF}(k_e)] \times E_d(k_e)\ \Delta\Omega \qquad (2.6.2)$$

$$I_F(k_e) = \Phi(k_e)[N_F\Sigma_F(Q_e)A_{F,F} + M_F(k_e)]\ E_d(k_e)\ \Delta\Omega \qquad (2.6.3)$$

The attenuation factors have the same definition as before, e.g. $A_{S,SCF}$ is the attenuation factor for scattering in the sample and attenuation in the sample, can and furnace. Similarly the multiple scattering cross sections have an equivalent definition as before. N_F is the number of furnace atoms in the incident beam.

2.7 VANADIUM OR STANDARD SAMPLE CALIBRATION

A unique characteristic of neutron scattering is the ability to perform an independent estimate of the instrumental calibration. This calibration consists of the unknown quantities, either

$$F_1(ke) = \Phi(k_e)\, E_d(k_e)\, \Delta\Omega \qquad (2.7.1)$$

in sections 2.1, 2.5 and 2.6 above, or

$$F_2(k_e) = \frac{E_d(k_e)}{E_m(k_e)}\, \Delta\Omega \qquad (2.7.2)$$

in section 2.3. With these definitions we can for example rewrite equations (2.5.1) and (2.5.2) which become, after normalizing to the monitor:

$$NRM_{SC}(Q_e) = F_2(k_e)[N_S\Sigma_S(Q_e)A_{S,SC} + N_C\Sigma_C(Q_e)A_{C,SC} + M_{SC}(k_e)] \qquad (2.7.3)$$

$$NRM_C(Q_e) = F_2(k_e)[N_C\Sigma_C(Q_e)A_{C,C} + M_C(k_e)] \qquad (2.7.4)$$

Estimation of these calibration constants is usually achieved with a standard vanadium sample because vanadium has a largely incoherent cross section and so it is believed that the differential cross section for vanadium can be estimated reasonably accurately, an assumption which of course is difficult to check! As described in section 2.9 the inelasticity correction has two principal terms, one relating to

scattering angle, the other proportional to temperature and inversely proportional to neutron energy, and since energy is being varied in a TOF experiment it is crucial to estimate this latter term correctly. Figure 2.4 shows the estimated single atom differential cross section at 20° scattering angle for a free vanadium nucleus at two temperatures. At the time of writing experiments are planned on LAD to determine if the estimated temperature dependence is indeed observed.

The normalized spectrum from vanadium is defined by

$$NRM_V(Q_e) = F_2(k_e)[N_V\Sigma_V(Q_e)A_{V,V} + M_V(k_e)] \qquad (2.7.5)$$

The quantity in square ([...]) brackets is the vanadium differential cross section which is estimated using exactly the same methods as in the previous section. This leads to a VANADIUM CALIBRATION, $CAL_V(Q_e)$, where

$$CAL_V(Q_e) = NRM_V(Q_e)/[N_V\Sigma_V(Q_e)A_{V,V} + M_V(k_e)] = F_2(k_e). \qquad (2.7.6)$$

In fact scattering from vanadium exhibits the usual statistical noise plus weak Bragg reflections due to the small coherent scattering amplitude. Since the data from the sample must be divided by CAL_V it is obviously undesirable to transfer either effect to the sample data, so an expansion in terms of Chebyshev polynomials is fitted to NRM_V with zero weighting of points in the region of Bragg peaks. This has the effect of smoothing out the Bragg peaks and noise without introducing any appreciable artifacts. However it is clearly important to check that this smoothing has in fact removed only the noise from NRM_V and none of the underlying structure. In any case whether to smooth or not is an option which can be overridden if needed. The computer programs associated with this section are described in section 3.9.

2.8 BASIC ALGORITHM TO DETERMINE DIFFERENTIAL CROSS SECTION

All of the main quantities needed to calculate the differential cross section (DCS) from the TOF diffraction data of the sample have now been described, and the algorithm ANALYSE (see section 3.10) is used to perform this operation. The stages are described in sequence for the case of a sample held in a can. Note that the arrow ⇒ is used to indicate that the result of an operation on the left hand side is placed in the quantity on the right. The symbol TOTAL applies to the total scattering, SINGLE applies to single scattering, and the suffixes S, C and B refer to sample, can and background.

1) Subtract background

$$TOTAL_{SC}(Q_e) = NRM_{SC}(Q_e) - NRM_B(Q_e)$$

$$TOTAL_C(Q_e) = NRM_C(Q_e) - NRM_B(Q_e)$$

2) Normalize to calibration

$$TOTAL_{SC}(Q_e) \Rightarrow TOTAL_{SC}(Q_e)/CAL_V(Q_e)$$

$$TOTAL_C(Q_e) \Rightarrow TOTAL_C(Q_e)/CAL_V(Q_e)$$

3) Subtract multiple scattering

$$SINGLE_{SC}(Q_e) = TOTAL_{SC}(Q_e) - M_{SC}(k_e)$$

$$SINGLE_C(Q_e) = TOTAL_C(Q_e) - M_C(k_e)$$

4) Apply absorption corrections

$$SINGLE_S(Q_e) = \frac{\left(SINGLE_{SC}(Q_e) - SINGLE_C(Q_e) \frac{A_{C,SC}}{A_{C,C}} \right)}{A_{S,SC}}$$

5) Divide by number of atoms in sample

$$DCS(Q_e) = \frac{SINGLE_S(Q_e)}{N_S}$$

If the furnace correction is being applied then the following modified sequence is used:-

1) Subtract background

$$TOTAL_{SCF}(Q_e) = NRM_{SCF}(Q_e) - NRM_B(Q_e)$$

$$TOTAL_{CF}(Q_e) = NRM_{CF}(Q_e) - NRM_B(Q_e)$$

$$TOTAL_F(Q_e) = NRM_F(Q_e) - NRM_B(Q_e)$$

2) Normalize to calibration

$$TOTAL_{SCF}(Q_e) \Rightarrow TOTAL_{SCF}(Q_e)/CAL_V(Q_e)$$

$$TOTAL_{CF}(Q_e) \Rightarrow TOTAL_{CF}(Q_e)/CAL_V(Q_e)$$

$$TOTAL_F(Q_e) \Rightarrow TOTAL_F(Q_e)/CAL_V(Q_e)$$

3) Subtract multiple scattering

$$SINGLE_{SCF}(Q_e) = TOTAL_{SCF}(Q_e) - M_{SCF}(k_e)$$

$$SINGLE_{CF}(Q_e) = TOTAL_{CF}(Q_e) - M_{SC}(k_e)$$

$$SINGLE_F(Q_e) = TOTAL_F(Q_e) - M_F(k_e)$$

4) Subtract furnace from sample and can

$$SINGLE_{SC}(Q_e) = \left[SINGLE_{SCF}(Q_e) - SINGLE_F(Q_e) \frac{A_{F,SCF}}{A_{F,F}} \right]$$

$$SINGLE_C(Qe_) = \left[SINGLE_{CF}(Q_e) - SINGLE_F(Q_e) \frac{A_{F,CF}}{A_{F,F}} \right]$$

5) Apply absorption corrections

$$SINGLE_S(Q_e) = \frac{\left[SINGLE_{SC}(Q_e) - SINGLE_C(Q_e) \frac{A_{C,SCF}}{A_{C,CF}} \right]}{A_{S,SCF}}$$

5) Divide by number of atoms in sample

$$DCS(Q_e) = \frac{SINGLE_S(Q_e)}{N_S}$$

2.9 INELASTICITY (PLACZEK) CORRECTIONS

Equations 1.2.9, 1.2.11 and 1.2.12 serve to define the inelasticity correction, $P(Q_e,\theta)$ in a TOF diffraction experiment: $P(Q_e,\theta)$ represents the difference between the static approximation $F(Q)$ and the TDCS, $\Sigma(Q_e)$. Strictly speaking to obtain $P(Q_e,\theta)$ one needs to know $F(Q,\omega)$ which preempts the need for a diffraction experiment since then the static structure factors (1.3.4) would be obtainable by direct integration of $F(Q,\omega)$. Obviously this is an impractical proposition, mostly because of the time that would be required in measuring the complete dynamic structure factor.

However in 1952 Placzek [5] showed that for nuclei much more massive than the neutron the correction adopts a form which is essentially independent of the detailed dynamics, and is related only to the nuclear mass, the sample temperature, the incident neutron energy, and the geometry and efficiency of the neutron detection process. Moreover at neutron energies well above those of any bound states that occur in the sample he showed that the correction to the interference term $S_{\alpha\beta}(Q)$ is zero to first order. These conclusions arose from the fact that the first two moments of $S(Q,\omega)$ can be estimated more or less exactly:

$$ {}^1S_\alpha(Q) = \int_{-\infty}^{\infty} \omega S_\alpha(Q,\omega)\, d\omega = \frac{\hbar Q^2}{2M_\alpha} \qquad (2.9.1) $$

$$ {}^2S_\alpha(Q) = \int_{-\infty}^{\infty} \omega^2 S_\alpha(Q,\omega)\, d\omega = \frac{k_B T \hbar Q^2}{M_\alpha} + \frac{\hbar^2 Q^4}{4M_\alpha^2} \qquad (2.9.2) $$

and

$$ {}^1S_{\alpha\beta}(Q) = \int_{-\infty}^{\infty} \omega\, S_{\alpha\beta}(Q,\omega)\, d\omega = 0 \qquad (2.9.3) $$

Here (2.9.1) and (2.9.3) are exact results, but (2.9.2) strictly only applies to a classical fluid.

Unfortunately Placzek's results cannot always be applied directly to thermal neutron diffraction because the conditions under which they apply are often not obtained. In particular the sampling factor (equation 1.2.10) rapidly drops to zero as k′ becomes less than k. Hence as in the fixed wavelength reactor experiment the scope for exciting high vibrational levels in a molecule depends on the incident energy. There is an extensive literature on the attempts to modify the original Placzek approach to include the cases where the system is only partly excited by the neutron. See for example the papers by Powles [6-11] and Egelstaff [4,12,13] and references therein. All of these involve lengthy algebra, and while there seems to be general agreement in the case of the self scattering for an atomic fluid the correct form of the terms for molecules, which involve a Q-depedent effective mass is still disputed. The advantage of the Placzek type of expansion is that in enables one to understand by inspection the effect of various instrument parameters on the inelasticity correction, in particular the flight path ratio, sample temperature, detector efficiency, and incident spectrum shape,.

As an example below is quoted the Egelstaff [4] formula for the self scattering inelasticity correction for an atomc fluid of nuclear mass M at temperature T, for a 1/E incident spectrum, at incident enrgy E_0:

$$P(Q_e,\theta) = -\frac{2ym}{M} X + \frac{m}{M}\frac{k_B T}{2E_0} Y \qquad (2.9.4)$$

where

$$X = \left[\frac{aA + a + 2}{a + 1}\right],$$

$$Y = \left[1 - 2y + \frac{4y(Aa+3)}{a+1} - \frac{2y\{a^2B - 6a(A+1) - 3(5a-1)\}}{(a+1)^2} \right]$$

and $y = \sin^2\theta$, m = mass of neutron, $a = 1/R = L/L'$, and A and B are detector constants:

$$A = 1 - \frac{\varepsilon}{k_e}\left[\frac{1}{E_{d(k_e)}} - 1\right]$$

$$B = A + \left(\frac{\varepsilon}{k_e}\right)^2\left[\frac{1}{E_{d(k_e)}} - 1\right]$$

with

$$E_d(k_e) = 1 - \exp(-\varepsilon/k_e)$$

and ε a detector constant which determines the efficiency. Further terms are needed in the Maxwellian region.

This formula gives the quantitative behaviour of the Placzek correction at large neutron energies, but also indicates qualitatively what will happen at all energies. In particular we see that the correction gets notably larger at low neutron energies, high temperatures, and small nuclear masses. Hence the often quoted maxim that the ideal diffraction experiment is performed at high energies and small scattering angles. The routine PLATOM described in Section 3.11 uses a modification of the Powles [10] formula derived by Howe, McGreevy and Howells [20]. Detailed comparison of this formula with the numerical methods described below shows some quantitative discrepencies which are not understood at the present time.

An alternative to the Placzek expansion is to define a model neutron scattering law $S(Q,\omega)$ which incorporates the properties defined in (2.9.1) and (2.9.2), or any alternative scattering laws which are know to represent $S(Q,\omega)$ correctly in the region of (Q,ω) space explored by experiment, and then perform the integral (1.2.9) numerically. This method is most useful when a particular scattering

law is known to apply, such as that for a diffusing particle or for a rigid molecular rotor, or when the nuclear mass is small: in all these cases the Placzek expansion is not helpful. Figure 2.5 shows a comparison between the numerical integration of the free particle $S(Q,\omega)$ (ideal gas formula) and equation (2.9.4) for a nucleus of mass 51 (vanadium) and scattering angle of 20°. Note that at this small angle the expansion formula gives good agreement with the numerical calculation: at larger angles such as 90° and 150° the agreement is much worse, although in every case the high Q limit is the same. Figure 2.6 shows the numerical calculation for a mass 2 particle at two tempertures. A pronounced temperature effect is seen. Moreover the correction now has a clear hump at $\sim 2\text{Å}^{-1}$ corresponding to the derivative of the incident spectrum. Results such as this can only be obtained by numerical integration.

Two computer programs exist to perform these numerical integrations: PLACID calculates the Placzek correction for an ideal gas, i.e. treating the particle as free. The other program is called PLATOF and it allows the user to input a table of $S(Q,\omega)$ values from a separate calculation. Both programs can be made available for general use if there is sufficient demand.

2.10 MERGING THE DATA TO FORM THE STRUCTURE FACTOR

Typically one will record the TDCS at several scattering angles in a TOF diffraction experiment. On LAD there are currently 14 groups of detectors, 7 on each side of the instrument. Which of these groups are to be combined requires a decision by the experimentalist. A typical approach might be as follows:

a) Correct each angle for inelasticity effects, particularly in the self scattering.

b) Plot all the spectra on top of each other

c) For each group choose a range of Q values over which this spectrum overlaps with at least one spectrum from a neighbouring group at higher or lower scattering angle, and ignore those spectra which clearly disagree with the others. Obviously this is a highly subjective point in the analysis, but if all has gone well with the experiment it should be fairly obvious where the overlaps occur. The object is to avoid combining different detector banks where there are clearly differences due to say not being able to perform the Placzek correction accurately, such as occurs with light atoms such as deuterium.

d) Merge the selected spectra over the selected Q range, using the MERGE command, see section 3.12 and below.

e) Finally perform any remaining normalizations as needed such as removing the incoherent scattering and dividing out the scattering cross section. The result should either be in the units of differential cross section (barns per steradian per atom/4π) or have dimensionless units as a structure factor, S(Q).

The merging of spectra is achieved by weighting each spectrum with the intensity with which it was measured. The weighting function is obtained from the corrected intensity data of the vanadium sample contained in the quantity

$$W_j(Q_e) = CAL_V(Q_e)*I_m(k_e) \qquad (2.10.1)$$

where the suffix j is used to label the j'th group of detectors. Hence if $\Sigma_j(Q_e)$ is the measured differential cross section for the j'th group, the merged differential cross section is obtained by forming the sum

$$\Sigma_M(Q_e) = \frac{\sum \Sigma_j(Q_e) * W_j(Q_e)}{\sum W_j(Q_e)} \qquad (2.11.1)$$

This is achieved with the MERGE command, section 3.12

2.11 ANALYSIS TO PAIR CORRELATION FUNCTION

The inversion of the S(Q) data to pair correlation function, g(r), i.e. inversion of equation 1.3.2, can be done by trivial Fourier transform. Routines GTOS and STOG (see section 3.13) are available to do this, and will allow the inclusion of a window or modification function if needed.

However such direct Fourier transforms will inevitably lead to spurious structure in the calculated distribution due to the finite extent and statistical noise present in the data. This has been the subject of a number of reports, including a preliminary one from the Rutherford Appleton Laboratory by Soper [21], which was presented at the ICANS-X meeting in October 1988. In this new method it is proposed to limit the fluctuations in r(g(r)-1) with increasing r to those that are compatible with the observed width of the peaks in S(Q). In this way the noise and truncation of the data are not reproduced in the simulated pair correlation functions, at the same time that excellent fits to the measured data are obtained. At the time of writing a full account of this technique has still to be prepared for publication, and the program, called MCGOFR, is not in a particularly user friendly form, so at presemt it must be run under careful supervision. Even so it is fully intended to make this program generally available to anyone interested in using it. The basic philosophy of the approach is described in Appendix C, which is a reproduction of the ICANS paper in full.

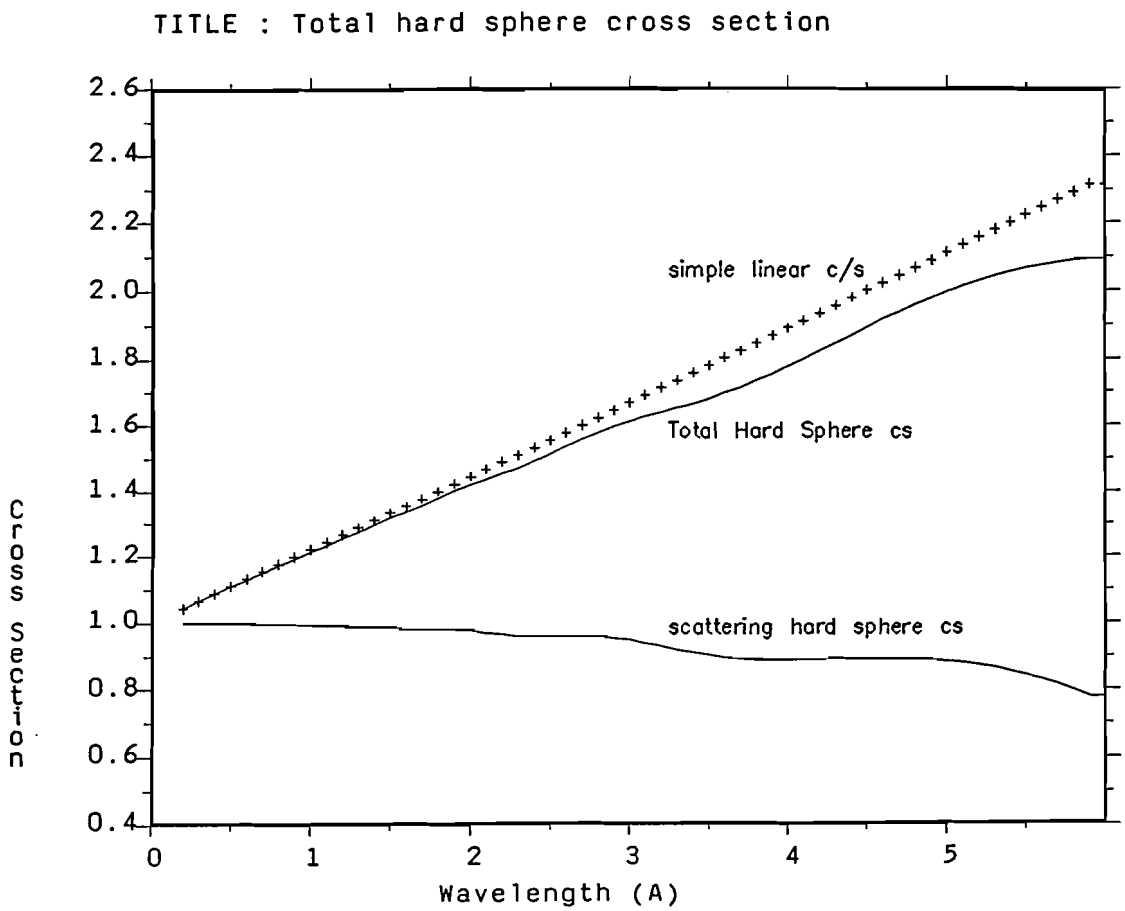

Figure 2.1 Calculated scattering and total cross section for a hard sphere fluid of density $\rho\sigma^3 = 0.5$, with σ=3.142. The fluid is assumed to have unit scattering cross section per atom, and the capture cross section is 0.4 at 1.8Å. The crosses correspond to a structureless fluid

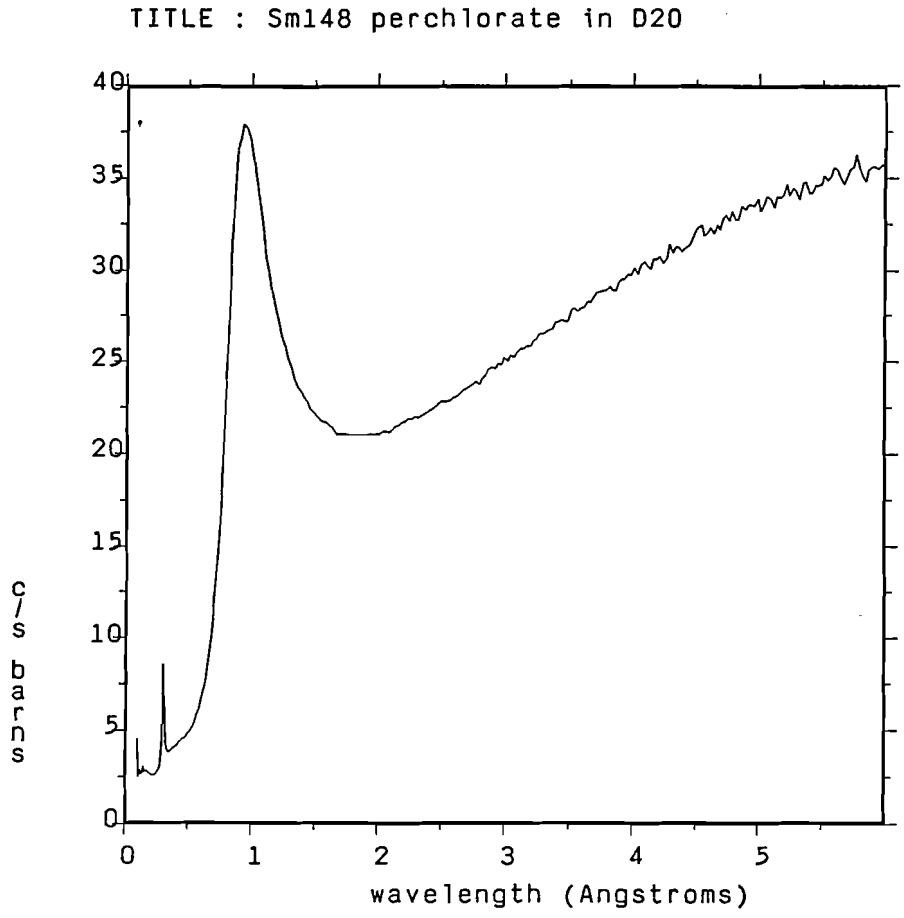

Figure 2.2 Measured transmission cross section for a solution of ^{148}Sm-perchlorate in D_2O. Note the pronounced neutron resonance near λ=1Å which arises from a ^{149}Sm impurity. Higher energy resonances are visible at shorter wavelengths.

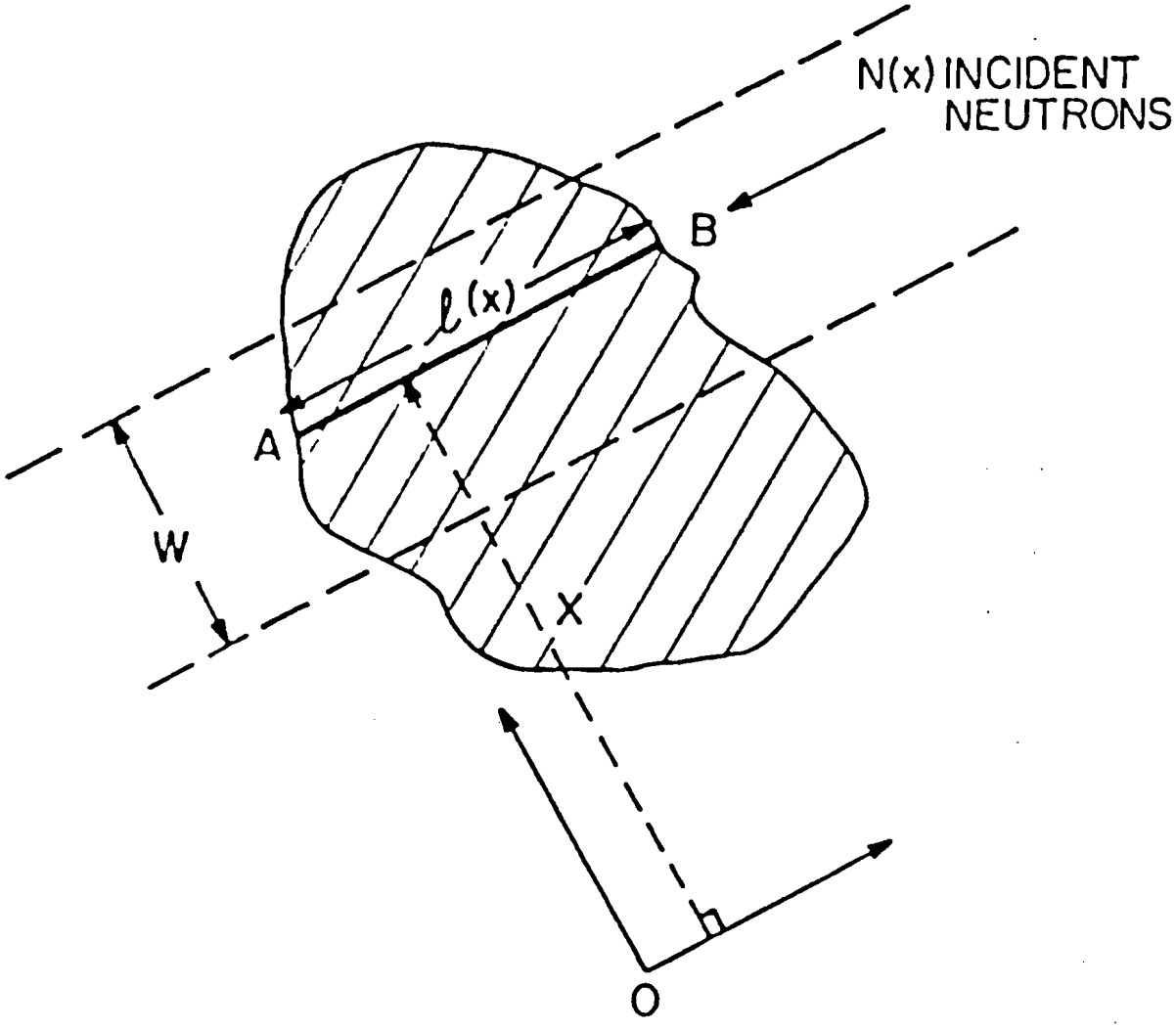

Figure 2.3 Geometry of transmission problem for an arbitrary shaped sample

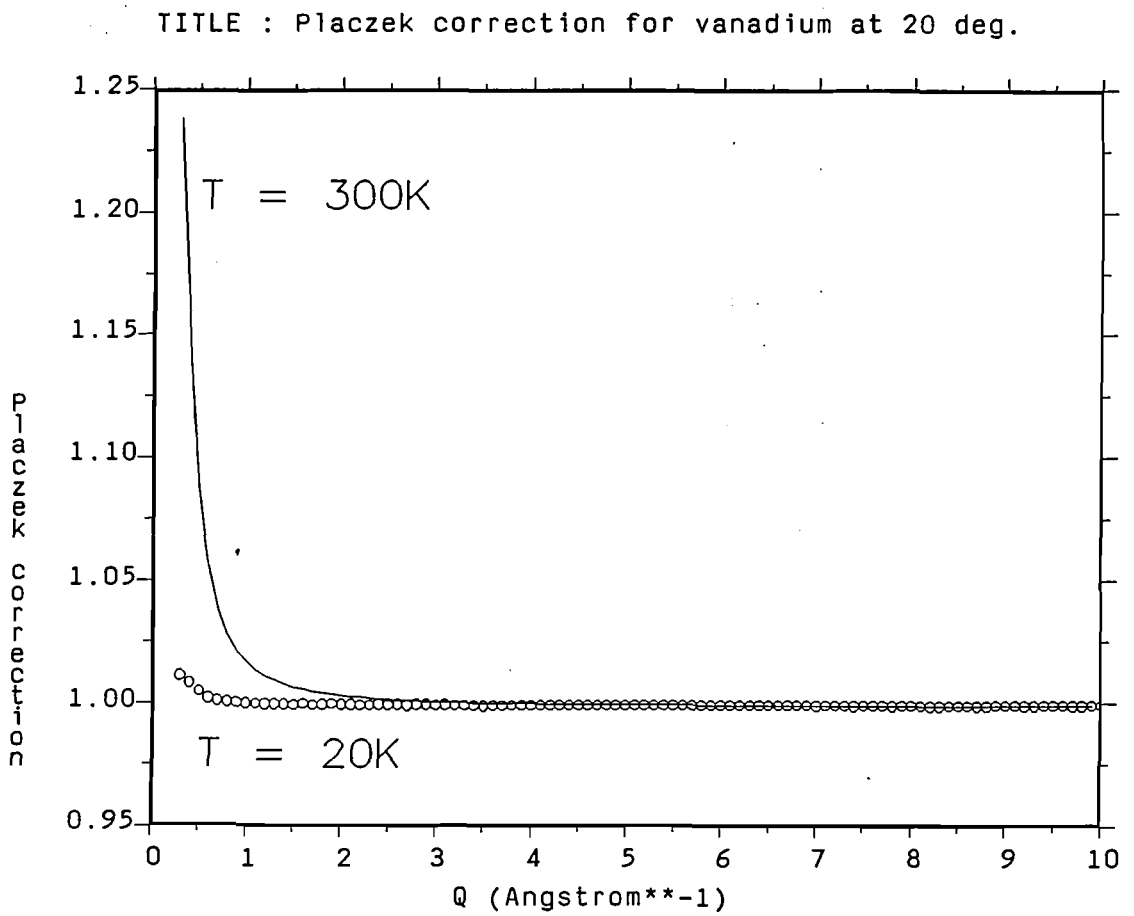

Figure 2.4 Calculated TOF recoil correction (1+P) for a free vanadium nucleus at two temperatures: 20K and 300K, and at a scattering angle of 20°. Note the large temperature effect at small Q values.

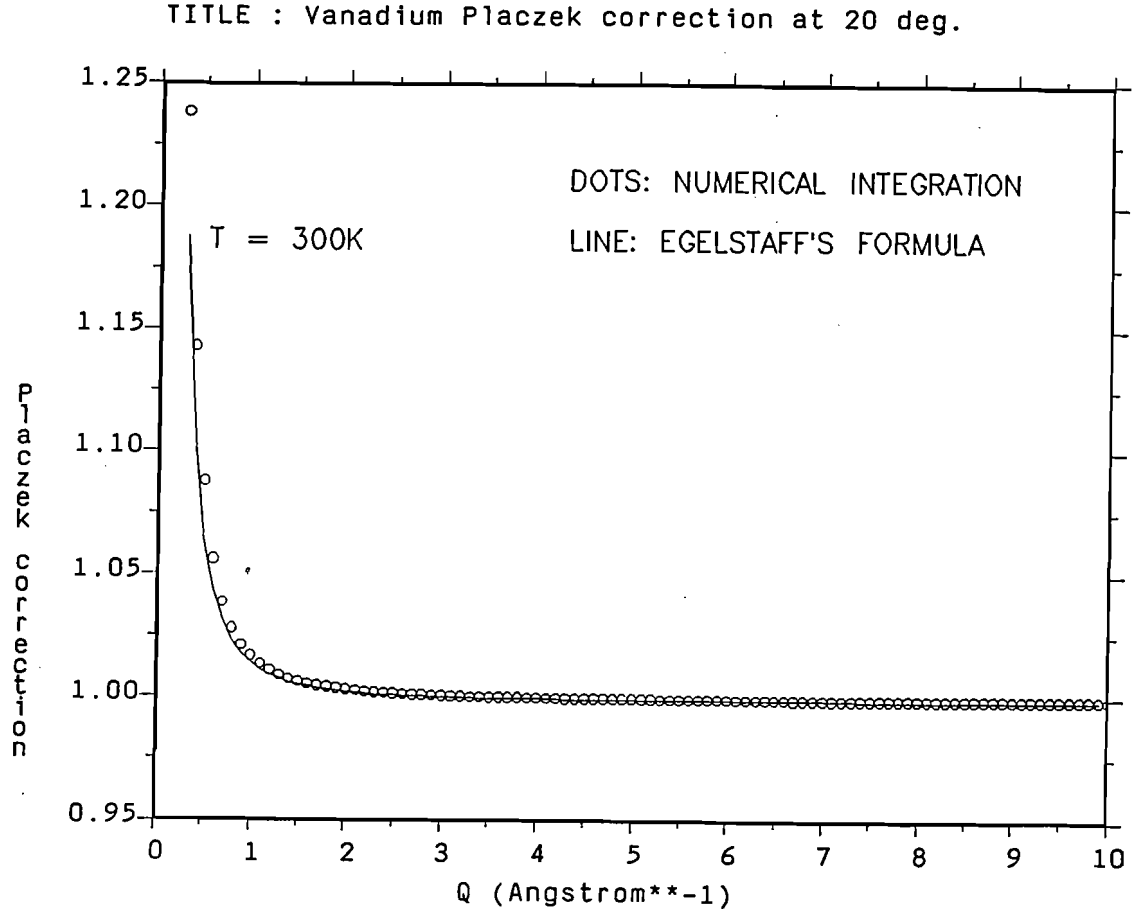

Figure 2.5 Comparison of numerical calculation of recoil correction for a vanadium nucleus at T=300K and scattering angle 20°, with Egelstaff's approximate formula, equation (2.9.4), which does not have the correct spectral dependence at small Q. Even so it gives good agreement at all Q values

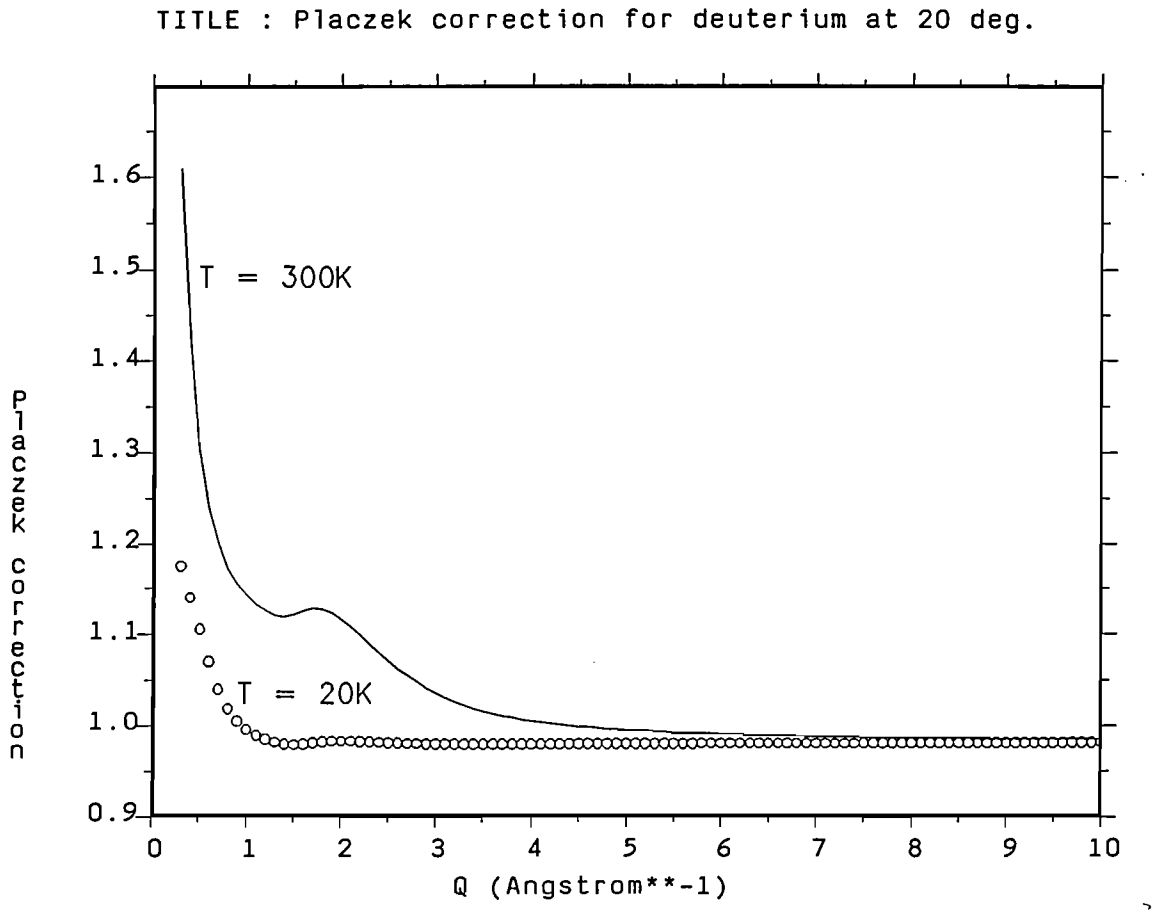

Figure 2.6 Recoil correction for a free deuterium atom at 20K and 300K. The scattering angle is 20°. Note again the large temperature effect at small Q, and that a pronounced structure appears due to the substantial energy transfers that take place in the scattering process,

SECTION 3

HOW TO RUN THE PROCEDURES

3.1 THE ISIS COMPUTING SYSTEM

3.1.1 The computers

The current ISIS computing system (sometimes referred to as PUNCH - PUlsed Neutron Computer Heirarchy) is illustrated below and is fully described in the PUNCH User Manual.

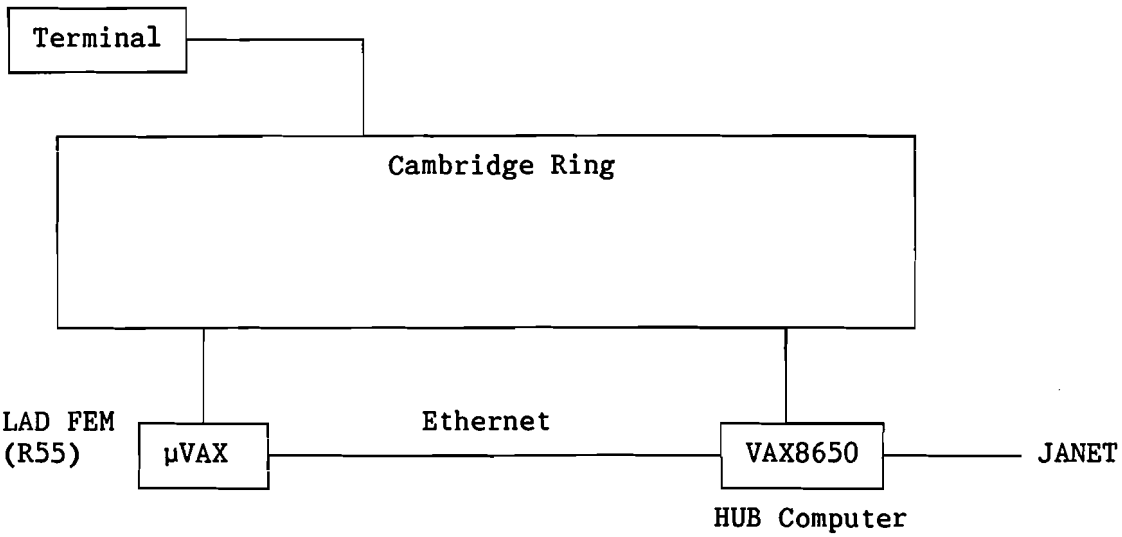

Each instrument is controlled by a Front End Mini (FEM) computer which in the case of LAD is a Micro-VAX 2. The central mainframe, referred to as the HUB, is a VAX8650.

The FEM and the HUB are connected by two network systems - the Cambridge Ring and Ethernet. The HUB is also the node for other wide area networks such as JANET, for UK universities, and DECnet, EARN and BITNET for world-wide access.

Users will be assigned their own username on the HUB (see Local Contact for details) for use in analysing data. The username will be of the form ABC01 where the letters are the initials of the user and the numerals take into account several users with the same initials. The same username may also be used to log on to the LAD FEM.

3.1.2 Getting started

>>>Note : any command typed into the computer should be followed by pressing the RETURN key (sometimes referred to as Carriage Return CR). This will be assumed throughout the manual.

To log on to the HUB ...

1. Press the BREAK key on the terminal until the prompt

DNS:

appears

2. Type CALL HUB
3. Press RETURN to make the prompt Username: appear
4. Type the username (eg ABC01)
5. In response to the prompt Password: type password
6. A short command routine will then be executed, setting the system ready for analysing LAD data, and then the user will be logged on to the HUB and able to commence data analysis. The command routine must be setup by the Local Contact during the first use of the username.

Periodically the user will be required to change the password. This is done by use of the command SET PASS.

Once logged on, the user ABC01 will have access to an area of disk space for storing files in the directory [ABC01] and any sub-directories of it. In these areas there are full access rights ie read,write,execute,delete. The user has limited rights usually read only to areas within [LADMGR]. Initially, when the data is collected, it is stored in the directory [LADMGR.DATA] on the FEM and automatically transferred to the HUB in the same directory. However, due to space restrictions the data is archived onto optical disk and deleted within a few days. Data files are restored by issuing the command RESTLAD when logged onto the HUB. This restores the raw data

files to the area [LADMGR.RESTORE], with the restore process taking a maximum of about 10 minutes. The data files are held in this area for a period of 3 days. Both these areas can be referred to by the logical name 'inst_data' - for example a directory listing can be obtained by DIR inst_data.

Programs and command files are stored in the area [LADMGR.PROGS] which has the logical name 'g_f'. (Note: a 'logical name' is simply a convenient synonym used to stand for a string of characters)

The user may wish to make use of sub-directories to help organise the files within his own area. In this case the following commands are useful:

CREATE/DIR [ABC01.ANA]	- create a sub-directory named [ABC01.ANA]
SET DEF [ABC01.ANA]	- set the default directory to be [ABC01.ANA]. This has the effect that subsequently the computer will assume that a file is in the directory [ABC01.ANA] unless another directory is specified.
SH DEF	- show the default directory.

3.2 DATA FILES AND BATCH SYSTEM

3.2.1 Data File Structure

The data on the FEM can be in 3 locations - the DAE, the CRPT or disk (either as a .SAV file or a .RAW file). On the HUB it is either .SAV or .RAW.

The convention used to name files involves 3 parts : a filename, an

extension and a version number. For data the filename is constructed from the instrument name (3 characters) and a 5 digit run number. The type of file is specified by the extension - for example SAV or RAW. The full name of the raw data file (version 1) for run 1234 for example is LAD01234.RAW;1 . In our programs we continue to use this form of nomenclature so that data for a specific sample can be recognised by its run number and the type of data by the extension name. Within the programs the instrument name and leading zeros in a run number need not be specified.

In all the above cases the file structure is the same. There is a header section which contains information supplied by the instrument control program (ICP) on the FEM.

There are sections on :

- -instrument parameters; for example detector angles, flight paths, spectrum numbers for detectors and monitors.
- -run parameters; for example date/time of start and end, number of protons, neutrons and frames.
- -sample parameters; for example title of run, dimensions.

These are followed by arrays containing :

- -time of flight which is stored as the time boundaries for the channels as specified by the ICP.
- -each spectrum as counts per channel.

Files are in binary format but ASCII versions of parts of the data can be provided.

The GENIE program can also create files in binary format but with a different layout. The file starts with a selection of parameters from the RAW data header section such as scattering angle and flight paths and is followed by arrays containing the values of x, y and error on y. Such binary files will be used extensively by our programs with the

type of data denoted by the extension.

Programs are available for converting these binary files to ASCII format.

3.2.2 Batch System

The batch system enables a program to be run non-interactively so as not to tie up the terminal. It is of most use for long programs, such as those used to calculate the absorption correction and the multiple scattering correction. Some useful batch related commands are as follows;

SUBMIT VAN01234.COM - submit the command file VAN01234.COM to be run by batch.

SHOW QUE *$BATCH - show the status of all batch queues.

DELETE/ENTRY=999 RLDE$BATCH - delete batch job 999 (the entry number 999 may be obtained by use of the SHOW QUE command) from queue RLDE$BATCH (for example).

SHOW SYS/BAT - shows all the batch jobs currently executing in the current processor and how much CPU time each has used. Note that if a job has been submitted to a different CPU from the current one the amount of time in that job can only be obtained by logging on to the appropriate CPU. This is not normally possible for HRPD, POLARIS and CRISP unless you know the password because these FEM's have limits on who can log on.

3.3 INSTRUMENT INFORMATION

3.3.1 Calibration

On a time-of-flight instrument the data must be converted from stored counts in channels to counts in other units such as wavelength, d-spacing and Q-vector. These conversions are determined by two standard equations :

$$t + \Delta = (m/h)\, L\lambda$$

$$\lambda = 2d \sin\theta \qquad \text{(Bragg's equation)}$$

where t is the time of flight
Δ is the origin in time determined by the electronics
L is the total flight path equal to the sum of the initial (l_1) and final (l_2) flight paths
λ is the wavelength
2θ is the scattering angle
d is the d-spacing of the powder peak

These parameters are determined with calibration experiments of two types. The first equation can be used with neutron absorption resonances which occur at fixed energy or wavelength. By measuring many resonances from different foils placed in the incident beam, values for Δ and L can be determined. Most resonances occur at high energies (~eV) (short times-of-flight) so these calibrations give good values for Δ.

The second equation of course leads to the familiar calibration using standard powders such as Ni, Al_2O_3 and MgO. These experiments will give values of Δ and the product $L\sin\theta$. At short times there are either no Bragg peaks or they cannot be resolved so that the value of Δ by this technique is not as reliable as that from resonances.

As pointed out in Appendix A the Bragg peaks have an asymmetric

shape which varies with scattering angle, so the peaks have to be analysed to take this into account.

The instrument calibrations are carried out by the Instrument Scientists and do not normally need to be repeated by the user. Nonetheless it is wise to look for discrepencies between the results from different scattering angles to determine if the supplied calibration is correct. The header sections of the .RAW data files should contain the correct values. On the FEM they are stored in a file called DETECTOR.DAT. If that file does not contain all the values or if they need changing a similar file can be created on the HUB to be used by our programs.

3.3.2 Spectrum numbering

All detectors and monitors are allocated a spectrum number. The physical detectors are mapped to spectrum numbers by software via a file called SPECTRA.DAT. These can be changed by the user at the start of an experiment, but in most cases a standard setup is used. The number of spectra and the number of channels per spectrum are defined on the FEM by the ICP and their product defines the storage capacity required and the maximum value is determined by the hardware in the FEM.

In the data analysis programs the spectra can be further combined for example according to scattering angle. This will in general be neccessary to reduce the volume of data and is particularly true for the scintillator modules which have a large number of detector elements. Subsequently a combined spectrum from several detectors is treated as though being at the average angle. In the case of LAD the detectors occur in groups at scattering angles of approximately 5°, 10°, 20°, 35°, 58°, 90° and 150° and the default way of combining the detectors is based on these groups.

Two of the spectra are always the monitors - one in the incident beam and the second in the transmitted beam.

The header section of the data files also keeps a record of the spectrum numbering and in our programs we make use of this data so that the user does not need to know them.

3.3.3 Time channels

The time channel structure is set up by the ICP and three basic structures are available : channel width constant with time, channel width proportional to time-of-flight and width proportional to the square of the time-of-flight. There can be up to five ranges of time-of-flight each with a choice of structure.

The constant channel width is the simplest but has the disadvantage that on converting to Q the data becomes squashed into the low Q region with the high Q region having widely spaced points. The second choice has the advantage that the channel widths are proportional to the resolution over the whole range since the resolution is constant in $\Delta t/t$ and $\Delta Q/Q$. For this option the distribution of points in Q is still on constant increment but not as bad as the first option. The last choice would provide constant increments in Q.

On LAD we have chosen the second option - that is the channel width is proportional to time-of-flight. There is only one region staring at 200 μs ending at 19500 μs just before the next pulse which arrives at 20 ms. The constant of proportionality is 0.002 which allows for about ten points across a Bragg peak at the backward angle (150°), highest resolution detectors. Since the resolution worsens as the scattering angle decreases and the constant does not change with angle, the number of points at the lower angles are higher than necessary.

The combination of unequal Q increments and the increments in general being smaller than neccessary for liquid and amorphous work means that rebinning of data in Q is always required.

TABLE 3.1

Example of DETECTOR.DAT file

LAD February 1989

Number of detectors, Number of user table parameters/detector
84 5

Det	Delta	Len2	Code	2theta	ut1	ut2	ut3	ut4	ut5
1	4.4	1.128	150	145.6	1.0	1.25	10.0	0.006	0.
2	4.4	1.128	150	145.6	1.0	1.25	10.0	0.006	0.
3	4.4	1.128	150	145.6	1.0	1.25	10.0	0.006	0.
4	4.4	1.128	150	145.6	1.0	1.25	10.0	0.006	0.
5	4.4	1.128	150	145.6	1.0	1.25	10.0	0.006	0.
6	4.4	1.128	150	145.6	1.0	1.25	10.0	0.006	0.
7	4.4	1.128	150	145.6	1.0	1.25	10.0	0.006	0.
8	4.4	1.128	150	145.6	1.0	1.25	10.0	0.006	0.
9	4.6	1.047	150	9.6	1.0	1.25	10.0	0.016	0.
10	4.6	1.047	150	9.6	1.0	1.25	10.0	0.016	0.
11	5.4	1.033	150	4.8	1.0	1.25	10.0	0.02	0.
12	5.4	1.033	150	4.8	1.0	1.25	10.0	0.02	0.
13	-0.7	-1.092	150	180.0	2.0	0.00244	44.0	0.001	0.
14	-0.95	1.260	150	0.01	2.0	0.00244	44.0	0.001	0.
15	-1.0	1.039	150	88.4	2.0	1.25	1.0	0.014	0.
16	-1.0	1.039	150	88.8	2.0	1.25	1.0	0.014	0.
17	-1.0	1.039	150	89.1	2.0	1.25	1.0	0.014	0.
18	-1.0	1.039	150	89.5	2.0	1.25	1.0	0.014	0.
19	-1.0	1.039	150	89.7	2.0	1.25	1.0	0.014	0.
20	-1.0	1.039	150	90.0	2.0	1.25	1.0	0.014	0.
21	-1.0	1.039	150	90.3	2.0	1.25	1.0	0.014	0.
22	-1.0	1.039	150	90.55	2.0	1.25	1.0	0.014	0.
23	-1.0	1.039	150	90.9	2.0	1.25	1.0	0.014	0.
24	-1.0	1.046	150	57.0	2.0	1.25	1.0	0.008	0.
25	-1.0	1.046	150	57.2	2.0	1.25	1.0	0.008	0.
26	-1.0	1.046	150	57.45	2.0	1.25	1.0	0.008	0.
27	-1.0	1.046	150	57.8	2.0	1.25	1.0	0.008	0.
28	-1.0	1.046	150	58.0	2.0	1.25	1.0	0.008	0.
29	-1.0	1.046	150	58.3	2.0	1.25	1.0	0.008	0.
30	-1.0	1.046	150	58.7	2.0	1.25	1.0	0.008	0.
31	-1.0	1.046	150	59.0	2.0	1.25	1.0	0.008	0.
32	-1.0	1.046	150	59.3	2.0	1.25	1.0	0.008	0.
33	-1.0	1.043	150	34.1	2.0	1.25	1.0	0.012	0.
34	-1.0	1.043	150	34.4	2.0	1.25	1.0	0.012	0.
35	-1.0	1.043	150	34.7	2.0	1.25	1.0	0.012	0.
36	-1.0	1.043	150	34.9	2.0	1.25	1.0	0.012	0.
37	-1.0	1.043	150	35.3	2.0	1.25	1.0	0.012	0.
38	-1.0	1.043	150	35.6	2.0	1.25	1.0	0.012	0.
39	-1.0	1.043	150	35.9	2.0	1.25	1.0	0.012	0.
40	-1.0	1.043	150	36.1	2.0	1.25	1.0	0.012	0.
41	-1.0	1.043	150	36.4	2.0	1.25	1.0	0.012	0.
42	-1.0	1.04	150	19.1	2.0	1.25	1.0	0.013	0.
43	-1.0	1.04	150	19.5	2.0	1.25	1.0	0.013	0.
44	-1.0	1.04	150	19.8	2.0	1.25	1.0	0.013	0.

45	-1.0	1.04	150	20.1	2.0	1.25	1.0	0.013	0.
46	-1.0	1.04	150	20.4	2.0	1.25	1.0	0.013	0.
47	-1.0	1.04	150	20.7	2.0	1.25	1.0	0.013	0.
48	-1.0	1.04	150	21.0	2.0	1.25	1.0	0.013	0.
49	-1.0	1.04	150	21.2	2.0	1.25	1.0	0.013	0.
50	-1.0	1.04	150	19.1	2.0	1.25	1.0	0.013	0.
51	-1.0	1.04	150	19.5	2.0	1.25	1.0	0.013	0.
52	-1.0	1.04	150	19.8	2.0	1.25	1.0	0.013	0.
53	-1.0	1.04	150	20.1	2.0	1.25	1.0	0.013	0.
54	-1.0	1.04	150	20.4	2.0	1.25	1.0	0.013	0.
55	-1.0	1.04	150	20.7	2.0	1.25	1.0	0.013	0.
56	-1.0	1.04	150	21.0	2.0	1.25	1.0	0.013	0.
57	-1.0	1.04	150	21.2	2.0	1.25	1.0	0.013	0.
58	-1.0	1.043	150	34.1	2.0	1.25	1.0	0.012	0.
59	-1.0	1.043	150	34.4	2.0	1.25	1.0	0.012	0.
60	-1.0	1.043	150	34.7	2.0	1.25	1.0	0.012	0.
61	-1.0	1.043	150	34.9	2.0	1.25	1.0	0.012	0.
62	-1.0	1.043	150	35.3	2.0	1.25	1.0	0.012	0.
63	-1.0	1.043	150	35.6	2.0	1.25	1.0	0.012	0.
64	-1.0	1.043	150	35.9	2.0	1.25	1.0	0.012	0.
65	-1.0	1.043	150	36.1	2.0	1.25	1.0	0.012	0.
66	-1.0	1.043	150	36.4	2.0	1.25	1.0	0.012	0.
67	-1.0	1.046	150	57.0	2.0	1.25	1.0	0.008	0.
68	-1.0	1.046	150	57.2	2.0	1.25	1.0	0.008	0.
69	-1.0	1.046	150	57.45	2.0	1.25	1.0	0.008	0.
70	-1.0	1.046	150	57.8	2.0	1.25	1.0	0.008	0.
71	-1.0	1.046	150	58.0	2.0	1.25	1.0	0.008	0.
72	-1.0	1.046	150	58.3	2.0	1.25	1.0	0.008	0.
73	-1.0	1.046	150	58.7	2.0	1.25	1.0	0.008	0.
74	-1.0	1.046	150	59.0	2.0	1.25	1.0	0.008	0.
75	-1.0	1.046	150	59.3	2.0	1.25	1.0	0.008	0.
76	-1.0	1.039	150	88.4	2.0	1.25	1.0	0.014	0.
77	-1.0	1.039	150	88.8	2.0	1.25	1.0	0.014	0.
78	-1.0	1.039	150	89.1	2.0	1.25	1.0	0.014	0.
79	-1.0	1.039	150	89.5	2.0	1.25	1.0	0.014	0.
90	-1.0	1.039	150	89.7	2.0	1.25	1.0	0.014	0.
81	-1.0	1.039	150	90.0	2.0	1.25	1.0	0.014	0.
82	-1.0	1.039	150	90.3	2.0	1.25	1.0	0.014	0.
83	-1.0	1.039	150	90.55	2.0	1.25	1.0	0.014	0.
84	-1.0	1.039	150	90.9	2.0	1.25	1.0	0.014	0.

The first column is the detector number; delta, l_2 and 2theta are as defined above; Code defines the instrument (150 is LAD); the parameters ut1-ut5 are user defined and in this case are :

ut1	detector type code 1=gas 2=scintillator
ut2 and ut3	parameters to calculate detector efficiency
ut4	resolution
ut5	spare

The calibration determines $L=l_1+l_2$, l_1 is taken to be the nominal value of 10.0m. If l_1 is not defined in the parameter section of the data files then l2 can be set to L for the purposes of unit conversion to wavelength.

3.4 OVERVIEW OF GENIE

For more details of this program the user should consult the GENIE Manual. We will restrict ourselves to comments on the general principles and the more important points in its operation.

The overall program structure is command driven, not by menu. However where possible the individual routines called by the commands will include a menu or question/answer structure for ease of use.

Workspaces are used for data manipulation. The number of workspaces and their size (array length) can be chosen by the user. However there is a limited memory space available so the product of the number of workspaces and their length must be within this limit. There must always be enough space for the graphics area and buffer areas. This will normally be set for you.

Command files can be used for repetitive operations and can also include terminal input. A command file is program run within GENIE which executes commands from a .COM file instead of the user typing in at the keyboard. Command files are run in GENIE by typing @ followed by the name of the .COM file which is to be run. The name must be prefixed by a directory name if the command file does not reside in the current default directory.

There is an initialisation command file that is automatically read on entering GENIE. This sets up values for the number of spectra and their size and the default disk directories.

The data in Workspaces can be written to binary files for subsequent reading back into workspaces.

External programs can be run to manipulate data in workspaces - these are the FUNCTION and TRANSFORM commands and are used in our programs for example to read in corrections parameters. Data in non-GENIE type files (usually ASCII) can be read into workspaces using

the Load command.

The units of x in the workspace can be changed provided that the workspace contains instrument parameters which are input via the SET PAR command. The y-values of the data in the workspaces are stored in the form of 'per unit of x' eg per microsec or per $Å^{-1}$. Care must be taken when changing units and dividing - for example the correct order is to change unit then divide. The option of scaling x to the y-unit can be removed with the SET Yunit command.

3.4.1 Simple Example of GENIE commands

In order to read in a sample and vanadium spectrum, divide and display as S(Q) the following operations are necessary :

```
>ASS 1234                    assign run number for sample
>W1=S1                       read spectrum 1 into workspace 1
>Set PAR 1 10 1. 150. 0 0    set parameters
>U/Q W1                      change units to Q
>ASS 1235                    assign run number for vanadium
>W2=S1
>Set PAR 2 10 1. 150. 0 0
>U/Q W2
>W3=W1/W2                    divide S by V to give S(Q)
>D W3                        display S(Q)
>L/X 0 20                    change range of X (ie Q)
>D/E                         display new Q range and with error bars
```

3.4.2 GENIE command files

Operations can be stored as a command file and such a file is provided for calculating the 'crude' S(Q), i.e. (sample-can)/vanadium, with no other corrections. The routine is started in GENIE with the command @g_f:SQRAW, that is, the command file is called SQRAW.COM in directory g_f. It prompts for sample, can and vanadium run numbers and

for the angle. The resulting "raw" S(Q) is displayed.

3.5 OVERVIEW OF PROGRAMS

The package provides a series of stand-alone Programs and GENIE routines which are to be run in a particular order :

Program NORM normalises RAW data and produces output files with extensions .MON and .NRM.

TRANSMISSION Routines calculate cross-sections from the transmission data with extension .MON and creates files with extension .MUT.

Program CORAL calculates the corrections using the files with extension .MUT and produces corrections files with extensions .ABS, .MUL or .REF.

Routine VANSM treats the reference or vanadium spectra using files with extensions .NRM and .REF and creates files with extension .SMO.

Routine ANALYSE takes the files with extensions .NRM, .ABS, .MUL and .SMO to produce the corrected S(Q) at each angle as an output file with extension .DCS.

Routine PLATOM calculates the self scattering at each angle, creating an output file with extension .SLF. Routine INTERFERE subtracts the self scattering in the .SLF file from the total scattering in the .DCS file to yield the interference scattering which is placed in a file of extension .INT.

Routine MERGE combines the individual angles in a file with extension INT or DCS to produce a single S(Q) in a file with extension .SOQ.

Routine STOG transforms S(Q) to g(r) and GTOS transforms g(r) to S(Q).

The diagram below shows the normal sequence of operations, and Appendix D summarizes the filename extensions which are produced.

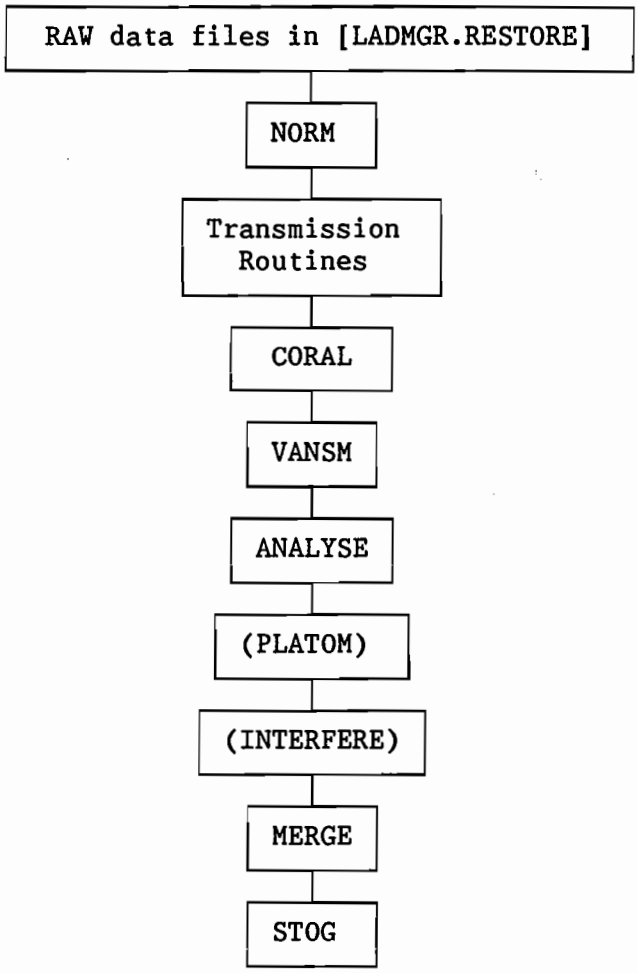

The operations in brackets are optional and can be skipped if necessary. This will typically happen when the inelasticity correction is either not needed or not calculable.

3.6 PROGRAM NORM

Version 4.1 March 1989

3.6.1 Introduction

This program NORMalises the RAW data - that is it takes detector spectra, corrects for deadtime, divides by the monitor spectrum, converts from time-of-flight to Q-vector, combines spectra and outputs results to files.

The following operations are carried out on all spectra :

- the time-of-fight is converted to wavelength using the parameters contained in the RAW file. Each spectrum has the same range of time-of-flight so because each spectrum may have a different flight path the wavelength range will differ. Before manipulating spectra they must therefore be rebinnned onto a common wavelength range (this also includes the same increment in wavelength).
- the counts are corrected for detector dead time. This requires the total frames for the run which is taken from the parameter section.
- the error is taken to be the square root of the count.

The program is in two sections each producing an output file which can subsequently be read into GENIE using the REad command.

3.6.2 Monitor files

This section creates a file with the extension .MON containing the two monitor spectra.

The incident monitor is just converted to wavelength. The transmission monitor is converted to wavelength, rebinned to the wavelength range of the incident monitor and divided by the incident monitor spectrum. The purpose of dividing by the incident monitor

spectrum is to allow for the possibility of variations in moderator temperature leading to changes in the flux wavelength distribution as well as scaling all runs to a same neutron flux. It is therefore in a form suitable for calculating the transmission cross-section.

3.6.3 Detector files

This section deals with the detector spectra and creates a file with the extension .NRM. The spectra can be 'grouped' together in a manner defined in a data file. A default version called GROUPS.DAT is available for LAD in the instrument program directory (G_F:).

The operations are :

- the individual spectra are read, converted to wavelength and normalised to the incident monitor spectrum as outlined above. This must be done on the individual detectors in wavelength and not after addition or converting to Q in order to take correct account of the shape of the monitor spectrum.
- the individual detectors are converted into counts per Q - each spectrum is rebinned onto a specified Q range and constant Q increment and the spectra within a defined group are added.

The default grouping for LAD creates a file of 14 groups corresponding to the 7 scattering angles on either side. The groups are in pairs in increasing angle.

3.6.4 Operation

The program is a stand-alone program similar in operation to GENIE and is started with the command NORM.

The program prompt is n> .

The command RUN defines run numbers to be used.
The command GRoup defines the spectra group structure.
The command BEGIN starts the program looping over all groups.

The command CALib initialises reading of the detector table (optional).

The sequence of commands is as follows :

>SET DIR or DISK	)	default values on
>SET INST	)	entry to program
>SET EXT	)	
>CAL		if required
>GR		
>RUN		
>BE		to begin operation
>EX		to exit program

The HELP facility is also available within the program. The command Help will provide brief comments on the NORM commands whilst Help GENIE gives information on GENIE commands.

***** IMPORTANT NOTE: At the time of writing NORM contains a bug which ***** means it can only be run on one set of data, i.e. one sequence ***** of commands as above. On completion it must be exitted and ***** restarted with the NORM command again for each set of .RAW ***** files.

3.6.5 Description of Commands

A full description of the commands now follows :

B E g i n

This command begins the automatic looping over all the groups as defined by the Group command.

The routine prompt is begin>

The routine will ask for :
increment in Q (delta_q) default is 0.02
maximum Q value (q_max) default is 50.

Alternatively the two parameters can be included with the command in the form BE delta_q q_max.

Each spectrum/group will be rebinned at constant delta_q where the q_values are integer multiples of delta_q ie N*delta_q. The minimum rebinned q_value is the first multiple of delta_q greater than the minimum q_value of the raw data. The maximum rebinned q_value is the last multiple of delta_q less than the maximum q_value of the raw data or the defined maximum q_value whichever is the smaller.

If the CAL command has previously been issued the values of the calibration constants will be changed.

There is an error message if a run number has not been given or if the groups have not been defined and the command is aborted.

C A L i b

This command initiates the changing of the values of the calibration constants. The new values must be in the file DETECTOR.DAT which must exist in the current directory. The new values are displayed as they are read in.

The command must be issued before both the RUN and BEgin commands. The monitor data is read during RUN so its parameters will not be changed unless CALib is issued before it.

There is an error message if the number of detectors is wrong or if the detector numbers are out of sequence and the parameters are not changed.

The option can be removed with the qualifier /N.

G R o u p

The group command defines the group structure of the spectra.
The routine prompt is group>

There will be a request to input a filename. A <CR> will default to the file G_F:GROUPS.DAT in the LADMGR program area, otherwise type the name of the file to be read (with directory if necessary).

The group structure (as in the file) is as follows :
first line : number of groups
subsequent lines (one for each group) :
number of spectra, the spectra numbers
Up to 25 groups are allowed, each with up to 25 spectra.
The spectra should be in increasing angle.

There is one qualifier /TYPEIN which allows the group structure to be typed in directly. There will be prompts for input ; the structure is similar to that in the file.

If the group file does not exist or if more than 25 groups are defined there is an error message and the command is aborted.

R U N

Defines the run numbers. The command is :

RU <run1> <run2> ...

Up to 8 runnumbers may be specified.

The output file will take the name of the first run number specified and will contain a sum over all the runs.

3.6.6 Example of GROUPS.DAT file

Standard Groups.dat file for LAD
corresponding to detector layout on February 1989

14	number of groups
1 11	5° gas L
1 12	5° gas R
1 9	10° gas L
1 10	10° gas R
8 42 43 44 45 46 47 48 49	20° scintillator L
8 50 51 52 53 54 55 56 57	20° scintillator R
9 33 34 35 36 37 38 39 40 41	35° scintillator L
9 58 59 60 61 62 63 64 65 66	35° scintillator R
9 24 25 26 27 28 29 30 31 32	60° scintillator L
9 67 68 69 70 71 72 73 74 75	60° scintillator R
9 15 16 17 18 19 20 21 22 23	90° scintillator L
9 76 77 78 79 80 81 82 83 84	90° scintillator R
4 1 2 3 4	150° gas Left
4 5 6 7 8	150° gas Right

The average angles produced by these groupings are :

4.8°, 9.6°, 20.23° , 35.27° , 58.08° , 89.69° and 145.6°.

3.6.7 Batch operation

The program can also be run in batch mode. A command file must be created in the following format :

```
$ norm
> gr
<return>
> run n1 n2 ....
> be delta_q q_max
> ex
$ exit
```

The job is submitted to the batch queue with the SUBMIT command, for example if the command file is called TEST.COM the job is started with SUBMIT TEST.

3.6.8 Reading output files

The data in the .MON and .NRM files can be read into a workspace using a standard READ command. For example, to read the fifth group of NRM into the second workspace type

Read W2 LAD01234.NRM 5 after the prompt >.

The following GENIE command files carry out the standard operations similar to SQRAW ie calculating a 'crude' S(Q) (see section 3.4.2). There are 2 versions:

SQGRP	operates on individual groups
SQANG	operates on angles as in the default grouping

The routines prompt for sample, can and vanadium run numbers and for the group number or angle, as appropriate.

3.7 TRANSMISSION ROUTINES

The transmission cross-section of a sample in a t-o-f experiment (and thus the absorption correction) cannot be calculated from the individual atomic cross-sections (eg. by assuming a 1/v dependence of the absorption cross-section) because of the effect of S(Q). Hence the transmission is calculated from the experimental data (for both sample and vanadium) - see section 2.4

These command files for GENIE calculate the transmission cross-section from the monitor data in either the .RAW files or in .MON files. The former is useful for checking the sample during the run whilst the latter is for the subsequent analysis. Two forms of sample geometry can be treated : cylindrical and flat plate. So the corresponding 2 routines are :

TCR	cylindrical geometry	.RAW data
TFR	flat plate geometry	.RAW data
TCM	cylindrical geometry	.MON data
TFM	flat plate geometry	.MON data.

To run these GENIE command files the user should go into GENIE and type @g_f:tcr for example.

The routines prompt for the sample and background run numbers and then divide sample by background to give the transmission. NOTE: if the sample is in a container then the correct background to use is the empty container run number, NOT the 'nothing in the beam' background. The next prompt is for the binning parameters - default values or input values. Then a Function program is entered to calculate the cross-section - TRANSCYL for cylindrical geometry or TRANSFLAT for flat plate geometry.

The result is displayed and the routine prompts for a choice of recalculating or outputting the result to an ASCII file suitable for the corrections programs - this file has the sample runnumber and

extension .MUT. See section 2.4 for further information on the calculation of the total cross-section.

The program TRANSCYL can take into account 2 concentric cans or 1 can plus a furnace, i.e. there are 4 radii defining 3 annuli. The routine will calculate the cross-section of annulus 1 and requires the cross-sections for annuli 2 and 3 as input. The following input is required :

- beam width
- radius 1 default=0. (ie =0 for solid sample)
  (= inner radius for empty can)
- radius 2 (= outer radius of sample)
- radius 3 default=0. (ie no can)
  (= outer radius of can)

if can is defined (ie non-zero value for radius 3)

- radius 4 default=0. (ie no furnace or second can)
  (= furnace/second can outer radius)

- sample number density in atom or mol per $Å^3$
  if can is defined can number density
  filename for cross-section data
  if furnace is defined furnace number density
  filename for cross-section data

The cross section file consists of the total scattering and absorption cross-sections at a series of wave-lengths. A file can be created using the program CSFILE. Standard files for vanadium (VAN.MUT) and titanium-zirconium (TIZR.MUT) are available in the program directory (g_f). If a cross-section data file does not exist there is an error message and the routine is aborted.

A subtlety occurs on LAD associated within the transmission monitor which does not sample the transmitted beam uniformly, but instead samples the beam on a square grid with 5mm between elements. This means the cross section determined from the transmission monitor

readings can be significantly in error, particularly if the sample does not attenuate the beam very much or if the sample is much thinner than the beam. This effect is also pronounced when the transmission of a thin sample container is being measured. In such cases the beam width can be regarded as an adjustable parameter, which is altered until the cross section of the vanadium rod comes out as expected: this should then be used as the "effective" beam width for the samples. If the container attenuation is so small to make the transmission readings unreliable then one of the standard .MUT files should be used for the container cross section

The program TRANSFLAT requires the following input :

- sample thickness
- sample number density in atom or mol per $Å^3$

The .MUT files can be read into GENIE with the command

```
LO W1 LAD*****.MUT g_F:read_cs
```

which puts the cross section into workspace 1

A straight line fitting program is available to fit a straight line through the cross section data. This is accessed by typing

```
FU w1 g_F:fit_line w2
```

which puts the straight line fit to the data in w1 into w2. This is useful for determining the asymptotic values of the measured cross sections.

3.8 PROGRAM CORAL

Version 4.1 March 1989

3.8.1 Introduction

The stand-alone program CORAL is used to set up a calculation of either an absorption correction or a multiple scattering correction. The actual calculations use several minutes of computer time and so they are performed in batch, with the program CORAL setting up the necessary input.

The scheme described in section 2.5 is used to perform the calculations. They may be performed for either a cylindrical or a flat plate sample, with or without a container.

The corrections calculated by CORAL may be performed for either a .NRM file or a .RAW file, although in the recommended sequence of analysis it is a .NRM file which is corrected. In order to perform either calculation a file containing the total cross-section is required. In normal use the .MUT file calculated by the TRANSmission programs may be used for this.

The absorption and multiple scattering corrections for a sample may be performed in either order. In the case of vanadium the recommended sequence of analysis involves performing only a multiple scattering correction at this stage, using the special CORAL command VA.

The program CORAL uses the following file naming conventions (for correcting the run LAD01234.NRM for example):

	Absorption Correction	Multiple Scattering Correction	Vanadium Correction
(Created before Batch Job)			
File Containing Commands to Run Batch Job:	ABS01234.COM	MUL01234.COM	VAN01234.COM
File Containing Input Parameters for Batch Job:	LAD01234.AIN	LAD01234.MIN	LAD01234.MIN
(Created during Batch Job)			
File Containing Log of Batch Job:	ABS01234.LOG	MUL01234.LOG	MUL01234.LOG
File Containing Batch Job Result:	LAD01234.ABS	LAD01234.MUL	LAD01234.REF

(Files named CYLMUL.IN and CYLMUL.OUT are also used during the multiple scattering calculation, but are deleted after successful operation.)

As well as the usual input parameters such as dimensions, this program requires a description of the beam profile and the total cross section as a function of wavelength. This cross-section data is in a data file with extension MUT as produced by the TRANSmission program. It can also take into account several annuli surrounding a sample (eg can and furnace) and masked beams (e.g. beam width smaller than sample diameter).

The location of the input run is defined using the SET commands. The default directory is set on entry to the instrument data area, e.g. [LADMGR.DATA] for LAD, and the default extension is RAW. All output goes to the current directory.

3.8.2 Operation

The program is a stand-alone program similar in operation to GENIE but without any display options and is started with the command CORAL.

The program prompt is c>

The sequence of commands is as follows :

```
SET EXT              (if required - default is RAW)
SET DISK or DIR      (if required - default is [LADMGR.DATA])
SET INS              (if required - default is LAD)
SET GEOM C or F      (if required - default is C)

RUN  <runnumber>

SA or VA

CA                   if required

BE
OUT [option]
SUB
```

In the program some of the parameters have fixed values while others are set to default values. When a default can be changed its value is printed and <RETURN> keeps the default - otherwise type in the new value.

The HELP facility is also available within the program. The command Help on its own will provide brief comments on the CORAL commands whilst Help Genie gives information on Genie commands.

When running CORAL it is important to type the full sequence of the above commands from RU to BE before typing OUT, otherwise errors in the output files can occur. Thus if when in SAMPLE or CAN or VANADIUM or

BEAM a typing error occurs, then the whole sequence from RUN (inclusive) should be typed again to ensure the output files are correct

3.8.3 Hints on running

The cylindrical input file format in 3.8.4 is used for both the absorption and the multiple scattering programs. The only change neccessary to the parameters is the step size (line 4). The MS calculation can have a larger step size than the absorption (by up to an order of magnitude). Typically, for MS use 0.1 and for absorption 0.02.

The flat plate input file is also used for both correction programs but line 3 is only nesseccary for the multiple scattering and default values have been set at 0.001 for accuracy and 100 planes.

The MS program assumes an input file with extension MIN and creates an output file with extension MUL and a lineprinter listing with extension LIS. The filename for all three files is the same.

The corrections programs are called CYLABSTOF, CYLMULTOF, FLTABSTOF and FLTMULTOF and are in the instrument program directory, ie [ladmgr.progs] or logical name g_F on LAD.

There are command files also in [ladmgr.progs] for running the programs called RUNABS and RUNMUL with one parameter - the filename. All created files will be in the current directory.

The programs take up to 15 mins of CPU time (especially the cylindrical multiple scattering program), so submitting to batch processing is highly recommended. Two further command files are available to make this easier and they assume that the filenames have the form LAD{runnumber} where {runnumber} is 5 digits - the same format as .RAW files. These commands in [ladmgr.progs] are SUBABS and SUBMUL and assume that the runnumber only has 3 digits. When running from the

[lad] area the abbreviations SUBA and SUBM can be used eg SUBA 123 or SUBM 234. All created files will be in the current directory.

If a program runs out of CPU time the problem is probably due to a step size that is too small. Resubmit with a larger step size - say a factor two larger. This should only occur for samples of large radius eg greater than 10mm.

The use of CORAL removes all these complications and avoids detailed knowledge of the operating system.

Do not run two versions of the same option at the same time - for example, wait for an ABS or MUL program to finish before starting a new version. ABS and MUL can be run at the same time.

If you are logged on at a terminal there will be a message from CORAL when a batch job has finished.

In the course of setting up the input files to run the corrections programs you will need to specify the capture cross section at 1.8Å. The value needed should be checked by looking at the measured cross sections since the SCATTERING cross section is determined from the TOTAL cross section by means of the relation

$$\sigma_s(\lambda) = \sigma_t(\lambda) - \sigma_a(\lambda).$$

Therefore IF for some reason the capture cross is LESS than its barn book value, e.g. due to an error in the sample composition, then simply using the 'barn book' value could lead to a NEGATIVE scattering cross section in the multiple scattering routines. In other words the capture cross section typed into CORAL must be consistent with the total cross section values in the .MUT files used.

Finally note that when running the multiple scattering for a container on its own the multiple scattering run is set up with the SA command (and not the CA command), i.e. the container must be treated as

a sample in this case.

3.8.4 Description of commands

A full description of the commands now follows :

Inputs parameters associated with the neutron beam and the instrument.

The routine prompt is beam>.

If neither a SA or VA command has previously been issued an error message is printed and the routine is aborted.

For **CYLINDRICAL** geometry the parameters are (in cm):

Incident beam width

Incident beam height default 4.0

The following assumptions are made concerning the beam, although the programs are designed to accept more general cases. If alternative conditions are known to exist then the input .AIN and .MIN files must be modified outside of CORAL and before the jobs are submitted to batch

a) The collimation to the detector is set to 4cm wide - this will be wider than the sample in most cases.

b) The neutron beam height (defaulted to 4cm) will in general be less than the sample height (defaulted to 6cm). The neutron beam is centred on the centre of the sample.

c) The profile across the beam is constant and the beam is symmetric about the sample centre.

For **FLAT** plate geometry the only parameter is :

The angle between the incident neutron beam and a line perpendicular to the sample plane. The default value is 0., that is sample perpendicular to the beam. It is assumed that the sample is an infinite plate.

The routine also reads the data file (RAW or NRM) to obtain the number of angles and their values. The angle for each group will be printed.

Inputs parameters associated with a can and other annuli such as radiation shields.

The routine prompt is can>

For **CYLINDRICAL** geometry the parameters are :

Outer radius of annulus (cm) (for single can radius 3)

For **FLAT** plate geometry the parameters are :

Thickness of can at front (cm)

Thickness of can at back - default front value

COMMON parameters are :

Number density in atom or mol per $Å^{-3}$

Absorption cross-section @1.8Å in barns

File name for cross-section data - there is NO default file name.

If the file does not exist an error message appears and the routine is aborted.

There is one qualifier - MANY - which is invoked for more than one annulus . [At present restricted to 2 annuli]. This would be used for cases involving shields etc. When used the routine prompts for the number of annuli and the above set of parameters is repeated for each annulus. If not specified the default is one annulus.

The routine reads the number of wavelengths in the cross-section data file and if this differs from that in the sample file an error message is printed.

G E o m

The sample geometry can be changed using the SET command.

The command SET Geom Cyl

invokes cylindrical geometry whereas

the command SET Geom Flat

invokes flat plate geometry.

On entering the program the default is Cylindrical.
This command must be issued before any of the SA, VA or CA commands.

O U t p u t

This initiates output of parameters to a file.

The command O {option}

creates a file with the extension AIN or MIN (as specified by the option parameter) and the name will be that specified in the RUN command. If the option is not specified the routine prompts for a value.

{option} can take the values :
- Van for vandium corrections
- Abs for absorption correction
- Mul for multiple scattering correction

The routine prompt is out>

For **CYLINDRICAL** geometry the parameter is :

step size (cm) the default values are :
- 0.1 for VAN and MUL
- 0.02 for ABS

For **FLAT** plate geometry the parameters are :

for multiple scattering only		
accuracy	default	0.001
number of planes	default	100

The name of the data file created is also printed.

If a run number has not been given an error message is printed and the routine is aborted. The same happens if the option value is incorrect.

R U n

The output filename is defined with the command

RUN {run number}

If the runnumber is not specified, its value is asked for.

For the Vanadium it would be the vanadium run number. The sample run number is used for absorption and multiple scattering in the sample. If a can is present its run number is used for the can multiple scattering

S A m p l e

Inputs parameters associated with the sample.

The routine prompt is sam>

For **CYLINDRICAL** geometry the parameters are :

Sample height (cm) default 6.0

First radius (cm) default 0.0 for solid rod

Second radius (cm)

For **FLAT** plate geometry the parameters are :

Sample thickness (cm)

COMMON parameters are :

Number density in atom or mol per $Å^3$

Absorption cross-section @1.8Å in barns

File name for cross-section data - if only <RETURN> is typed itdefaults to a file with runnumber and extension .MUT eg LAD00123.MUT.

The routine checks that the data file exists ; if it does, the routine reads the number of wavelengths in the cross-section data file and uses that value. If the file does not exist it prompts for a value.

The job is submitted to the batch queue to run the corrections programs with the command

SUB {runnumber}

If {runnumber} is not specified the value given in the RU command is used and the correction option is that defined by the last Output command issued.

If {runnumber} is specified it refers to a file with that runnumber, not that given by the RUn command. The routine will ask for the correction option. This will normally be used to submit a job using a file created in a previous session on Coral.

There will be a LOG file with a name of the form ABS{runnumber} or MUL{runnumber} with extension .LOG.
The output from the programs will be in files with name LAD{runnumber} and extension .MUL, .ABS or .REF (for the VAN).
Lineprinter output will have extension .LIS.

Inputs parameters associated with vanadium.

The routine prompt is van>

For **CYLINDRICAL** geometry the parameters are :

Beam height (cm) default = 6.0

Vanadium radius (cm) assumes a solid rod

For **FLAT** plate geometry the parameter is :

Vanadium thickness (cm)

COMMON parameters are :

Number density default = 0.072 atoms/Å^3

Absorption cross-section @1.8Å default = 5.04 barns

File name for cross-section data - if <RETURN> is typed it defaults to file with runnumber and extension .MUT eg LAD00123.MUT.

The routine checks that the data file exists ; if it does, the routine reads the number of wavelengths in the cross-section data file and uses that value. If the file does not exist it prompts for a value.

3.8.5 Format of data files

For **CYLINDRICAL** geometry the format for the input data file to the programs is :

line	parameters
1	title
2	number of profile values
3	the profile values
4	step size for calculation (cm)
5	number of detector angles
6	the angle values
7 .1	height of sample
7 .2and.3	position of incident beam edges
7 .4and.5	position of detected beam edges
7 .6and.7	bottom and top of incident beam
7 .8and.9	bottom and top of scattered beam
8	number of annuli in sample (na)
9	radii of annuli (na+1) values
10 .1	number density in atom or mol/Å^3
10 .2	absorption c/s at 1.8Å
11	filename of total (scat+abs) c/s data
12	as 10 for next annulus
13	as 11 " " "

and so on.

For **FLAT** plate geometry the format for the input data file to the programs is :

line	parameters
1	title
2	angle between sample and beam

3		accuracy and number of planes calculation
4		number of detector angles
5		the angle values
6		number of cans plus sample
7		thicknesses of sample and can (front and back)
8	.1	number density atom or mol/$Å^3$ for sample
8	.2	absorption c/s at 1.8Å for sample
9		filename of sample total (scat+abs) c/s data
10		as 8 for can
11		as 9 for can

3.8.6 Format of output files

The .ABS files consist of a tabulation of the absorption factors, such as $A_{S,SC}$ for example, for every wavelength and scattering angle specified in the input file. The format is:-

no. of wavelengths
bank no. (not necessarily group no.), scattering angle of bank

then for each wavelength the values of

$\lambda(Å)$ $A_{S,S}$ $A_{S,SC}$ $A_{C,SC}$ $A_{C,C}$

This is repeated for each bank (normally 7 banks for LAD)

The .MUL files have a similar format. Using the notation of section 2.8 it is:-

no. of wavelengths
bank no. (not necessarily group no.), scattering angle of bank

then for each wavelength the values of

λ(Å) SINGLE(λ) M(λ) TOTAL(λ)

3.9 ROUTINE VANSM

This is a GENIE command file that removes the Bragg peaks from the vanadium spectra, puts a smooth line through the data, and divides by the calibration correction as described in section 2.7. This calibration correction is obtained by combining the results of the single and multiple scattering correction in the file with extension .REF with a vanadium Placzek correction estimated using the program g_F:N_PLAVAN, which uses the same formalism as that used for the sample Placzek correction described in section 3.11.

The routine reads the vanadium data from the file with extension .NRM and smooths using Chebyshev polynomials. The Bragg peaks are removed at the same time by ignoring the region around the peaks in the fitting procedure. The fitting routine defaults to 10 polynomials but this can be changed if required.

The routine is run from GENIE by typing @G_F:VANSM .

The routine just simply for the vanadium run number and a corresponding background run number and automatically loops through the groups. It requires a file with extension .REF to exist in the current directory, as produced by the VA command in CORAL. The smoothed result is output to a file with extension .SMO. Spectra from the SMO file can be read using the standard GENIE READ command.

It is recommended that users check that a satisfactory smooth line has been put through the vanadium data. This can be done by displaying the contents of workspaces 1 - n (n is the number of groups) after running VANSM. These workspaces contain the difference between the original .NRM data for each detector group and the smoothed version,

original .NRM data for each detector group and the smoothed version, but BEFORE the calibration correction has been applied. The command for this would be:

D/L W5 to display the difference for detector group 5

The user may wish to experiment with fitting Chebyshev polynomials of order other than the default 10:
-Before running VANSM diagnostic output may turned on by typing (in GENIE) v19=1.
-Similarly typing v20=15 sets the polynomial order to 15 for example.
The ideal polynomial order is selected so that the residual given in the diagnostic output has settled down to a value almost independent of polynomial order. Thus a suitable procedure for selecting an appropriate polynomial order involves first doing a test fit with diagnostic output on a very large (~50→100) polynomial order.

3.10 ROUTINE ANALYSE

This GENIE command file takes the spectra data and applies the corrections to produce the differential scattering cross section. The routine is invoked with the command

@g_F:ANALYSE

The routine reads sample and can data from the NRM files, the smoothed vanadium from the SMO file and corrections from the ABS and MUL files. It carries out the following operations as described in section 2.8:

- subtract background from sample
- divides sample by vanadium
- subtracts multiple scattering from sample
- if can is present :
  - subtract background from can

- divide can by vanadium
- subtract multiple scattering from can
- apply absorption correction to can
- subtract can from sample

- apply absorption correction to sample
- divide by sample calibration constant.

This is done on all groups specified and the results written to a file with extension .DCS. (Note that the sequence of operations given above is necessary in order that the corrections be performed properly.)

The ANALYSE routine requires the following input :

- option of can or no can
- sample, background and can run numbers
- range of groups to be used
- sample calibration constant which :

**** for CYLINDRICAL samples is the number of atoms or scattering units in the beam x 10^{-24}

**** for FLAT PLATE samples is the product of atomic number density (in atoms per $Å^3$) and the thickness of the sample in cm.

Spectra from the .DCS file can be read using the standard GENIE READ command.

(Note DCS stands for Differential Cross Section.)

3.11 ROUTINES PLATOM AND INTERFERE

PLATOM is a GENIE function to evaluate the self scattering from the sample. This routine uses the approach described by Powles [6] and extended by Howe, McGreevy and Howells [20] (see section 2.9) which

involves an expansion in powers of M^{-1} and derivatives of the detector efficiency and flux distribution. The user should decide whether or not this approach is acceptable for his particular experiment. It is intended to eventually offer programs implementing other alternative approaches to inelasticity correction. The routine PLATOM is executed by entering GENIE and typing:-

@g_f:PLATOM

A .NRM file is required for input so as to obtain the required Q-scale. (The default directory must be set to that of the .NRM file before entering GENIE.)

The GENIE function PLATOM can be applied to a multi-component system and requires the following input :

- number of atom species and for each one :
  - its fractional concentration (these should add to one)
  - its atomic weight. (in atomic mass units, ^{12}C=12.0)
  - its total scattering cross-section (in barns)
  - sample temperature (in units of Kelvin - used to calculate mean atomic kinetic energy in sample)

The user should check that the calculation of the self scattering is acceptable by using GENIE plots to check whether the corrected differential cross section oscillates about the calculated self scattering. At high Q the differential cross section (LAD01234.DCS) should tend to the average level given by the self scattering (LAD01234.SLF). This check may be performed by using GENIE to DISPLAY the self scattering and then to PLOT the differential cross-section on top (or vice versa). For example:

```
> READ W1 LAD01234.DCS 5
> READ W2 LAD01234.SLF 5
> D W1
> P W2
```

(Programming note: If the user makes changes to the routine PLATOM.COM to suit his own requirements he should be aware that it makes use of the GENIE variable v18.)

The GENIE routine INTERFERE is used to calculate the interference (or distinct as it is otherwise known) scattering by subtracting the self scattering (in the .SLF file) from the differential scattering cross-section (in the .DCS file). This routine is invoked by entering GENIE and typing:-

```
@g_f:INTERFERE
```

3.12 ROUTINE MERGE

This GENIE command file combines selected areas of spectra from different groups into one composite S(Q) as defined in section 2.10. For input it requires the sample .DCS or .INT file, the vanadium .SMO file and the vanadium .MON file to be present in the user's area. The output is in the file with extension .SOQ. Before running this command file the user must determine by plotting the results from ANALYSE or INTERFERE to determine which groups and which Q ranges for each group he or she wishes to merge. The routine is invoked by typing:-

```
@g_F:MERGE
```

3.13 ROUTINES STOG AND GTOS

These GENIE functions carry out the Fourier Transform of S(Q) to g(R) and its inverse g(R) to S(Q). They are invoked with the GENIE TRANSFORM command. Otherwise the required input by the user should be fairly straightforward. The command is for example, after the GENIE

```
TR W1 g_f:STOG W2
```

etc. Note that for these routines to work correctly it essential for both S(Q) and g(r) to oscillate about unity.

APPENDIX A RESOLUTION OF A TIME-OF-FLIGHT DIFFRACTOMETER

The three dimensional quality of the transforms (1.2.1) or (1.2.2) has an important consequence when examining the effect of resolution broadening on peaks in $S(\underline{Q})$. Figure A1 shows a projection of scattering space onto the $(Q,\theta,\phi=0)$ plane - in effect the Ewald sphere for the diffraction experiment. $\underline{k}$ and $\underline{k}'$ are the incident and scattered wave vectors, which are assumed to have the same magnitude, and the scattering angle is $2\theta_0$. With this geometry $|\underline{Q}_0| = 2k\sin\theta_0$. In fact two spheres, separated in Q by ΔQ_0, are shown corresponding to the edges of the time channel under consideration. The combination of angular uncertainty, pulse width and timing uncertainty means that at each time channel the detector probes a volume of reciprocal space (shown as the shaded area in figure A1) whose magnitude is given approximately by

$$\Delta\underline{Q} = Q_0^2\cos\theta_0\Delta\theta_D\Delta\phi_D\Delta Q_0 = Q_0^2\Delta\Omega\Delta Q_0/4\sin\theta_0 \qquad (A1),$$

provided ΔQ_0 and $\Delta\Omega$ are not too large. Here $2\Delta\theta_D$ and $\Delta\phi_D$ are the effective polar angular widths of the detector, and $\Delta\Omega = 2\sin 2\theta_0\Delta\theta_D\Delta\phi_D$ is the solid angle of the detector. Note that since $\Delta\Omega$ is fixed for a given detector position, the volume of reciprocal space probed by the detector varies as $Q_0^2\Delta Q_0/\sin\theta$.

This volume of reciprocal space is not sampled uniformly by the detector. Instead we describe the distribution of $\underline{Q}$ vectors probed by the detector for a given scattering angle and time-of-flight channel by a RESOLUTION function, $R(\underline{Q},\underline{Q}_0)$, which incorporates all the effects which affect resolution e.g. pulse width, flight path uncertainty, angular uncertainty. For conservation reasons the resolution function must be normalizable:

$$\int d\underline{Q}\, R(\underline{Q},\underline{Q}_0) = 1. \qquad (A2)$$

where the integral is taken in the volume around $\underline{Q}_0$. With this definition we can write down the measured structure factor (as opposed to that which would ideally be measured with infinitely sharp

resolution) as

$$S_M(\underline{Q}_0) = \int d\underline{Q}\ S(\underline{Q})\ R(\underline{Q},\underline{Q}_0) \qquad \text{(A3)}$$

The definition (A2) ensures that if, for example, $S(\underline{Q})$ is everywhere unity (e.g a structureless fluid or purely incoherent scatterer) then $S_M(\underline{Q}_0)$ is also everywhere unity as expected.

The consequence of this convolution on the measured pair correlation function can be seen if we insert (1.2.1) into (A3).

$$S_M(\underline{Q}_0) = 1 + \rho \int d\underline{Q}\ R(\underline{Q},\underline{Q}_0) \int d\underline{r}\ (g(\underline{r}) - 1)\ \exp(i\underline{Q}.\underline{r})$$

$$= 1 + \rho \int d\underline{r}\ (g(\underline{r}) - 1)\ R(\underline{Q}_0,\underline{r}) \qquad \text{(A4)}$$

where

$$R(\underline{Q}_0,\underline{r}) = \int d\underline{Q}\ R(\underline{Q},\underline{Q}_0)\ \exp(i\underline{Q}.\underline{r})$$

$$= \exp(i\underline{Q}_0.\underline{r}) \int d\underline{Q}\ R(\underline{Q},\underline{Q}_0)\ \exp[i(\underline{Q}-\underline{Q}_0).\underline{r}]. \qquad \text{(A5)}$$

The simple Fourier transform in (1.2.1) is now replaced by a more complicated function which in general will not have a direct inversion. However if the Fourier transform of the resolution function (A5) can be calculated then the problem is still amenable to forward transform techniques such as maximum entropy methods with no loss in computing time because the inherent linearity of the transform is preserved.

The resolution function is frequently estimated by convoluting the various contributions to the resolution function together. Such a convolution strictly assumes the contributions are orthogonal which is only partly correct. However the convolution approach is valid in two limits, and probably gives satisfactory approximate results in intermediate cases as well. At small scattering angles geometric

effects dominate the resolution which usually means the effects of pulse width and flight path uncertainty can be ignored. On the other hand, at large scattering angles where geometric considerations assume less importance the resolution is dominated by the neutron pulse width, in which case the geometric effects can be represented by convolution of the pulse shape with a simple peak shape, usually Gaussian. The three main causes of resolution broadening will now be described briefly (see "Pulsed Neutron Scattering" by Colin Windsor [1]): the intrinsic pulse width for a given neutron energy or wavelength, Δt, the flight path uncertainty to the detector, ΔL, and the scattering angle uncertainty due to the finite size of the moderator, sample and detector.

A1.1 The neutron pulse shape

The pulse width is determined by moderator characteristics and so is independent of flight path and scattering angle and so is certainly orthogonal to the other contributions to the resolution function. It leads to an uncertainty in the neutron's incident velocity, v, or wave vector, k, for a given time channel. The wave vector uncertainty in turn contributes to the uncertainty in the magnitude of $|\underline{Q}|$, but not to the direction of $\underline{Q}$.

The neutron pulse shape at the moderator as a function of time t and neutron velocity v_0, is given by

$$P(t,v_0) = (\Sigma_s v_0 t)^2 \exp(-\Sigma_s v_0 t) \qquad \text{(A6)}$$

in the epithermal region, and this must be convoluted with a longer exponential tail in the thermal region [see Colin Windsor's book or notes from Andrew Taylor, RAL-84-120 (1984)]. For full details see the paper by Ikeda and Carpenter, Nucl. Inst. Meth.,A235, 553 (1985). Σ_s is the macroscopic cross section of the moderating material. Note that the pulse shape is the same irrespective of whether it is presented as function of t or v_0. When it reaches the detector after a flight path

length L the pulse shape is unchanged, but it is shifted in time by $t_0 = L/v_0$. Hence the pulse shape as a function of time at the detector is

$$P(t,t_0,v_0) = [\Sigma_s v_0(t-t_0)]^2 \exp[-\Sigma_s v_0(t-t_0)]. \qquad (A7)$$

The pulse width correction arises in practice because we fix the time for a particular channel and evaluate the contribution of all reciprocal lattice points to that time channel by virtue of the velocity uncertainty of the neutron. In that case v_0 is the smallest neutron velocity that can reach the detector at time $t=t_0$. Hence the distribution of neutron velocities v (always greater than v_0) for this time channel is given by

$$P(t_0,v,v_0) = [\Sigma_s t_0(v-v_0)]^2 \exp[-\Sigma_s t_0(v-v_0)]. \qquad (A8)$$

For liquids and amorphous diffraction there is the additional complication arising from the inelastic scattering of the sample. However since the interference inelasticity correction tends to be small in many cases it is unlikely that inelasticity will have a very pronounced effect on the observed resolution. Thus for the present purpose it will be assumed that the scattering is elastic.

We write $\hbar k=mv$, where k is the neutron wave vector and m the neutron mass, and with $k_0 = mL/\hbar t_0$, $Q=2k\sin\theta$ and $Q_0 = 2k_0\sin\theta$, the pulse shape in reciprocal space appears as

$$P(Q,Q_0) = [\Sigma_s L(Q-Q_0)/Q_0]^2 \exp[-\Sigma_s L(Q-Q_0)/Q_0]. \qquad (A9)$$

In this form the advantage of going to a longer flight path can be seen explicitly: as L is made larger the pulse decays more rapidly and becomes narrower in reciprocal space. Also it will be seen that FWHM of the resolution function, $\Delta Q/Q=\Delta\lambda/\lambda=$ constant for a given total flight path.

A1.2 Flight path uncertainty

The flight path uncertainty arises because we necessarily must use finite size moderators, samples and detectors. Therefore it depends closely on the particular instrumental geometry. Furthermore it cannot be regarded as decoupled from the scattering angle uncertainty since different points in the moderator, sample and detector may define different scattering angles as well as different flight paths. Therefore the normal approach is to treat the flight path uncertainty as part of the geometric contribution to the resolution of a diffractometer. It is incorporated into the scattering angle uncertainty as an "effective" angular uncertainty.

A1.3 Scattering angle uncertainty

The scattering angle uncertainty of recorded events in the detector lead to an uncertainty in $\underline{Q}$, $\Delta\underline{Q}$, both in direction and magnitude, in a manner which varies depending on the precise details of the instrument geometry. Normally for accurate numbers the geometric contribution to the resolution function has to be determined by computer simulation of a model of the instrument, or by measuring the profile of Bragg peaks. Because the results of such a simulation indicate that the geometric contribution is usually quite symmetric, except at very small scattering angles, it is useful to represent the angular uncertainty with an effective angular width for the detector, $2\Delta\theta_D$. In fact the geometric contribution is usually found to be roughly Gaussian in $\Delta\theta$, where $2\Delta\theta$ is the difference between the nominal scattering angle of the detector, $2\theta_0$, and the actual scattering angle, 2θ, of a particular neutron event in the detector. Provided $\cot\theta_0\Delta\theta_D$ is ~10% or less and $\Delta\theta$ has a symmetric distribution about θ_0, then the geometric contribution to the resolution is roughly symmetric irrespective of whether it is presented as a function of wavelength, time or Q.

For the geometric contribution a reasonable approach is to assume that the scattering angles probed by the detector are distributed in a

Gaussian manner about $\theta=\theta_0$. This assumption can be verified to be approximately correct for the typical instrumental geometries which occur in practice. In that case we describe the distribution by

$$P(\theta,\theta_0) \sim \exp[-(\theta-\theta_0)^2/2\gamma^2) = \exp[-\Delta\theta^2/2\gamma^2] \qquad (A10)$$

where γ describes the angular width of the distribution and it is assumed that $\gamma << \theta_0$. Writing $\Delta Q \simeq 2k\cos\theta_0\Delta\theta = Q_0\cot\theta_0\Delta\theta$ we see that the geometric contribution to the resolution function in reciprocal space is represented by

$$R_G(Q,Q_0) \sim \exp[-\Delta Q^2/2Q_0^2\gamma_Q^2] = \exp[-(Q-Q_0)^2/2Q_0^2\gamma_Q^2] \qquad (A11)$$

where $\gamma_Q = \gamma\cot\theta_0$. The normalization condition (A2) with (A1) then requires that

$$R_G(Q,Q_0) = A\exp[-(Q-Q_0)^2/2Q_0^2\gamma_Q^2] \qquad (A12)$$

where

$$A = \frac{1}{\sqrt{(2\pi)Q_0^2\sin\theta_0\Delta Q_0\Delta\phi_D\gamma_Q}}.$$

In solving the integral (A2) for this function we note that the integral over ϕ coordinate of the detector does not affect the magnitude of Q, and we have assumed that the incident wave vectors are distributed uniformly over ΔQ_0. This form exhibits the well known result that the width of the geometric contribution, $\Delta Q/Q$, to the resolution function is constant for a given scattering angle, and varies with scattering angle θ_0 as $\cot\theta_0$.

A1.4 Application to liquids and amorphous materials diffraction

For an instrument such as LAD (and SANDALS when it comes on stream) the geometric term dominates the resolution function for scattering angles below about 40°. Since this is the important measuring region, as far as minimizing Placzeck corrections is concerned, we can safely assume that an expression such as (A12) will adequately represent the resolution of the diffractometer. With this choice the Fourier transform of the resolution function (A5) can be evaluated analytically. First we note that for this case (and also polycrystalline materials) the integrals over the directions of $\underline{Q}$ in (A3) can be done immediately to give

$$S_M(Q_0) = \frac{1}{\sqrt{(2\pi)}Q_0\gamma_Q}\int_0^{+\infty} dQ\, \exp\left[-\frac{(Q-Q_0)^2}{2Q_0^2\gamma_Q^2}\right] S(Q). \qquad (A13)$$

Inserting the definition for S(Q) (1.2.2) into (A13) leads to the result:

$$S_M(Q_0) = 1 + 4\pi\rho\int_0^{\infty} dr\, r^2(g(r) - 1)\, R(Q_0,r) \qquad (A14)$$

where

$$R(Q_0,r) = \frac{1}{\sqrt{(2\pi)}Q_0\gamma_Q}\int_0^{\infty} dQ\, \exp\left[-\frac{(Q-Q_0)^2}{2Q_0^2\gamma_Q^2}\right]\frac{\sin(Qr)}{Qr}.$$

Writing $Q=Q_0 + Q'$ and assuming that always $|Q'| \ll Q_0$, this last integral can be solved analytically using standard integral tables (see Gradshteyn and Ryzhik, p 480 and p495, 1980 edition, Academic Press, London). To second order in γ_Q the result is

$$R(Q_0,r) = \left[\frac{\sin(Q_0r)}{Q_0r} - \gamma_Q^2\cos(Q_0r)\right]\exp\left[-\frac{r^2Q_0^2\gamma_Q^2}{2}\right]. \qquad (A15)$$

Therefore the main effect is that that the exact transform of equation

(1.2.2) is modulated by a Gaussian decay caused by the finite resolution in Q space.

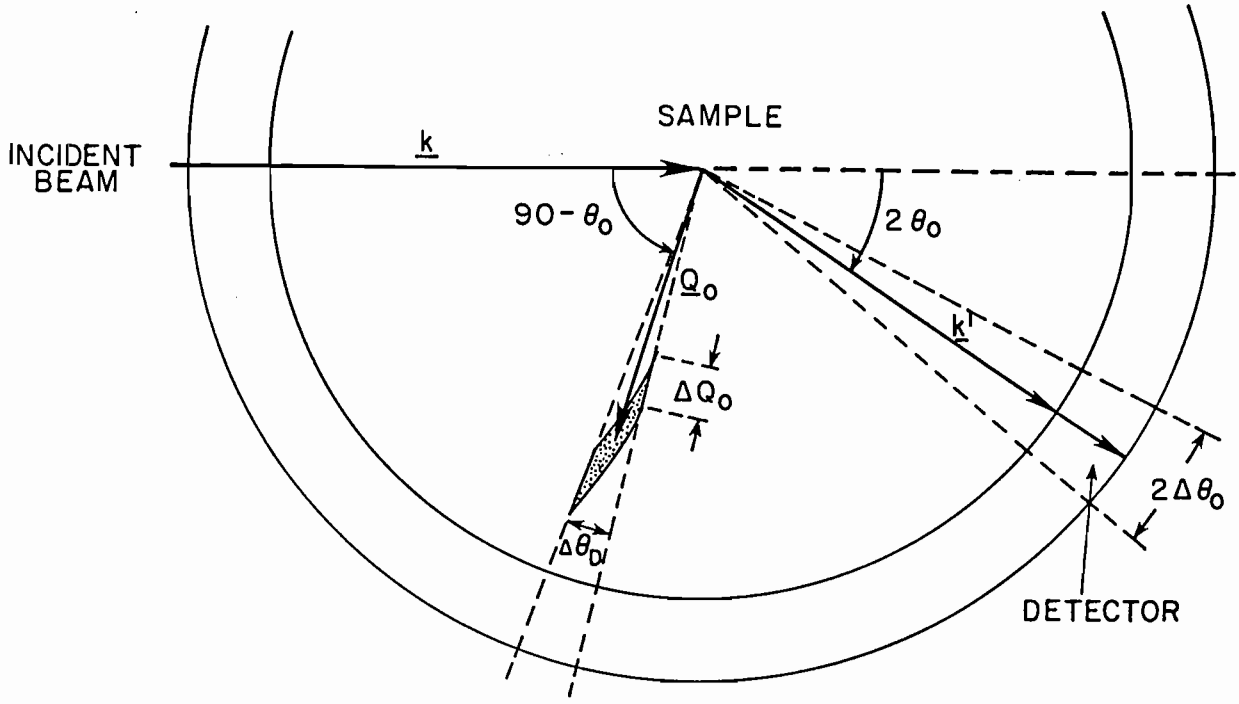

Figure A1 Geometry of scattering in reciprocal space

APPENDIX B ESTIMATING THE COUNT RATE ON A TOF DIFFRACTOMETER

Because the features in a liquid or amorphous material's diffraction pattern are rather broad (compared to crystalline powder diffraction) the requirements for resolution are relatively relaxed (provided very large Q values are not needed), but an adequate count rate can be crucial to obtaining a useful result, particularly for those experiments which involve differencing datasets as a function of pressure, temperature, isotope, etc. In these cases the differential behaviour is usually more important than the total scattering pattern. Therefore count rate is almost always the primary quantity of interest. Typically the data are mapped out as a function of Q in bins of width say $\Delta Q=0.05\text{Å}^{-1}$, and the quantity of interest in rating the performance of a diffractometer is therefore the count rate per Q-bin per unit volume of standard scatterer which is normally vanadium:-

neutrons / s / 0.05Å^{-1} / cm^3 of vanadium (B1).

This definition serves to normalize out differences between instruments which are purely geometric in origin, (usually the size and shape of the beam at the sample position).

This number is also useful to know for a given diffractometer: a rough estimate of the count rate for a given sample can be obtained by multiplying it by the volume of sample times the ratio of sample scattering cross section to vanadium scattering cross section. It would be helpful therefore if this number could be specified for all liquids diffractometers so that realistic intercomparisons could be be made. For convenience we shall refer to the count rate number according to (B1) as the "C-number" for a given diffractometer.

For reactor experiments the count rate is almost independent of Q, but for pulsed sources the spectrum falls as 1/Q in the epithermal region. In addition the detector efficiency is proportional to $\lambda \sim 1/Q$, so the measured count rate falls as $1/Q^2$. In practice efficiency corrections mean that the intensity falls more like $1/Q^{1.7}$, but even so

there is a dramatic fall in measured count rate with increasing Q, as shown in figure B1, where the measured spectrum for LAD at a scattering angle of 20° is displayed.

For the methane moderator at ISIS, the parameter that describes the epithermal flux is Φ_o and at 100μA proton current and 750 MeV energy, this has the value for a moderator area of 100 square cm, (see Table 1.1)

$$\Phi(E) = 2.7 \times 10^{12}/E^{0.92} \text{n/eV/sr/100cm}^2\text{/s} \qquad \text{(B2)}$$

Now $E \sim Q^2$ so $\Phi(Q) = 2(E/Q)\Phi(E)$

$$\simeq 5.4 \times 10^{12}/Q \text{ n/Å}^{-1}\text{/sr/100cm2/s}$$

$$= 2.7 \times 10^{11}/Q \text{ n/0.05Å}^{-1}\text{/sr/100cm2/s.} \qquad \text{(B3)}$$

Using these values the expected count rate on LAD can be estimated. It is assumed that:-

(i) the collimator views most of the active area of moderator;
(ii) the incident flight path is 10m;
(iii) the sample is a cube of vanadium, 10 x 10 x 10mm^3 in volume (corresponding to a 30% scatterer);
(iv) detector is 30% efficient (corresponds to a ^{3}He tube at 2eV, and Q≃10Å^{-1} for 20° scattering angle);

then the scattered count rate per unit detector solid angle is

$$2.7 \times 10^{11} \times 0.3 \times 1.0 \times 10^{-6} \times 0.3 / 4\pi Q$$

↑ moderator; ↑ fraction scattered by sample; ↑ sample solid angle at moderator; ↑ detector efficiency

$$= 1940/Q \text{ n/0.05Å}^{-1}\text{/sr/s/cm}^3\text{V}. \qquad \text{(B4)}$$

It will be noted that this number, which of course applies strictly only to the epithermal region of the spectrum, is **independent** of scattering angle for a given Q value. The fact that count rates vary for different scattering angles in practice arises primarily from variations in detector solid angle and efficiency. For LAD at $2\theta = 20°$ the detector area is $2 \times 0.04 \times 0.2 m^2$ and the final flight path is 1.0m, and so for $Q = 10Å^{-1}$ the C-number is $3.1n/0.05Å^{-1}/s/cm^3V$. The C-number is quoted at $Q = 10Å^{-1}$ since it is important to remember the very rapid decline in count rate at a pulsed diffractometer with increasing Q value.

Figure B1 shows that the measured C-number is much lower at $\sim 0.7n/0.05Å^{-1}/s/cm^3V$ for this Q value (and $\sim 22n/0.05Å^{-1}/s/cm^3V$ at $Q = 1Å^{-1}$), and the reason for this disagreement is not known at the present time. It should be born in mind of course that for most experiments several LAD detector banks can be combined so that the count rate should be multiplied by a factor of ~2-3 to get a realistic estimate of likely count rates. Even so the very rapid fall in count rate with increasing Q is clear from figure 5.

For the new glass diffractometer at IPNS, GLAD, the estimated C-number assuming a full complement of detectors at the same Q value is $\sim 20 - 25n/0.05Å^{-1}/s/cm^3V$ at $Q = 10Å^{-1}$, (Montague and Price, 1988, private communication), which includes the factor of 2.5 enhancement which has taken place since the booster target was installed.

Finally for the D4B diffractometer at ILL the measured neutron flux on the sample is 4×10^7 n/cm^2/s for a wavelength of 0.7Å, so the C-number for the standard cube of vanadium would be

4×10^7	x	0.3	x	5.5×10^{-4}	x	0.67	x	0.15 / 4π
↑		↑		↑		↑		↑
flux		fraction scattered by sample		detector solid angle for 0.05Å^{-1} bins		detector effic.		sampling factor

$$= 53 \text{ n/0.05Å}^{-1}\text{/s/cm}^3\text{V}.$$

The sampling factor arises here because the present detector does not scan all scattering angles simultaneously. This number is entirely in accord with the observed count rate from a sample of vanadium placed in the neutron beam on D4B (A C Barnes, 1988, private communication).

Comparison of the D4B C-number with figure B1 shows that when several angles are combined the LAD diffractometer is already as intense as D4B, but only in a narrow region of Q, around Q≃1Å^{-1}. Outside this region the intensity falls off rapidly.

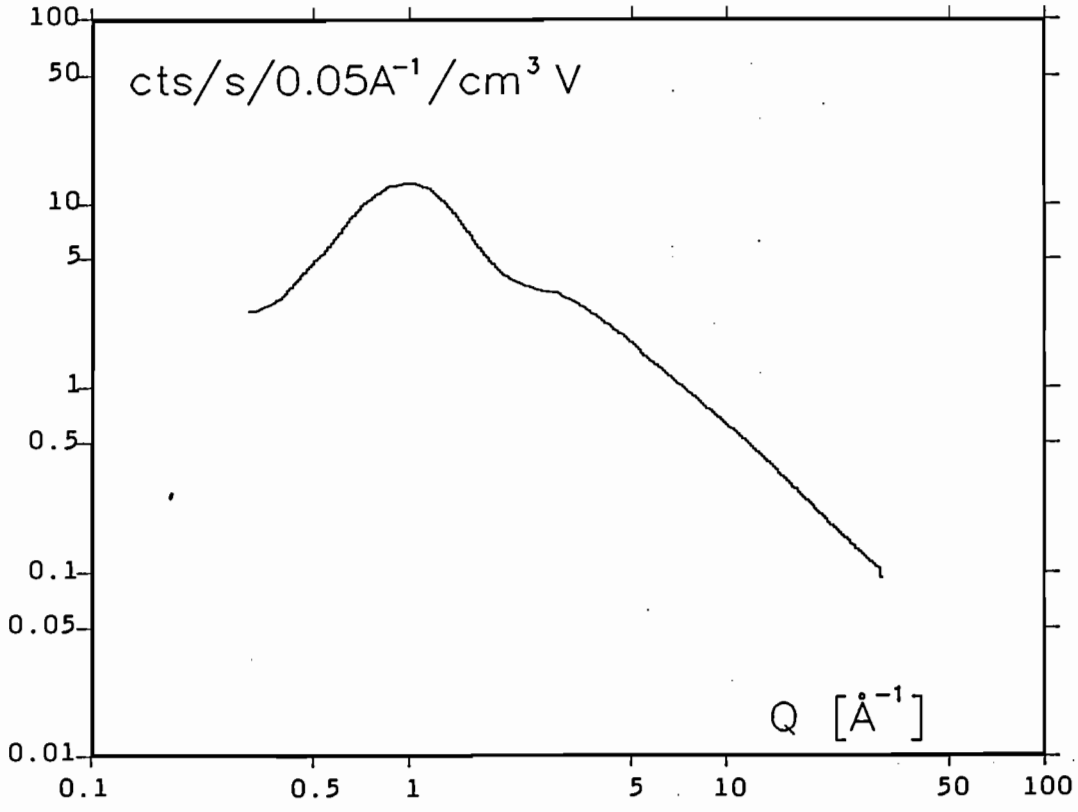

Figure B1 Measured count rate (or "C-number" - see text) for LAD at 20° scattering angle as a function of Q. Note the log axes.

APPENDIX C MAXIMUM ENTROPY METHODS IN NEUTRON SCATTERING: APPLICATION TO THE STRUCTURE FACTOR PROBLEM IN DISORDERED MATERIALS

C.1 Introduction

A broad class of problems in neutron scattering involve the inversion of a set of measurements, the data D_i, to a desired distribution function, N_j, the N_j being related to the D_i via a transform of some kind:-

$$D_i = \mathrm{Tr}\left\{ N_j \right\}, \qquad i,j = 0,1,\ldots,\infty \tag{C1}$$

This inversion is often impossible or ill-conditioned for several reasons:-

(a) the transform may not be linear;
(b) the data may be incomplete, i=i1 ... i2;
(c) the data are measured at discrete points;
(d) the data may be noisy;
(e) the data may have systematic errors.

Because of the ill-conditioning it is likely that several or perhaps a large set of distributions N_j can be regarded as consistent with the measured data.

Over the years a large number of methods have evolved to cope with the variety of difficulties which arise in the inversion of incomplete data. Of these it is claimed, Jaynes [22], that the Maximum Entropy (ME) approach, which attempts to avoid producing any information which is not justified by the data, provides an independent assessment of all the possible solutions to a particular problem, and so leads to that solution which is "maximally non-committal" with respect to the unmeasured data. This is achieved via an entropy metric which is usually defined as

$$H = - \sum_j N_j \ln \{N_j/P_j\} + \sum_j N_j - \sum_j P_j \qquad (C2)$$

where P represents a "prior" distribution which incorporates previous knowledge about the distribution not contained in the data. The second and third terms are introduced in (C2) in the event that N and P are not normalizable distributions. In the absence of any other information the ME solution, which attempts to maximize H, is simply N = P for all j. When constrained by additional information, i.e. the measured data, the entropy falls below its maximum value. The object of the ME method therefore is to find that solution for N which satisfies the data but which also keeps H as near as possible to its maximum value. It will be seen that this definition of H only exists if $N_j, P_j > 0$.

The goodness of fit to the data is usually measured by a χ-squared statistic or R-factor:

$$R_f^2 = \sum_i (D_i - M_i)^2 \; / \; \sum_i D_i^2 \qquad (C3)$$

where M_i is an estimate (or "model") of the i'th data point obtained from the estimated trial N distribution via (1). With this definition a "quality factor", or Q-factor, which represents how well a particular solution satisfies the dual constraints of entropy maximization and fit to the supplied data, is defined as

$$Q_f^2 = - H + xR_f^2, \qquad (C4)$$

where x is an undetermined positive multiplier which controls how closely the model fits the data. Therefore it is the Q-factor which is to be minimized, with x determined by constraining the R-factor to a predefined value.

In setting up the ME solution for a given experimental situation, there are two questions that need to be confronted. Firstly what is the

most appropriate distribution space, the N distribution, in which entropy is to be calculated? Secondly, what is the most reasonable choice for the prior distribution, or P distribution. It is frequently assumed that the prior distribution should be uniform even though the existence of the data implies that the real distribution is anything but uniform. Unfortunately both of these questions are often ignored in the literature, there being an implicit assumption that somehow maximizing entropy will cover up all the difficulties. In the sections that follow I will apply the ME method to the problem of calculating the pair correlation function for a liquid or amorphous material from structure factor data. I will demonstrate that the obvious choice for the distribution N is in fact quite inappropriate in this case, and that the result of ME analysis can depend markedly on the choice of prior distribution. Full details on the correct choice for the N and P distributions for the entropy estimation for this problem are given elsewhere, but some examples of the results are shown here. The conclusions to be drawn are applicable to many other applications where ME techniques are used.

C.2 Solution of the Maximum Entropy Problem

The general solution of the ME problem is a highly non-linear problem and several solutions exist, mostly using sophisticated search procedures, Bryan and Skilling [23]. I have a developed a Monte Carlo (MC) solution to this problem which has several attractive features. In particular it is simple to execute, can allow error bars on the calculated distributions to be estimated if needed, and by virtue of the stochastic process intrinsic to MC calculations is unlikely to get stuck in local phase space minima. The object of the MC calculation is to set up an ensemble of distributions such that each member occurs with probability

$$p(Q_f^2) = \exp\{-\lambda Q_f^2\} \qquad (C5)$$

with λ a positive multiplier which determines the size of the Q-factor

and its fluctuations: as λ is made larger so the Q-factor is driven smaller and the fluctuations become smaller. Full details of this algorithm are given elsewhere, and will not be elaborated further here. However it will be noted that in all the examples given below λ is kept as large as possible, so that fluctuations are held to a minimum and the individual trial distributions lie indistinguishably close to the ME solution. Typical run times for this algorithm, which might involve 500,000 individual moves, are ~10 minutes of cpu on a VAX 8650, assuming 200 data points and 500 points in the N distribution.

C.3 The Structure Problem in Disordered Systems

The underlying transform in the structure of liquids and amorphous materials is in principle a straightforward Fourier transform:

$$S(Q) = 4\pi\rho \int_0^\infty r\{ g(r)-1 \} \sin(Qr)\, dr \qquad (C6)$$

where S(Q) is the measured structure factor, as a function of wave vector transfer, Q, and g(r) is the underlying pair distribution function as a function of radial distance r from an atom at the origin. The atomic number density is ρ. Inverting this transform directly can lead to significant transform errors because the data can never be measured over a complete range of Q values and in any case invariably contain some form of error, statistical or systematic. Typically one introduces the constraint of only calculating g(r) at certain values of r, according to the Lado [24] rules for Fourier transforms, i.e. $\Delta r = \pi/Q_{max}$. Furthermore a "window" function is often invoked to further reduce the effects of noise in the calculated distribution function.

This problem is readily amenable to ME analysis. In particular there is apparently an obvious choice for the N distribution by virtue of the normalization

$$4\pi\rho \int_0^\infty r^2\{ g(r)-1 \}\, dr = -1 + \rho\chi k_B T \qquad (C7)$$

where χ is the isothermal compressibility and T is the absolute temperature. Hence the "obvious" choice for the N distribution is simply

$$N_j = N(r_j) = 4\pi\rho r_j^2 g(r_j)\Delta r \qquad \text{(C8)}$$

where Δr is the bin width of the discretized distribution. Figures C1 and C2 show the effects of applying ME analysis to the problem of transforming the hard sphere structure factor to pair correlation function. In this case the input S(Q) is known exactly within the Percus-Yevick approximation but is a particularly severe test of any transform method because g(r) for hard spheres is discontinuous at $r=\sigma$, the hard core diameter. In this case the density was chosen such that $\rho\sigma^3 = 0.5$, and a large Q limit of $Qmax = 15/\sigma$ was imposed on the S(Q) data, with $\sigma = 1$Å. In figure C1 the prior distribution is

$$\begin{aligned} P_j &= 0 && \text{for } r_j < \sigma \\ p_j &= 4\pi\rho r_j^2\Delta r && \text{for } r_j > \sigma, \end{aligned} \qquad \text{(C9)}$$

while for figure C2 the prior distribution is set at

$$\begin{aligned} P_j &= 0 && \text{for } r_j < 0.75\sigma \\ p_j &= 4\pi\rho r_j^2\Delta r && \text{for } r_j > 0.75\sigma. \end{aligned} \qquad \text{(C10)}$$

In either case the fit to the data was the same, (R-factor = 1%); however it is readily apparent that the two results for g(r) are not the same. In particular the distribution in figure C2 has greater entropy than figure C1 (-2.064 for figure C2 compared to -2.534 for figure C1) when measured against the uniform prior, thus confirming that the algorithm has found the true maximum entropy solution for figure C2. This result is apparently at odds with our intuition which might tend to favour the one in figure C1 as being less "structured", if the word "structure" in this case is taken to indicate the number

and size of peaks and valleys in the calculated distribution. In fact the distribution in figure C1 is very close to the known exact solution, Throop and Bearman [25].

The difference between the two solutions is manifested in Q space not in the region of the input data, where the two solutions give equally good fits, but beyond the input region. Figure C3 shows the calculated structure factor for the distribution in figure C2, and also the difference between model and data. It is seen that immediately beyond the data (Q ~ 15-16 $Å^{-1}$) there is a strange cusp in the S(Q) from figure C2, a phenomenon which has been seen before, Root, Egelstaff and Nickel [26]. The ripples seen in figure C2 become suspect when it is realized they have a period of ~ $2\pi/Q_{max}$, where Qmax is the largest Q value for the input data. Hence it is concluded that maximizing the entropy has not avoided the truncation ripples associated with the discontinuity in the input data at Q=Qmax. For measured datasets which usually have a noise component, the discontinuities become important since there is effectively a discontinuity at every data point.

C.4 Solution of the Discontinuity Problem

Two solutions to the problem of discontinuities are proposed. The first is to effectively force S(Q) to be everywhere continuous and have continuous derivatives. To see how to do this a well known theorem from Fourier transforms is invoked, Lighthill [27]. From (6) it can be seen that the n'th derivative of S(Q) is given by

$$S^n(Q) = 4\pi\rho(-1)^{n/2} \int_0^\infty r^{n+1}\{ g(r)-1 \} \sin(Qr)dr \qquad \text{for n=even} \qquad (C11)$$

and

$$S^n(Q) = 4\pi\rho(-1)^{(n-1)/2} \int_0^\infty r^{n+1}\{ g(r)-1 \} \cos(Qr)dr \qquad \text{for n=odd}$$

Therefore if {g(r)-1} converges slower than $1/r^{n+2}$ as $r \to \infty$, there will be discontinuities in the n'th derivative. On the other hand if $\exp(\alpha r)\{g(r)-1\}$, where α is a finite positive number, is convergent as $r \to \infty$ then $r^{n+2}\{g(r)-1\}$ is also convergent at large r for all n. For the hard sphere pair correlation function the exponential decay of {g(r)-1} with increasing r is an analytic consequence of the theory which describes the hard sphere structure factor, Perry and Throop [28]. For other liquid and amorphous structures the requirement that S(Q) be continuous and have continuous derivatives is a necessary consequence of there being no long range order in the material.

This exponential constraint leads to a simple revision of the definition of the N and P distributions, namely

$$N_j' = \exp(\alpha r_j) * N(r_j) = 4\pi\rho \exp(\alpha r_j) r_j^2 g(r_j) \Delta r \qquad (C13)$$

and

$$\begin{aligned} P_j' &= 0 && \text{for } r_j < \sigma \\ P_j' &= 4\pi\rho \exp(\alpha r_j) r_j^2 \Delta r && \text{for } r_j > \sigma. \end{aligned} \qquad (C14)$$

The primed distributions are used instead of the unprimed distributions in the definition of entropy, equation (2). Otherwise the calculation proceeds as before. The inverse correlation length, α, is determined from the width of the narrowest peak in S(Q), or by inspection of the large r behaviour of g(r). Hence for a previously unknown dataset it may be necessary to redetermine its value once an initial solution has been achieved.

Figures C4 and C5 show the results of applying this exponential constraint in the definition of entropy, with α = 1.8/Å. It can be seen that the ripples in figure C2 have been largely eliminated in figure C4, and that the problem of the cusp in S(Q) at Q=Qmax has now been

erradicated (figure C5). The fit is a good as before (R-factor = 1%), and the entropy is only marginally lower than for figure C2, being equal to -2.096.

C.5 Coping with Truncation Effects

It is apparent in figure C4 that some truncation effects may still be present in the estimated distribution functions. These arise because in estimating the change in Q-factor at each move, there is a sum over the input data which in effect is a Fourier transform of the difference $D_i - M_i$. Since the change in Q-factor at each move is the driving force behind the calculation this Fourier transform can give rise to exactly the same truncation effects seen in a direct transform of the raw data. My solution to this difficulty is to evaluate the transform only at the allowed r values ($r_j = j\pi/Qmax$), and then interpolate the result onto the required grid of r values by linear interpolation.

Figure C6 shows the result of doing this for the same input dataset as before. Now it will be noted that truncation effects are diminished even further: the result is now approaching that of figure 1, but with greater entropy (H = -2.141).

C.6 Conclusion

The foregoing text has described the application of the ME method to the calculation of the pair correlation function from structure factor data for liquid and amorphous materials. The main conclusion is that ME does not automatically guarantee that the results are free from artifacts associated with noise and truncation in the data. To avoid these artifacts it is necessary to build into the distributions used to calculate entropy known physical constraints which must be satisfied, whatever the detailed form the distributions are to take. For the structure factor problem these constraints include the requirement that the structure factor must everywhere be continuous and have continuous

derivatives, and that the fluctuations in the distributions away from the prior distribution are not biassed by the truncation of the input data. Further details and applications of the Monte Carlo algorithm used here are available elsewhere as well as a discussion of the present approach in the context of other recent attempts at the structure factor problem.

C.7 Acknowledgement

I would like to acknowledge invaluable discussions on the subject matter of this paper with S. Baer, T. Gaskell, and N. Rivier.

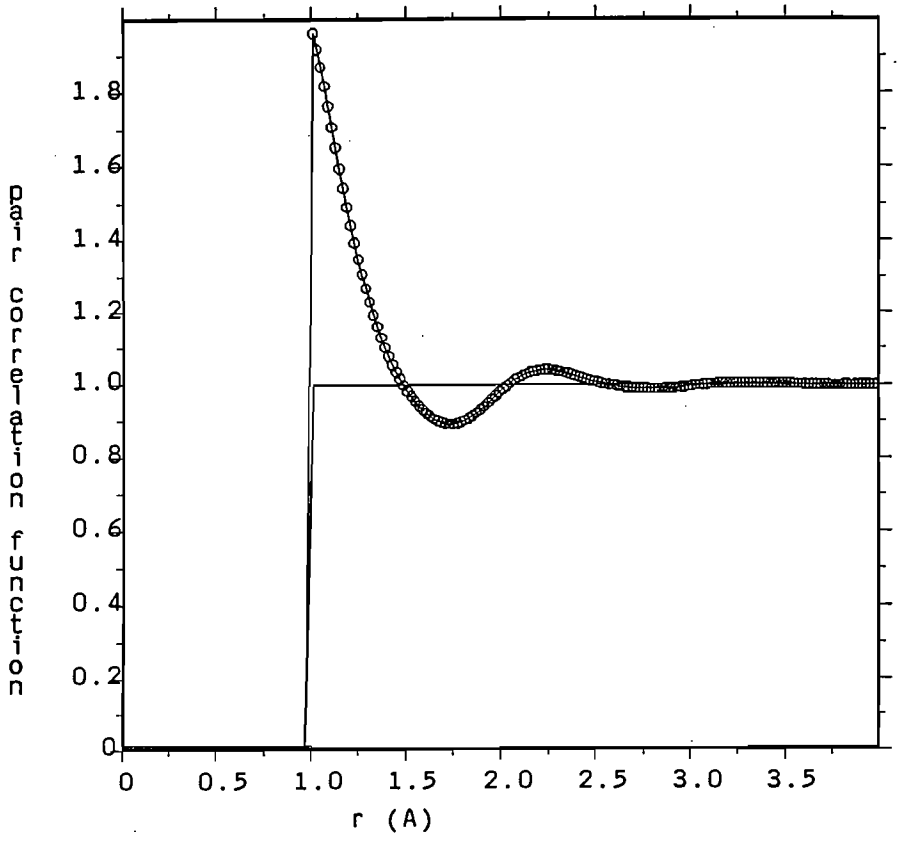

Figure C1 Maximum entropy pair correlation function derived from Percus Yevick hard sphere structure factor. The S(Q) data were truncated at Q = 15Å^{-1}, and the prior distribution used is zero in the region r = 0 to r = 1Å. The circles show the calculated distribution and the line shows the prior.

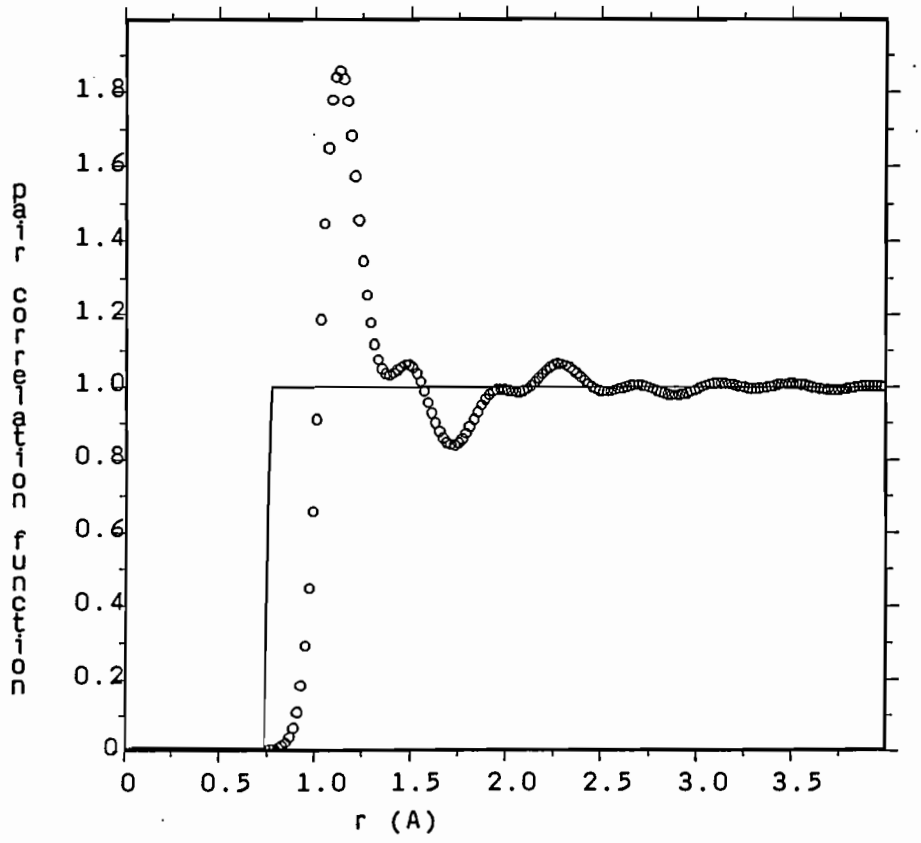

Figure C2 Same calculation and notation as for figure 1 except that the prior is zero in the region r = 0 to r = 0.75Å.

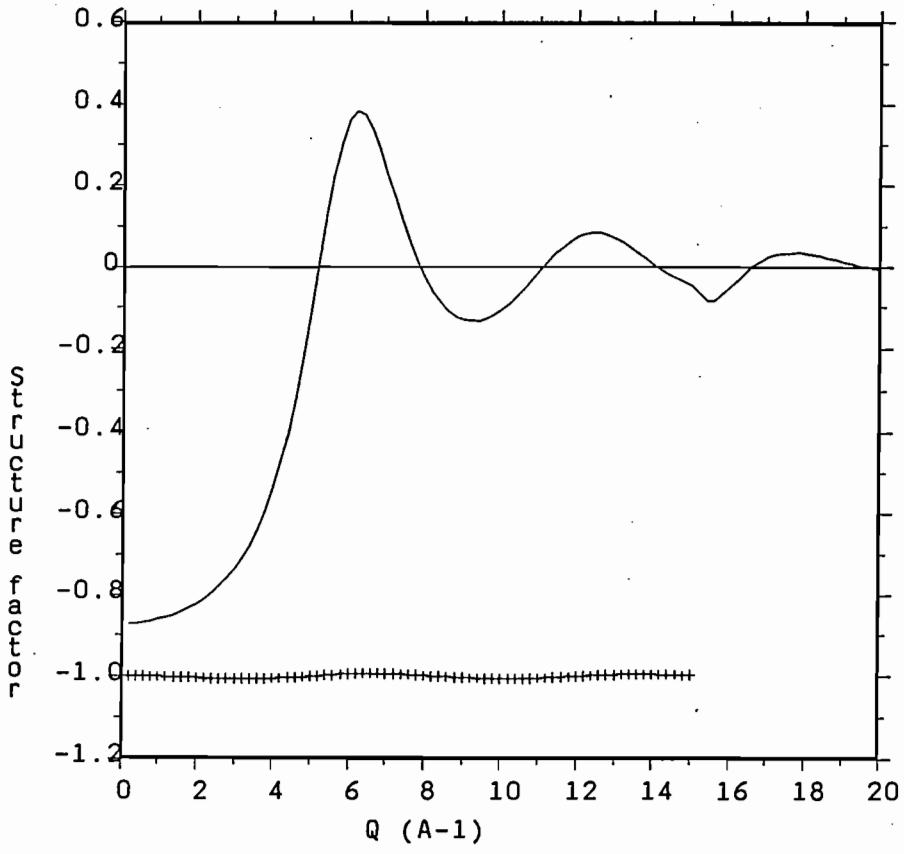

Figure C3 Maximum entropy structure factor corresponding to the correlation function of figure C2. The crosses show the residual between fit and data shifted below zero by unity.

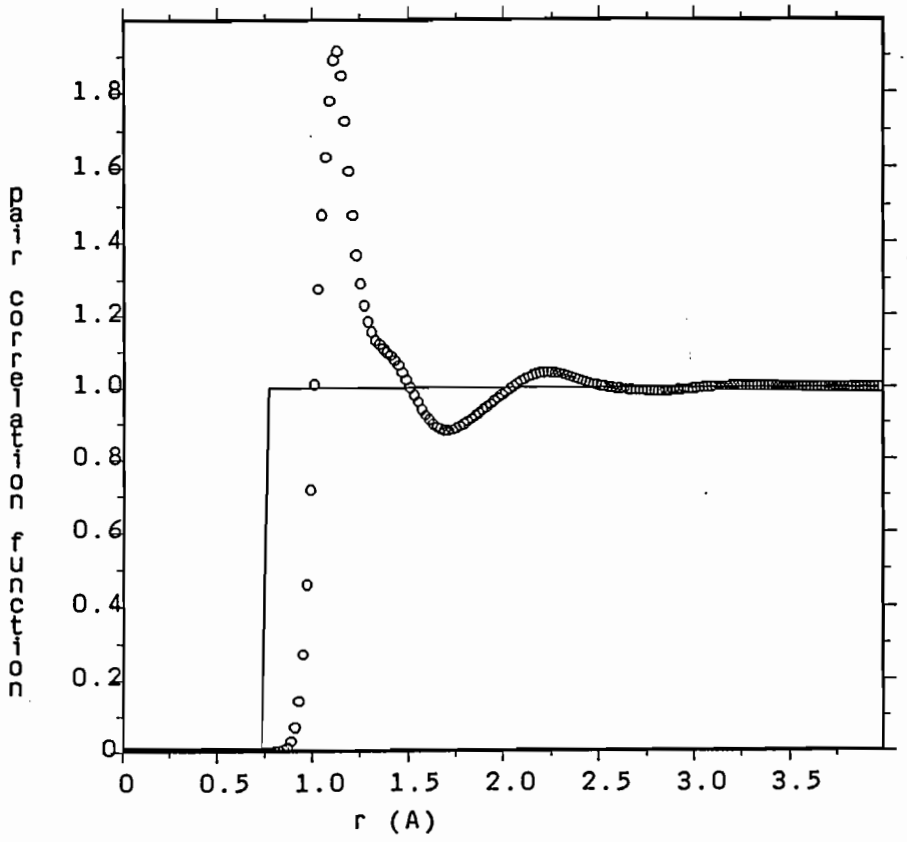

Figure C4 Maximum entropy pair correlation function as for figure 2, but this time derived using the exponential weighting on the distributions used to calculate the entropy, as described in the text.

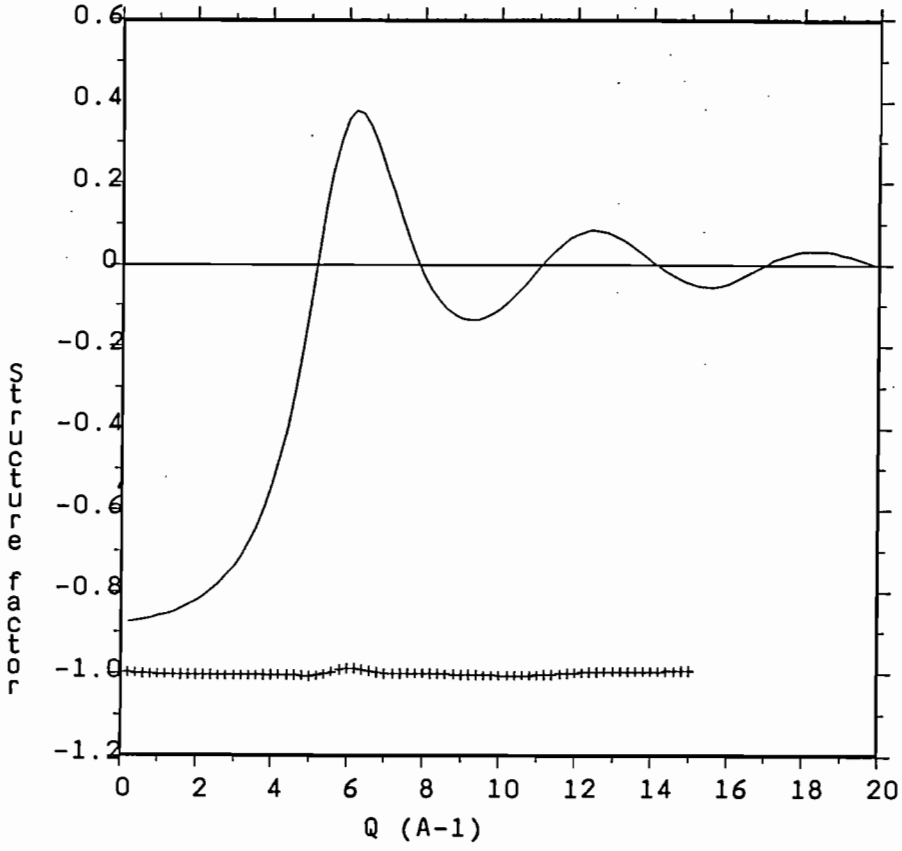

Figure C5 Maximum entropy structure factor corresponding to figure 4. Note that the cusp near Q = 15/Å is absent in this case.

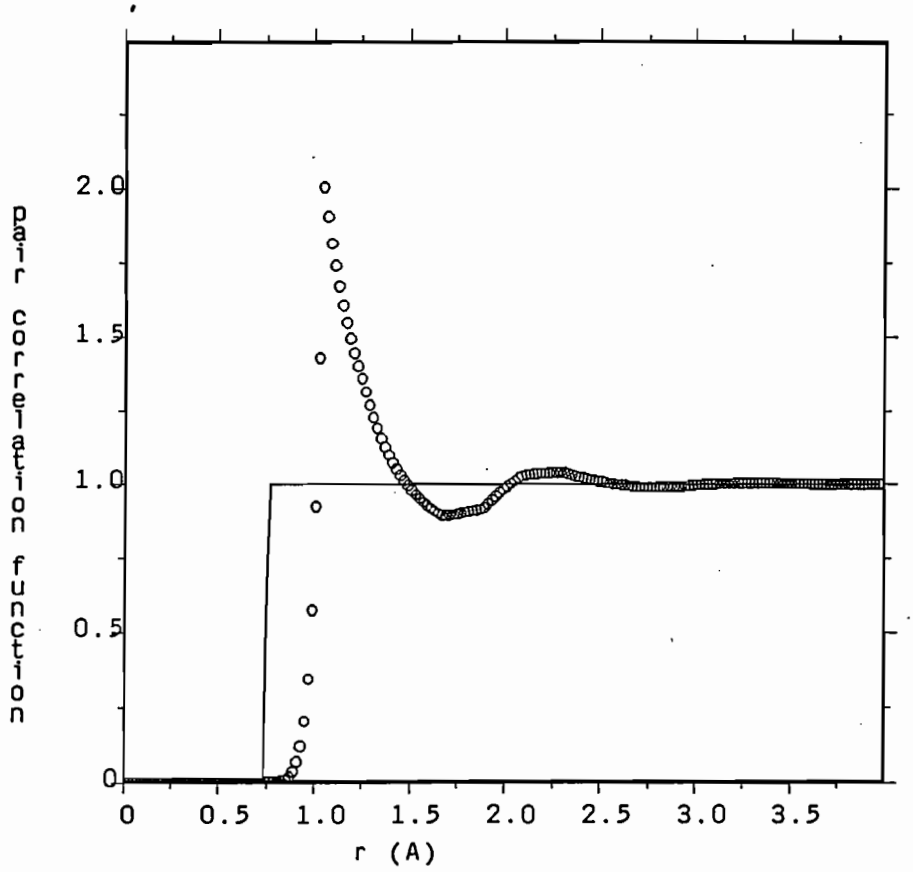

Figure C6 Maximum entropy pair correlation function as before, but this time using the fluctuations in the Q-factor linearly interpolated between the allowed discrete Fourier values.

APPENDIX D GLOSSARY OF FILE EXTENSIONS.

This appendix contains a list of the file extensions used by the ATLAS suite of programs together with a brief description of their contents. The files are listed in most likely order of usage. (Note the word 'extension' indicates the second part of the name of a file, occurring after the dot. eg the extension of file 'LAD01234.NRM;2' is 'NRM'.) Except where indicated otherwise, all files are written by a GENIE WRITE command so that the spectra may be read from them and displayed by use of the GENIE READ command. An ASCII file contains normal characters and the ASCII file LAD01234.AIN for example may be inspected either by $TYPE LAD01234.AIN or by $ED LAD01234.AIN . The program producing the file is indicated in {brackets}. The number of spectra in the file is indicated in [brackets], with n_spect indicating the number of raw spectra collected by the instrument and n_group indicating the number of detector groups.

Extension	Description
COM	A file containing commands to run programs. Can be used to run a batch job.
RAW	The raw data as collected on the neutron scattering instrument. There are a large number of spectra in the file, corresponding to the detector/electronic configuration of the instrument. The spectra are recorded as a function of time of flight. They may be read by GENIE by use of the ASSIGN command followed by DISPLAY S1 (for example). {ICP} [n_spect]
SAV	The contents of these files are of the same type as for the RAW files. The difference is that a SAV file is created by doing an UPDATE followed by a STORE on the instrument before the run is ENDed. Hence the SAV file does not contain the data for the full duration of the

run. {ICP} [n_spect]

NRM — Initial reduction of the experimental data. The file contains a small number of spectra, each of which corresponds to a group of a number of detectors. The spectra are stored as a function of momentum transfer Q. The data are corrected for deadtime and divided by incident beam monitor spectrum. {NORM} [n_group]

MON — The two monitor spectra as a function of neutron wavelength. The transmission monitor spectrum is on the same wavelength scale as the incident monitor spectrum and is divided by the incident monitor spectrum. {NORM} [2]

MUT — The cross-section of the sample as a function of wavelength as calculated from the measured transmission. This is an ASCII file and may be read into GENIE workspace Wn using >>load Wn LAD01234.MUT g_f:read_cs {Transmission Routines} [1]

AIN — The input parameters for a batch job to calculate an attenuation correction. An ASCII file. {CORAL/absorption}

ABS — The result of an attenuation correction calculation. An ASCII file. {CORAL/absorption}

MIN — The input parameters for a batch job to calculate a multiple scattering correction. An ASCII file. {CORAL/multiple scattering}

MUL — The result of a multiple scattering correction calculation. An ASCII file. {CORAL/multiple scattering}

REF — The result of a vanadium multiple scattering correction

calculation. An ASCII file. {CORAL/vanadium}

LOG — A LOG file is produced when a program is run by the batch system. It contains the output that would have gone to the screen if the program had been run interactively. The contents of the file may be inspected by TYPEing it, or EDiting it. It is recommended that LOG files are generally deleted. {Batch}

SMO — This file contains the vanadium spectra as a function of Q. The data are smoothed (Bragg peaks removed) and corrected for multiple scattering and inelasticity. {VANSM} [n_group]

DCS — The single differential cross-section of the sample as a function of Q. The data are normalised and corrected for attenuation and multiple scattering. {ANALYSE} [n_group]

SLF — A SLF file contains the calculated self scattering for the sample as a function of Q. {eg. PLATOM} [n_group]

INT — The distinct scattering for the sample as a function of Q, obtained by subtracting the self scattering from the total scattering. {INTERFERE} [n_group]

SOQ — The final S(Q) for the sample, obtained by merging data from different detector groups. {MERGE} [1]

APPENDIX E NEUTRON ABSORPTION RESONANCES

Z	Element	Resonance energies (eV)			
17	^{35}Cl	400			
23	V	170			
25	Mn	350			
27	Co	140			
29	^{63}Cu	600			
	^{65}Cu	240			
30	^{67}Zn	220	450		
	^{68}Zn	510			
31	^{69}Ga	110	350		
	^{71}Ga	95	300		
32	Ge	100	110	200	
33	As	46	95	250	
34	Se	2.6	210	270	
35	Br	35	55		
36	Kr	28	41	110	
38	Sr	3.5	600		
40	Zr	300	700		
41	Nb	35	42	95	
42	Mo	12	45	70	
43	Tc	5.6	20	40	
44	Ru	10	15	25	
45	Rh	1.2	34	46	
46	Pd	3	13	25	
47	^{107}Ag		16	40	
	^{109}Ag		5	30	40
48	Cd	0.18	19	29	
49	In	1.5	4	9	12
50	Sn	40	45	65	
51	Sb	6	15	21	
52	Te	2.3	8.5	25	
53	I	20	31		
54	Xe	5	9.4	14	

55	Cs	6	22	50			
56	Ba	25	80				
57	La	7					
59	Pr	85	210				
60	Nd	4.3	45	55			
61	Pm	5.4	6.9	7.0	16		
62	^{147}Sm		3.4	18			
	^{149}Sm		0.1	0.9	5	9	15
	^{152}Sm		8				
63	Eu	0.5	1	2.5	3.4		
64	Gd	2.1	2.6	2.9	6.3	7	
65	Tb	3.3	11				
66	Dy	1.7	2.7	3.7			
67	Ho	3.9	12.8				
68	Er	0.45	0.58	4.4	6	9	
69	Tm	3.9	14	17.5			
70	Yb	0.6	7.9	13			
71	Lu	0.14	2.6	5.2			
72	Hf	1.1	2.4				
73	Ta	4.3	10.3	14			
74	W	4.2	7.6	18.8			
75	Re	2.16	4.4				
76	Os	6.7	9.0	10.3			
77	Ir	0.66	1.3	5.4			
78	Pt	12	20				
79	Au	4.9	60	80			
80	Hg	23	32				
81	Tl	240					
88	Ra	0.5					
90	Th	22	23	60			
91	Pa	0.4	5				
92	^{233}U	1.8	2.3	6.8			
	^{234}U	5.2					
	^{235}U	8.8	11.7	12.4	19.3		
	^{236}U	5.4					
	^{238}U	6.67	20.9				

93	Np	0.5	1.5		
94	^{238}Pu		2.9	10	18
	^{239}Pu		0.3	7.8	11
	^{240}Pu		1.06	20.5	
	^{241}Pu		0.3	4.3	
	^{242}Pu		2.7		
95	Am	0.3	0.6	1.3	

References

1. Windsor C, 1981 "Pulsed Neutron Scattering", Academic Press

2. Taylor A D, 1984 Rutherford Appleton Report RAL-84-120

3. van Hove L, 1954, Phys. Rev. 95, 249

4. Egelstaff P A, 1987, "Neutron Scattering", Ed. K Sköld and D L Price, Ch 14, Academic Press Series - Methods of Experimental Physics, Vol 23, Part B.

5. Placzek G, 1952, Phys. Rev., 86, 377

6. Powles J G, 1973, Mol. Phys. 26, 1325

7. Rickayzen G and Powles J G, 1976, Mol. Phys. 32, 301

8. Powles J G and Rickayzen G, 1976, Mol. Phys. 32, 323

9. Powles J G, 1978, Mol. Phys. 36, 1161

10. Powles J G, 1978, Mol. Phys. 36, 1181

11. Powles J G, 1979, Mol. Phys. 37, 623

12. Egelstaff P A and Soper A K, 1980, Mol. Phys., 40, 553

13. Egelstaff P A and Soper A K, 1980, Mol. Phys., 40, 569

14. Koester L, Rauch H, Herkens M, Schröder, 1981, "Summary of Neutron Scattering Lengths", KFA-Jülich report no. 1755

15. Sears V F, 1984, "Thermal-Neutron Scattering Lengths and Cross Sections for Condensed-Matter Research", Atomic Energy of Canada Limited, Chalk River, Ontario, Canada, AECL Report No. 8490

16. Soper A K and Egelstaff P A, 1980, Nucl. Inst. Meth., 17

17. Paalman H H and Pings C J, 1962, J. Appl. Phys., 33, 2635

18. Blech I A and Averbach B L, 1965, Phys. Rev. 137A, A1113

19. Sears V F, 1975, Adv. Phys. 24, 1

20. Howe M A, McGreevy R L, Howells W S, 1989, J. Condensed Matter, in press.

21. Soper A K, 1988, Proceedings of ICANS-X , held in Los Alamos, Oct. 1988, to appear as IOP conference proceedings

22. Jaynes E T, 1982, Proc. of the IEEE. 70, 939

20. 23. Bryan R K and Skilling J, 1984, Monthly Not. Astr. Soc., 211, 111

24. Lado F, 1971, J. Comput. Phys. 8, 417

25. Throop G J and Bearman R J, 1965, J.Chem. Phys. 42, 2408

26. Root J H, Egelstaff P A, and Nickel B G, 1986, Inst. of Phys. Conf. Ser. No. 81
"Neutron Scattering Data Analysis, 1986", ed. by M W Johnson, IOP Bristol.

27. Lighthill M J, 1959, "Introduction to Fourier Analysis and Generalised Functions", Cambridge University Press.

28. Perry G and Throop G J, 1972, J.Chem. Phys. 57, 1827